NASA CR-66908

A STUDY OF ASEPTIC MAINTENANCE BY PRESSURIZATION

By Donald J. Cheater, Robert J. Homsey,
Maurice E. Long, John F. Sontowski

Prepared under Contract No. NAS1-9174 by
GENERAL ELECTRIC COMPANY
Re-Entry and Environmental Systems Division
Philadelphia, Pennsylvania

for

NATIONAL AERONAUTICS AND SPACE ADMINISTRATION

TABLE OF CONTENTS

		Page No.
TABLE OF CONTENTS		i
LIST OF FIGURES		iii
LIST OF TABLES		vi
LIST OF PHOTOGRAPHS		vii
GLOSSARY OF TERMS		viii
1.0	SUMMARY	1
2.0	INTRODUCTION	5
2.1	Background	5
2.2	Program Formulation	7
3.0	ANALYTICAL STUDIES	10
3.1	High Velocity Experiment Design	10
3.1.1	Flow Chamber Design Analysis	10
3.1.1.1	Configuration Analysis	10
3.1.1.2	Vibration Analysis	32
3.1.2	Experiment Test Parameter Analysis	40
3.1.2.1	Physical Considerations	41
3.1.2.2	Dimensional Analysis	45
3.1.2.3	Minimum Pressure Requirements	50
3.2	Microbial Motion In Flow Fields	57
3.2.1	Response to Turbulent Flow	57

TABLE OF CONTENTS

			Page No.
		3.2.2 Penetration By Large Contaminants	62
		3.2.3 Behavior At Reduced Ambient Pressure	71
4.0	EXPERIMENTAL PROGRAM		82
	4.1	Apparatus Description	82
		4.1.1 Quiescent Tests	82
		4.1.2 High Velocity Tests	87
	4.2	Test Protocol	92
		4.2.1 Quiescent Procedures	92
		4.2.2 High Velocity Procedures	100
	4.3	Apparatus Validation	108
		4.3.1 Flow Characterization	108
		4.3.2 Hole Characterization	113
		4.3.3 Aerosol Particle Distribution	115
		4.3.4 Microbial Challenge Conditions	122
5.0	RESULTS AND DISCUSSION		127
	5.1	Quiescent Program	127
	5.2	High Velocity Program	131
6.0	CONCLUSIONS		138
7.0	RECOMMENDATIONS		141
APPENDIX A - Equations of Motion For Spore Particles			143
APPENDIX B - Wind Tunnel Fan - Vibration Analysis			161
APPENDIX C - Air Velocity Calculations			173
APPENDIX D - High Velocity Test Results - Tabular			174

LIST OF FIGURES

Figure No.	Title	Page
3.1.1	Spore Particle Travel Distance to Achieve 0.9 and 0.99 Free Stream Speed	15
3.1.2A	Initial Flow Chamber Design	17
3.1.2B	Second Flow Chamber Design	17
3.1.3	Exploded View of Membrane Holder	18
3.1.4	Dependence of Flow Chamber Pressure Losses on Design Parameters and Flow Rates	19
3.1.5	Comparison of Available 5" Fan Capability to Optimum Capability Required	20
3.1.6	Impeller Type Selector	22
3.1.7	Comparison of Available 9" Fan Capability to Optimum Capability Required	24
3.1.8	AMP Flow Chamber Design	26
3.1.9	Comparison of Available 12" Fan Capability to Optimum Capability Required	28
3.1.10	Definition of Expansion and Contraction Angles	29
3.1.11	Flow Chamber Fan System	33
3.1.12	Dynamic Model of Fan Shaft	35

LIST OF FIGURES

Figure No.	Title	Page
3.1.13	Structural Modification to Alter Resonant Frequency	38
3.1.14	Challenge Geometry	42
3.1.15	Visualization of Spore Motion	50
3.1.16	Relationship of P_{∞} to P_m	55
3.1.17	Effect of Impinging Air Stream Velocity on Microbial Penetration	56
3.2.1	Spore Motion Relative to Flow	59
3.2.2	Membrane Holder Visualization	64
3.2.3	Penetration Threshold for One Micron Particle in Vacuum Condition	79
4.1	Quiescent Experimental Apparatus	83
4.2	Aerosol Dispenser	85
4.3	Aerosol Sampling Apparatus	88
4.4	Membrane and Viable Culture Tube Holder	91
4.5	Test Procedure - Quiescent Tests	93
4.6	Quiescent Test Procedure Checkout Sheet	94
4.7	Test Procedure - High Velocity	102
4.8	High Velocity Test Procedure Check	103

LIST OF FIGURES

Figure No.	Title	Page
4.9	Air Flow Through 20 Micron Opening	110
4.10	Air Flow Through 205 Micron Opening	111
4.11	Air Flow Through 980 Micron Opening	112
5.1	Test Chamber	129
5.2	Effect of Impinging Air Stream on Microbial Penetration Through 20 Micron Holes	133
5.3	Effect of Impinging Air Stream on Microbial Penetration Through 200 Micron Holes	134
5.4	Effect of Impinging Air Stream on Microbial Penetration Through 1000 Micron Holes	135

LIST OF TABLES

TABLE NO.	TITLE	PAGE
3.1.1	Impeller and Shaft Physical Properties	37
3.1.2	Physical Parameters Governing Microbial Penetration	46
3.1.3	Minimum Pressure Drop ΔP to Prevent Penetration	53
3.2.1	Penetration Depths as Function of Efflux Velocity for 15 micron Particle	69
3.2.2	Penetration Depths as Function of Efflux Velocity for 20 micron Particle	69
3.2.3	Penetration Distance for 1 Micron Particle as a Function of Altitude; (ΔP = Stagnation Pressure)	75
3.2.4	Penetration Distance for 1 Micron Particle as a Function of Altitude (ΔP = 2 in. H_2O)	77
4.1	Performance of Millipore Filters	99
4.2	Particle Distribution - Quiescent Chamber	116
4.3	Particle Distribution - 30 mph (Collector-Millipore Filter)	118
4.4	Particle Distribution - 30 mph (Collector-Glass Slide)	119
4.5	Aerosol Stability in Wind Tunnel	121
4.6	Viable Aerosol Counts in Quiescent Chambers vs Sampling Point	123
4.7	Investigation Results Into Anomolous Quiescent Run	124
4.8	Aerosol Challenge to 1000 μ Diameter Holes	125
5.1	Quiescent Test Results Summary	128

LIST OF PHOTOGRAPHS

PHOTOGRAPH NO.	TITLE	AFTER PAGE NO.
P-0	Quiescent Test Chamber	83
P-1	High Velocity Wind Tunnel	88
P-2	High Velocity Wind Tunnel	88
P-3	Membrane Holder Assembly - High Velocity	89
P-4	Hole Characterization 150 x 170 Micron Hole	113
P-5	Hole Characterization 200 Micron Hole	114
P-6	Hole Characterization 1000 Micron Hole	114
P-7	High Velocity Aerosol Deposition	120

GLOSSARY OF TERMS

A	-	area
C_D	-	dynamic drag coefficient
D, d	-	diameter
$\mathcal{D}$	-	diffusion coefficient
E	-	Young's modulus
f_n	-	oscillation frequency
g	-	gravitational acceleration
K	-	Knudsen number
K_o	-	loss coefficient
L	-	length
λ	-	loss coefficient
m	-	mass
μ	-	viscosity
N_s	-	specific fan speed
n	-	number density
ω	-	angular velocity
P	-	pressure
ΔP	-	pressure differential
P_c	-	chamber pressure loss
ϕ	-	potential function
Q	-	volumetric flow rate
q	-	dynamic pressure
R, r	-	radius
r_f	-	revolutions/minute
ρ	-	density
R_e	-	Reynold's number
S	-	distance
τ	-	time constant
V	-	speed
W	-	weight
Z	-	height

Subscripts:

f	-	fan
h	-	hole
0	-	reference body
S	-	spore
∞	-	free stream

1.0 SUMMARY

A study of aseptic maintenance by pressurization has been conducted for the Langley Research Center of the National Aeronautics and Space Administration under Contract NAS1-9174. The study consisted of two phases. The first phase concentrated on increasing the confidence limits of the data previously obtained from the AMP I contract. Both studies have demonstrated that a pressure differential slightly above ambient across a membrane separating two quiescent gas chambers could prevent migration of microorganisms through a single microscopic hole against that pressure gradient. Spores of B. subtilis var. niger were aerosolized into a chamber and were presented by gravity to the hole at the bottom of the chamber. The holes, ranging in size from 19 microns to 1887 microns in diameter, were made in .012 inch thick membranes of aluminum. The viable spores which penetrated the hole were captured on an agar medium.

A total of 50 tests with pressure differentials ranging from 0.5 inches to 2.0 inches of water resulted in total exclusion of microorganisms from the detection medium.

During the early part of the quiescent testing, difficulty was

experienced when one test gave the appearance of penetration of a microorganism against a pressure gradient of 0.5 inches of water. Experimental evidence proved this to be a procedural flaw and resulted in the extention of the pre-incubation time from 24 to 48 hours to ensure the sterility of the assembled membrane prior to its hook-up to the test assembly.

The data obtained under quiescent conditions substantiates the theory that very low pressure differentials will effectively prevent passage of microscopic particles against the pressure gradient through a microscopic hole as long as the atmosphere on either side of the hole is quiescent. The experimental data clearly demonstrated that for all the hole sizes tested 0.5 inches of water stopped all of the particles that challenged the holes. The particle sizes were found not to exceed 35 microns in diameter. Even though the particle sizes were limited by the experimental conditions, theoretical analysis has shown that 0.5 inch of water will stop particles, under quiescent conditions, with diameters of up to approximately 200 microns.

The second phase of the study, which ran concurrently with the first, dealt with the increased pressure differential required to prevent passage of microorganisms through the hole under non-quiescent conditions. The experiments were performed in a unique wind tunnel facility specifically designed and constructed for this phase of the study.

The theoretical analysis of gas flow demonstrated that the presence of internal pressure slightly above the flow stagnation pressure on a membrane should prevent migration of one to two micron diameter particles. As the particle size and velocity increases, however, an increasingly larger differential pressure is required to prevent passage through the larger holes.

A total of 83 tests with hole sizes of 20, 200 and 1000 microns in diameter were run at pressure differentials ranging from 0 to 3.6 inches above ambient. These were run at wind velocities ranging from 10 to 35 mph. Results of the 20 and 200 micron diameter holes were very similar. Their threshold curves, up to 25 mph, have a constant slope and indicate a water pressure of 0.4 inches above ambient is sufficient to prevent penetration of airborne particles capable of being sustained at these velocities. As the wind velocity increases beyond 25 mph however, a slope change occurs (indicating an alteration in challenge conditions) and at the highest test velocity a 1.1 inch water pressure differential is required.

Results of the tests run with the 1000 micron diameter holes indicate that at 25 miles per hour and below, 1.8 inches water pressure is required to prevent penetration. Above 25 miles per hour, the differential pressure required to prevent penetration has not been firmly established. Pressures in excess of 3.5 inches above ambient have been found necessary

at speeds of 35 mph. A particle size dependence has shown up in all the hole sizes and it appears, therefore, that control of particle sizes is necessary when the protection of holes is to be accomplished using about 2.0 inches of water. In general, the use of pressure differentials, when flow disturbances exist on either side of a membrane, offer a workable solution where assembly sterilization and maintenance of asepsis are of prime importance.

2. INTRODUCTION

2.1 BACKGROUND

The program described herein addresses the problem of maintaining the sterility of a spacecraft by providing a barrier against recontamination from viable organisms.

Until the existence and nature of living forms on extra-terrestrial bodies are determined, such a program is necessary for interplanetary missions which require sterile flight vehicles to enter the atmosphere or land on the surface of extra-terrestrial planets.

Two basic concepts for sterilization of spacecraft have been brought forth in recent years. These are called "Terminal Sterilization" and "Assembly/Sterilizer" processing.

The concept of Terminal Sterilization refers to the assembly and checkout of a vehicle in a clean room, decontamination with a suitable biocide (ETO), sealing in a canister, and then exposing to dry heat sterilization. After this final dry heat sterilization, no access to the vehicle is possible without involving recontamination.

The assembly sterilizer system is an ultra-clean room facility

which permits decontamination and sterilization of the disassembled vehicle, and subsequent assembly, checkout, adjustment, and if necessary, repair of the spacecraft in a sterile environment.

When this sterilization cycle is completed, a canister will be utilized to maintain the sterility of the vehicle. This canister, being subjected to the rigors of manufacture, assembly and sterilization, may have microscopic holes present which would provide a port for recontamination. To avoid the possibility of recontamination by such means in either the assembly sterilizer or the canister, investigators have adopted the use of a positive pressure differential to achieve an outward gas flow through any leak to ensure the biological integrity of the system.

The AMP I studies proved to be a very sensitive method for the detection of microbial penetration through small holes in thin membranes. The theoretical and experimental studies have shown that such microorganisms do not penetrate under quiescent conditions when a positive pressure differential of as small as 0.5 inches of water pressure is applied across the membrane.

During the course of these studies, however, certain conditions were encountered which led one to believe that microbial penetration may result by non-quiescent conditions on either side of the membrane.

In light of these anomalies, it was deemed necessary to extend the scope of the AMP I contract to include these parameters in order to obtain data which would provide additional information on the feasibility of maintaining aseptic conditions by pressurization. Toward this end, the Aseptic Maintenance by Pressurization program described herein, was directed.

2.2 PROGRAM FORMULATION

The present AMP program was formulated to extend the quiescent testing of the AMP I program and to investigate the pressure differentials required to prevent the passage of microorganisms under non-quiescent conditions. The first phase, the quiescent work, was entirely experimental since the experiment design studies and the analytical studies of AMP I (Reference 2.1) were directly applicable. The testing used four identical sets of apparatus which were very similar to the AMP I equipment. The most significant difference was a re-designed membrane holder which successfully eliminated the existence of uncontrolled leaks. The entire test protocol and culture tube preparation techniques were carried over from the previous program with one exception. The pre-incubation was extended to 48 hours to ensure the sterility of the assembly prior to the initiation of a test. To maintain a constant procedure, a detailed check-out form was generated and used on each test run to record the actual

procedural steps that were followed. In addition to the basic test program, studies on the Millipore line filters were done to build confidence in their ability to maintain a sterile air flow to the culture tube. No violations of the filters were observed. The extensive use of AMP I techniques and hardware therefore allowed the greater majority of the effort on quiescent testing to be concentrated on the collection of data.

The second phase of the program dealt with the development of a facility and its use to investigate microbial penetration under non-quiescent conditions. This new aspect of the AMP work required both analytical and experimental activities. The analyses included:

Flow Chamber Design - an aerodynamically acceptable chamber was designed to accelerate spore particles up to 40 miles per hour in a closed circulation loop and to provide a stable condition for microbial challenge of membranes;

Microbial Motion in Flows - analysis was done to gain a quantitative understanding of the parameters controlling penetration at high velocities; i.e. particle speed, absolute pressure, pressure differential, particle mass, particle size, hole size, etc. The results were also used to identify the necessary test parameters and their variation in magnitude.

In addition, the analysis provided an improved insight into the quiescent results by providing an estimation of the effect of particle size on quiescent penetration.

The experimental program concentrated on the development of acceptable techniques to accomplish microbial challenges with velocities up to 40 mph and on the generation of penetration threshold curves for holes sizes of 20, 200 and 1000 microns in diameter. The methods for aerosol dispensing, culture tube preparation, and gas supply filtering were carried over from the quiescent test program. Like the quiescent program, the test runs were scheduled to last 72 hours to ensure adequate incubation time and hence reliable detection of spore penetrations. The same initial population of spores (8.5×10^9) were used and with the closed loop circulation provided a microbial challenge several orders of magnitude more severe than the quiescent challenges.

The results of both the analytical and experimental efforts were combined to extend the data to conditions not covered in the experiments; e.g. penetration at reduced ambient pressures corresponding to altitudes from sea-level to free-space vacuum and the spore particle size dependence of the pressure differential requirements to negate penetration.

3.0 ANALYTICAL STUDIES

3.1 HIGH VELOCITY EXPERIMENT DESIGN

3.1.1 Flow Chamber Design Analysis

3.1.1.1 Chamber Configuration

The investigation of penetration through holes by microbial spores has required the design and construction of a unique facility. The initial specifications for the facility included: (1) dispersal and closed loop circulation of a prepared sample in a free stream flow of up to 40 mph; (2) essentially "laminar" flow conditions just upstream of the test membrane; (3) minimal chamber flow losses to achieve a cost-effective design; (4) utilization of "off-the-shelf" monitoring and control equipment: and (5) simplicity in design to facilitate the accomplishment of short down times between experimental runs. The chamber configuration selected for AMP II was based on well established aerodynamic equations that have been successfully used in the design of large scale wind tunnels. The design margins were sufficiently conservative to permit trouble-free operation on all three chambers for the five month duration of the test program, to permit stable flow conditions during each test run, and to achieve the 40 mph speeds using only 40 percent of the drive motor capability. The simplicity of the

selected configuration also allowed the ready incorporation of design changes dictated by the results of the apparatus validation tests. The changes involved the loading of the structure to alter its resonant frequency (predicted by analysis), the addition of a grounded charge build-up, and the inclusion of a honeycomb structure to insure a stable flow state at the membrane surface.

A closed loop flow chamber was desired to provide to the test membrane a total number of microbial challenges which was at least comparable to the quiescent test challenge condition. An attempt to provide the challenge in one pass could fall below the necessary challenge level because of inhomogenieties in the spatial distribution of the microbes within the tunnel. Furthermore a closed loop system avoids bacterial contamination of adjoining laboratories.

The initial philosophy in selecting the chamber was governed by ease and economy construction. The first configuration was therefore square in its outline with each leg having identical and constant cross-sectional area and the corners rounded to minimize turbulence. The key analytical step was to evaluate the chamber flow losses as a function of the flow speed and to determine whether standard drive fans and motors would suffice over the speed range of 0 to 40 mph. The standard equation for flow loss as expressed in terms of a pressure change is:

$$P = K_o q_o \qquad (3.1.1.1)$$

where K_o is typically dependent on the flow tube length and diameter. In particular,

Cylinder:

$$K_o = \left(\lambda \frac{L}{D}\right)\left(\frac{D_o}{D}\right)^4 \qquad (3.1.1.2)$$

and:

Corners:

$$K_o = \left[0.10 + \frac{4.55}{(\log_{10} R)^{2.58}}\right]\left(\frac{D_o}{D}\right)^4 \qquad (3.1.1.3)$$

To provide quantitative values for ΔP, a selection of L/D, D, and R must be made and should be representative of the expected values for the final chamber configuration. The length of the flow chamber side was selected using three criteria; i.e. (1) length must be greater than the distance required for microbes to achieve free stream speeds; (2) length should be sufficient to allow dampening of any turbulence caused by flow turning a corner (rule-of-thumb used was $L \geq 7D$); and (3) chamber sizing must be consistent with the available laboratory space.

Motion of a microbe is described by:

$$m \frac{d\bar{v}}{dt} = C_D \tfrac{1}{2} \rho_\infty V^2 A \qquad (3.1.1.4)$$

where:

$$C_D = \frac{K}{Re} = \frac{24}{\frac{\rho_\infty V d}{\mu_\infty}}$$

$$A = \frac{\pi d^2}{4}$$

Hence Equation (3.1.1.4) becomes after substitution, rearrangement and integration:

$$V_s = V_\infty \left[1 - e^{-t/\tau}\right] \qquad (3.1.1.5)$$

and:

$$S_s = V_\infty \left[t - \tau V_s / V_\infty\right] \qquad (3.1.1.6)$$

where V_s is the spore speed, S_s is the spore distance traveled in time t, and $\tau^{-1} = \frac{24 \mu_\infty \pi \quad d}{8m}$. The expressions, which are derived in detail in Appendix A, are valid for Reynold's number of about 1.0 and below. It is shown in the Appendix that a 1 micron diameter spore moving 40 mph in air has a Reynold's number R_e = 1.22. For our purposes of visualizing what happens, it is therefore acceptable to assume Stokes' law applies over the velocity

range we are considering. Incidentally, it may be noted that Stokes' law gives C_D values smaller than those measured at $R_e \sim 1$ so that decelerations will not be over-estimated. Then for 1 micron diameter spores, the distances traveled in reaching 90% and 99% of the free stream speed are given in Figure 3.1.1. It can be observed that at 40 mph the 1 micron spore will reach 90% of the stream velocity in 4.3×10^{-4} feet.

It was assumed during the analysis (and later proven to be correct) that the greatest majority of particles to be encountered will be below 100 microns. The design of the chamber should be capable of accommodating such particles so that no significant perturbation to their velocity history occurs. The equation of motion for the 100 micron particles unfortunately cannot be accurately predicted using Equations 3.1.1.5 and 3.1.1.6 since their Reynold's number, R_e, is above 120 at 40 mph. However the experimentally derived, and therefore more accurate, values of C_D are higher than those predicted by Stokes' law. It is apparent then that a conservative chamber design should result if one uses Stokes' law for the value of C_D. Taking this approach, the distances traveled by a 100 micron particle in attaining 90% and 99% of the free stream speed are given in the upper curves of Figure 3.1.1. It can be seen that at 40 mph the 100 micron particle reaches 90% of the stream speed in 4.3 feet. Hence choosing a chamber leg to be at least four feet long insures most of the membrane challenges will occur within a few percent of the free stream speed.

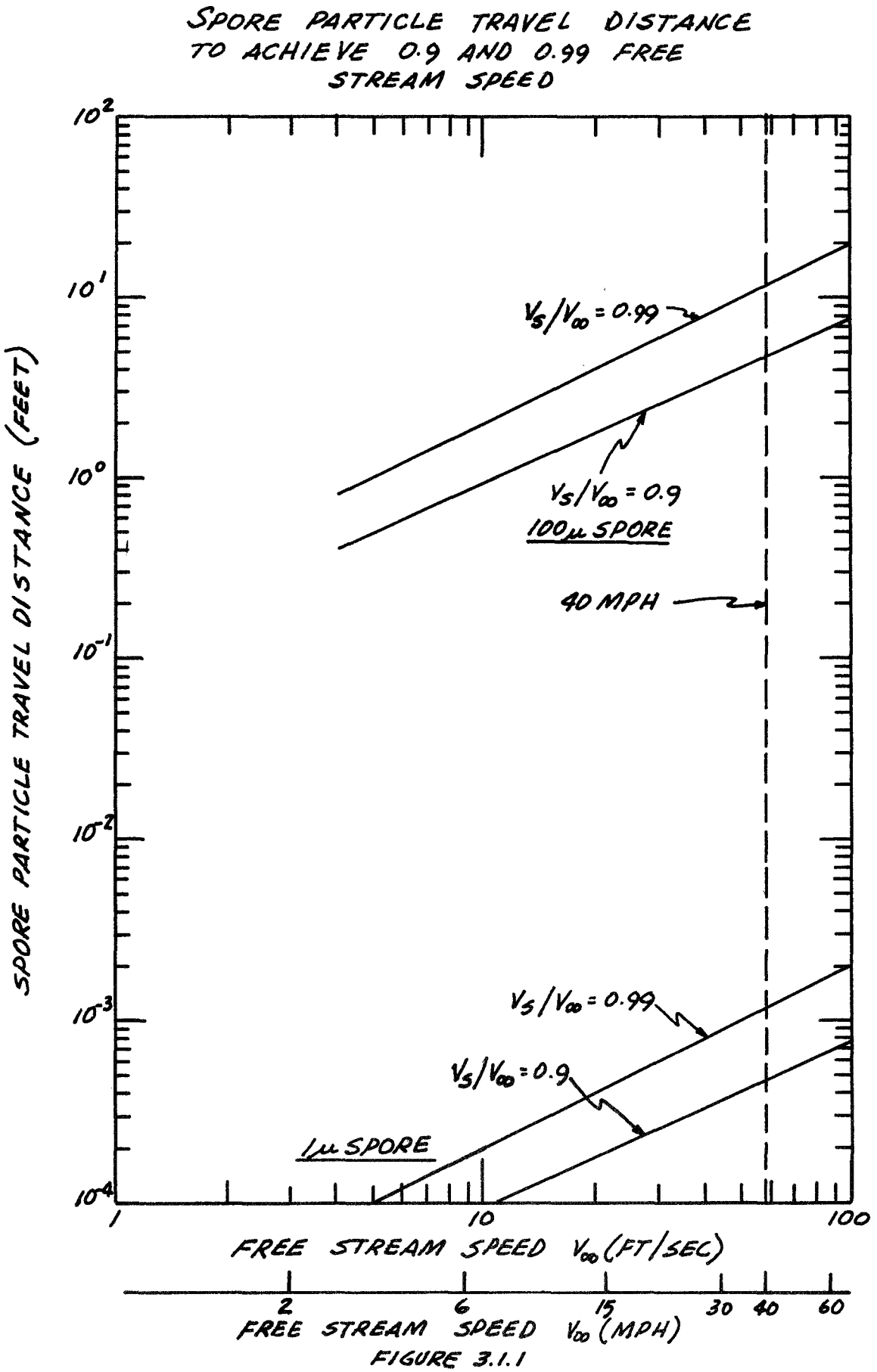
SPORE PARTICLE TRAVEL DISTANCE TO ACHIEVE 0.9 AND 0.99 FREE STREAM SPEED
SPORE PARTICLE TRAVEL DISTANCE (FEET)
10^2
10^1
10^0
10^{-1}
10^{-2}
10^{-3}
10^{-4}
$V_s/V_\infty = 0.99$
$V_s/V_\infty = 0.9$
100μ SPORE
40 MPH
$V_s/V_\infty = 0.99$
$V_s/V_\infty = 0.9$
1μ SPORE
1
10
100
FREE STREAM SPEED V_∞ (FT/SEC)
2
6
15
30
40
60
FREE STREAM SPEED V_∞ (MPH)

FIGURE 3.1.1

The initial selection of the chamber leg diameter was next made. Experience in aerodynamic wind tunnels has shown that for smoothness of flow after turning corners the test section in front of the model should be at least seven (7) times the section diameter. With a test section of about four (4) feet, a diameter of less than seven (7) inches is desired. Experience has also shown that for smooth flow around a target the tunnel cross-sectional area to target cross-sectional area should be in the ratio of at least 5:1. Since a 2 inch diameter target was being planned, the target's cross-sectional area would be 0.02 ft^2. Therefore the tunnel's area should be at least 0.1 ft^2 which corresponds to a diameter of 4.3 inches. Hence the tunnel dimension should lie between 7 and 4.3 inches.

The above considerations plus the consideration of the ease in construction led to an initial chamber design with the dimensions given in Figure 3.1.2.A. The attendent pressure loss as a function of stream speed was calculated using Equations 3.1.1.1 to 3.1.1.3 where the use of turning vanes has not been considered and the model is taken to be aerodynamically shaped as given in Figure 3.1.3 with $K_o = 0.1$. The results (curve 1 in Figure 3.1.4) when compared to the operating capabilities of available fans (Figure 3.1.5) clearly shows the impractical situation of requiring a drive motor with a rotational speed well in excess of 5000 rpm. The cost of such heavy duty units was considered incompatible with the program funding.

INITIAL FLOW CHAMBER DESIGN

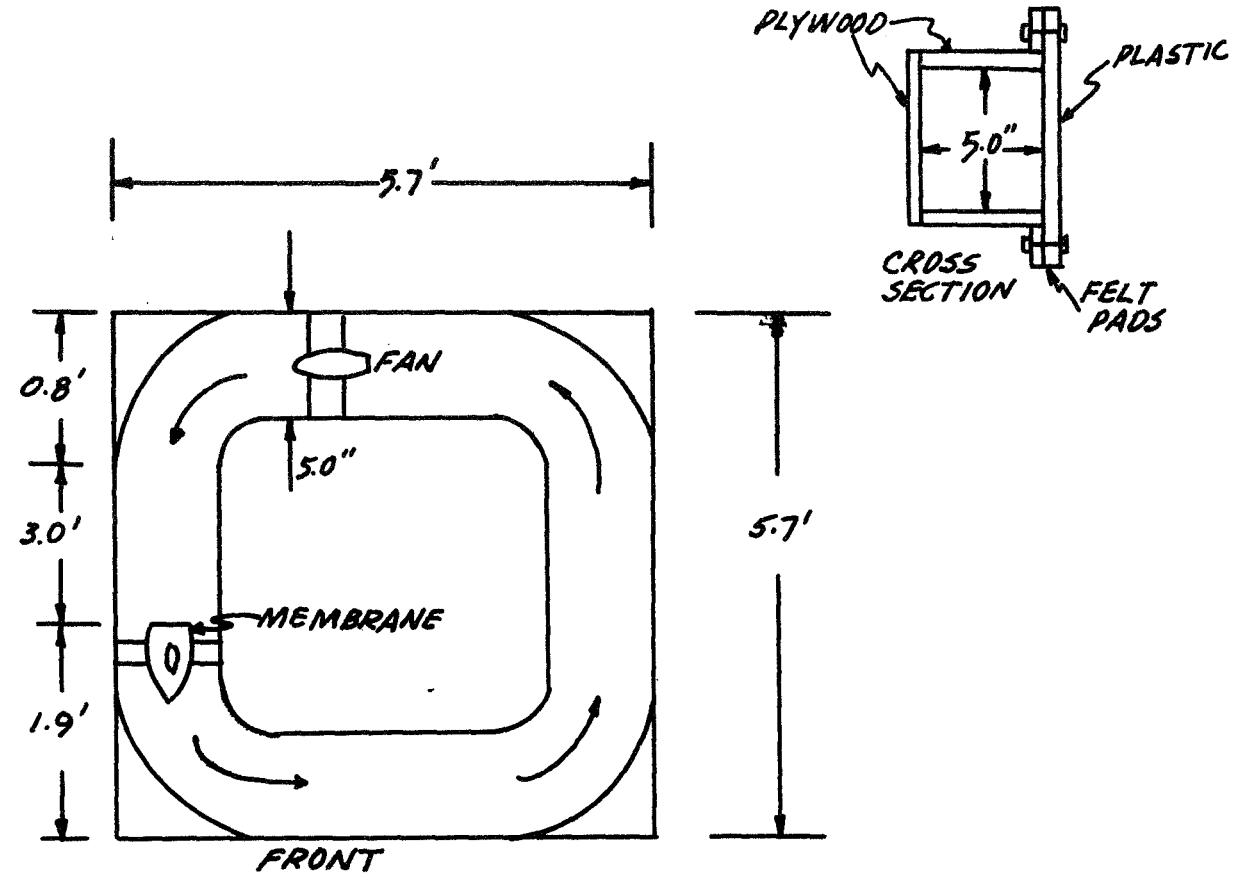

FIGURE 3.1.2 A

SECOND FLOW CHAMBER DESIGN

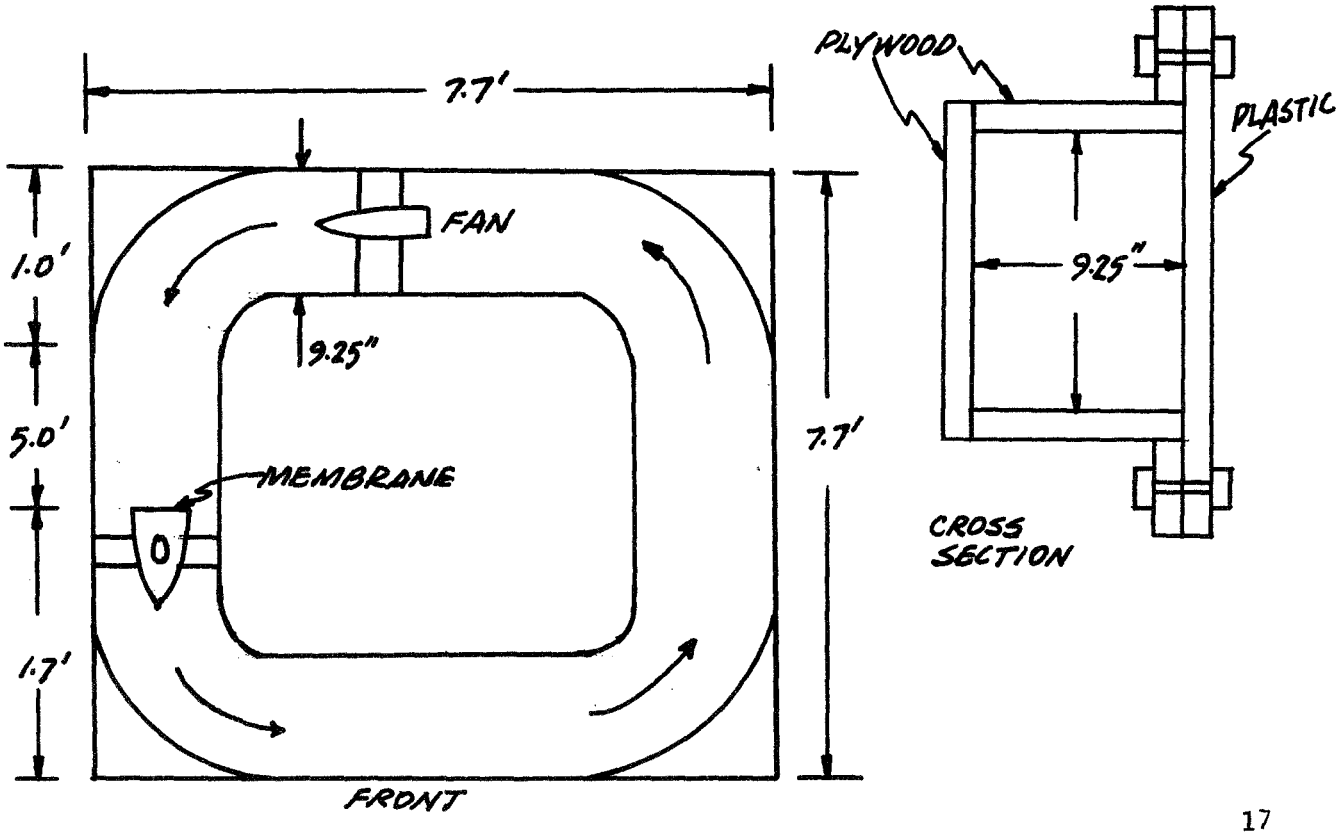

FIGURE 3.1.2 B

EXPLODED VIEW OF MEMBRANE HOLDER WITH AERODYNAMIC SHAPING ($K_0 = 0.1$)

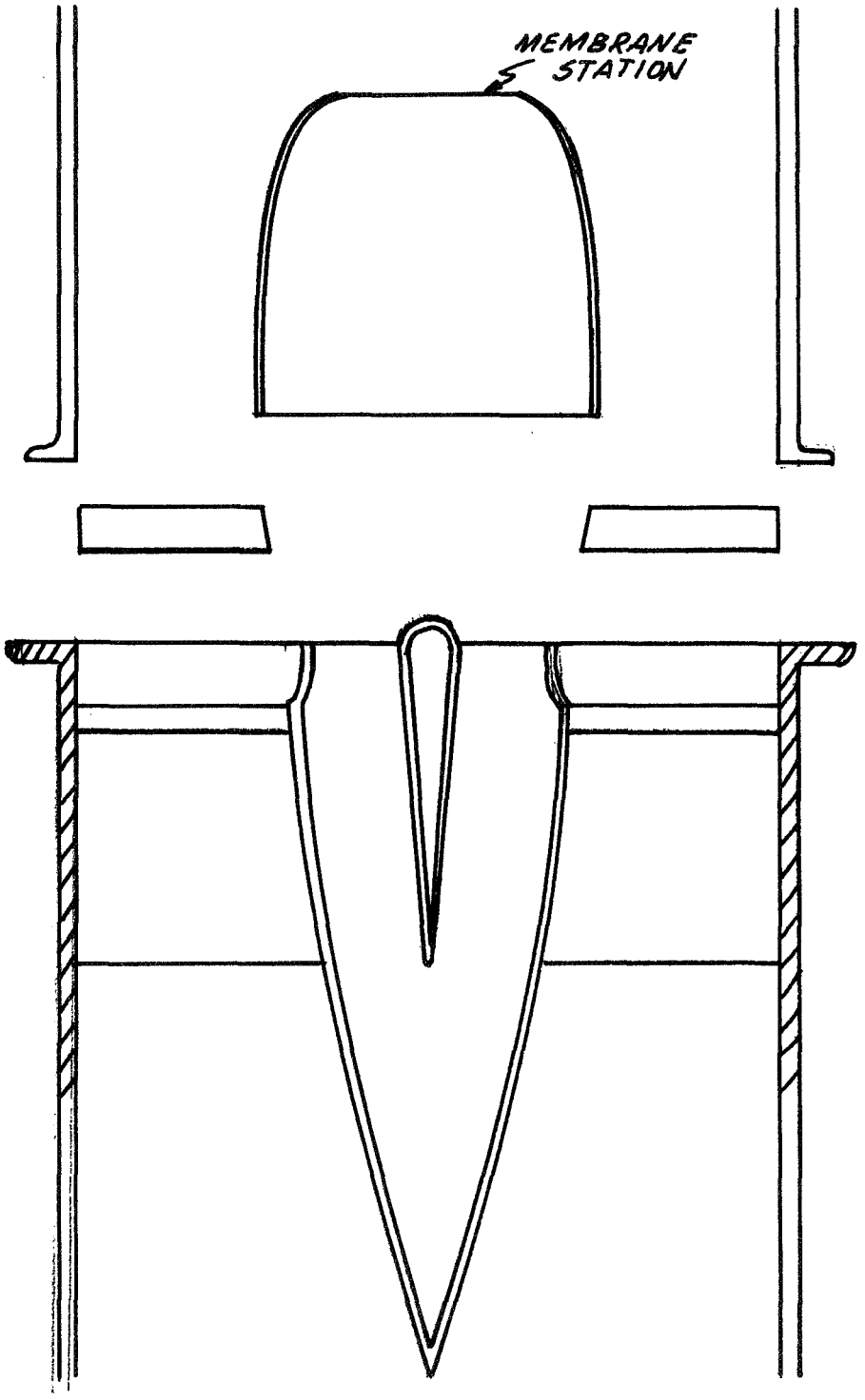

FIGURE 3.1.3

DEPENDENCE OF FLOW CHAMBER PRESSURE LOSSES ON DESIGN PARAMETERS & FLOW RATE

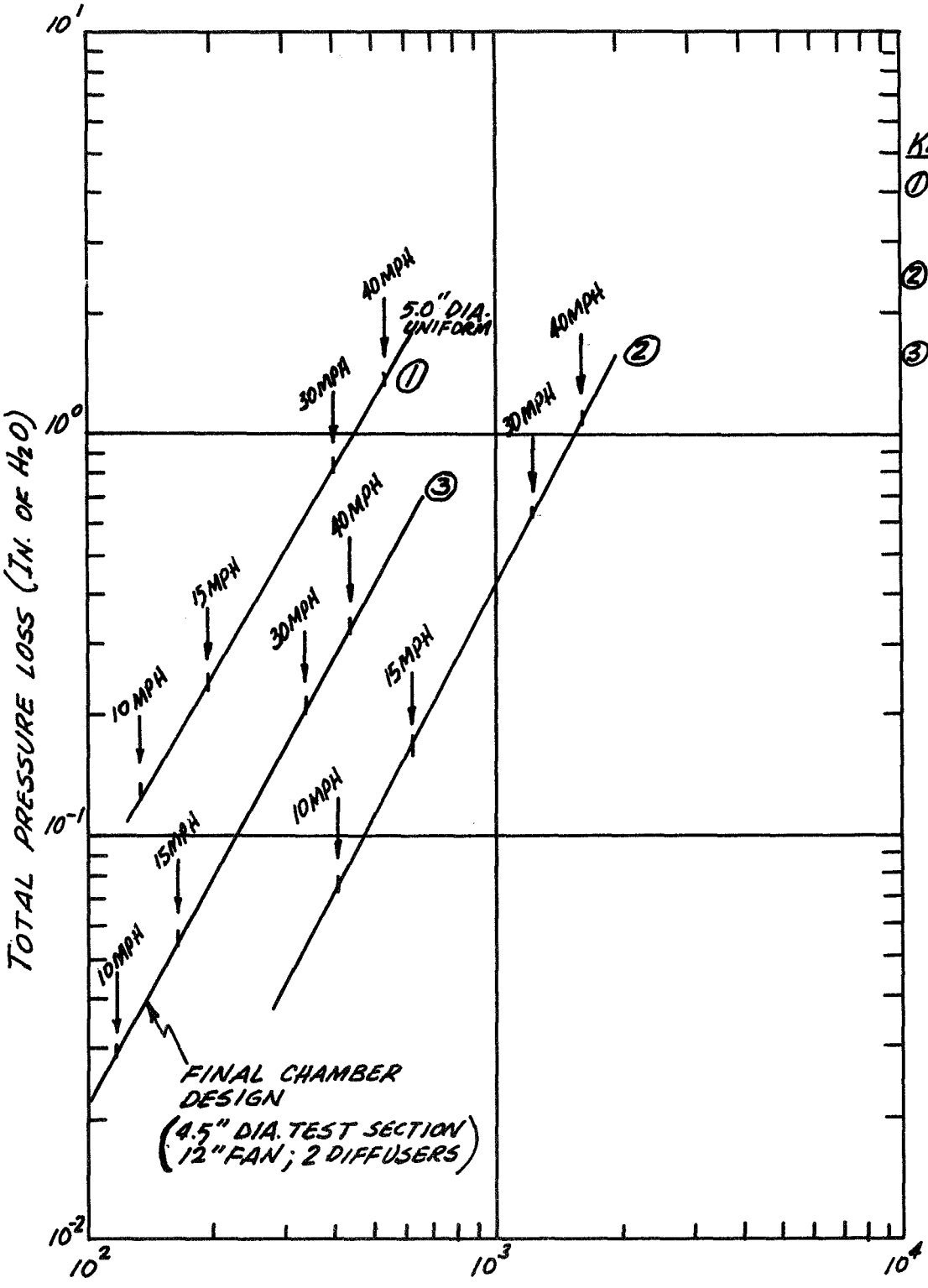

FIGURE 3.1.4

COMPARISON OF AVAILABLE 5" FAN CAPABILITY TO OPTIMUM CAPABILITY REQUIRED FOR THE 5" CHAMBER

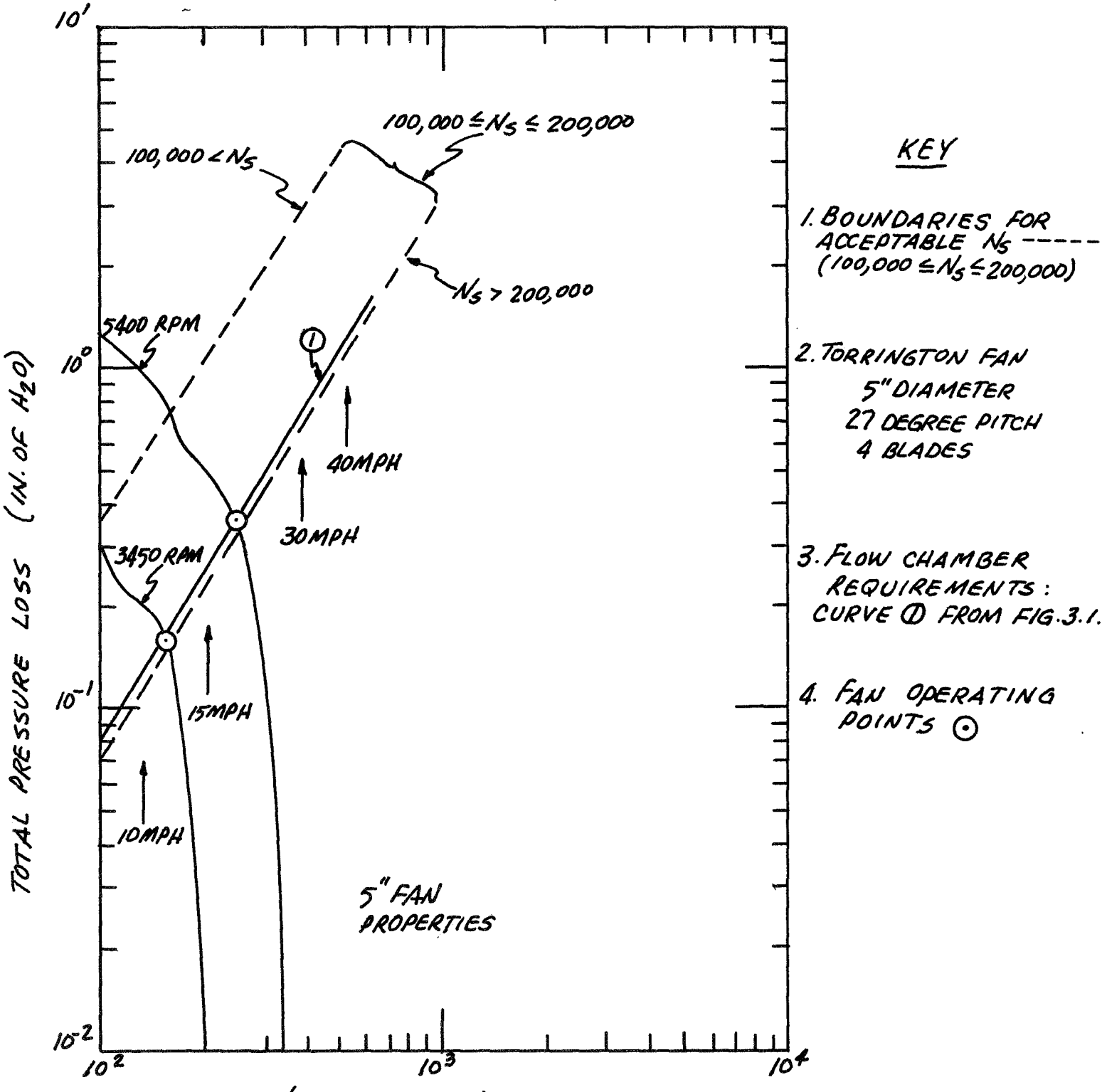

FIGURE 3.1.5

The impeller given prime consideration for the chamber was a propeller fan since its inherent design will provide less impedance to the flow of bacteria than will its companion the centrifugal impeller. Moreover, the widespread use of propeller fans will insure the ready availability of a unit with the proper characteristics for our application. The operating capabilities as given in Figure 3.1.5 are based on a propeller fan operating in its optimum specific speed of $100{,}000 \leq N_s \leq 200{,}000$ as obtained from a standard operating efficiency as given in Figure 3.1.6. The selection of N_s permits the dashed curves in Figure 3.1.5 to be generated from the relationship:

$$N_s = \frac{Q^{1/2} rf}{P_c^{3/4}} \qquad (3.1.1.7)$$

The fan properties given in the figure are measured values for a 5" fan supplied by the Torrington Fan Company. The crossing points of these curves with the chamber requirement curve are the only permissible fan operating conditions.

The undesirable operating speeds required by the 5 inch diameter chamber next led to consideration of a 9.25 inch diameter, uniform cross-section chamber (Figure 3.1.2.B). The larger diameter chamber provides a lower pressure loss as predicted by the inverse dependence to D in

IMPELLER TYPE SELECTOR (PEAK EFFIENCY AT WIDEST PART OF BAR)

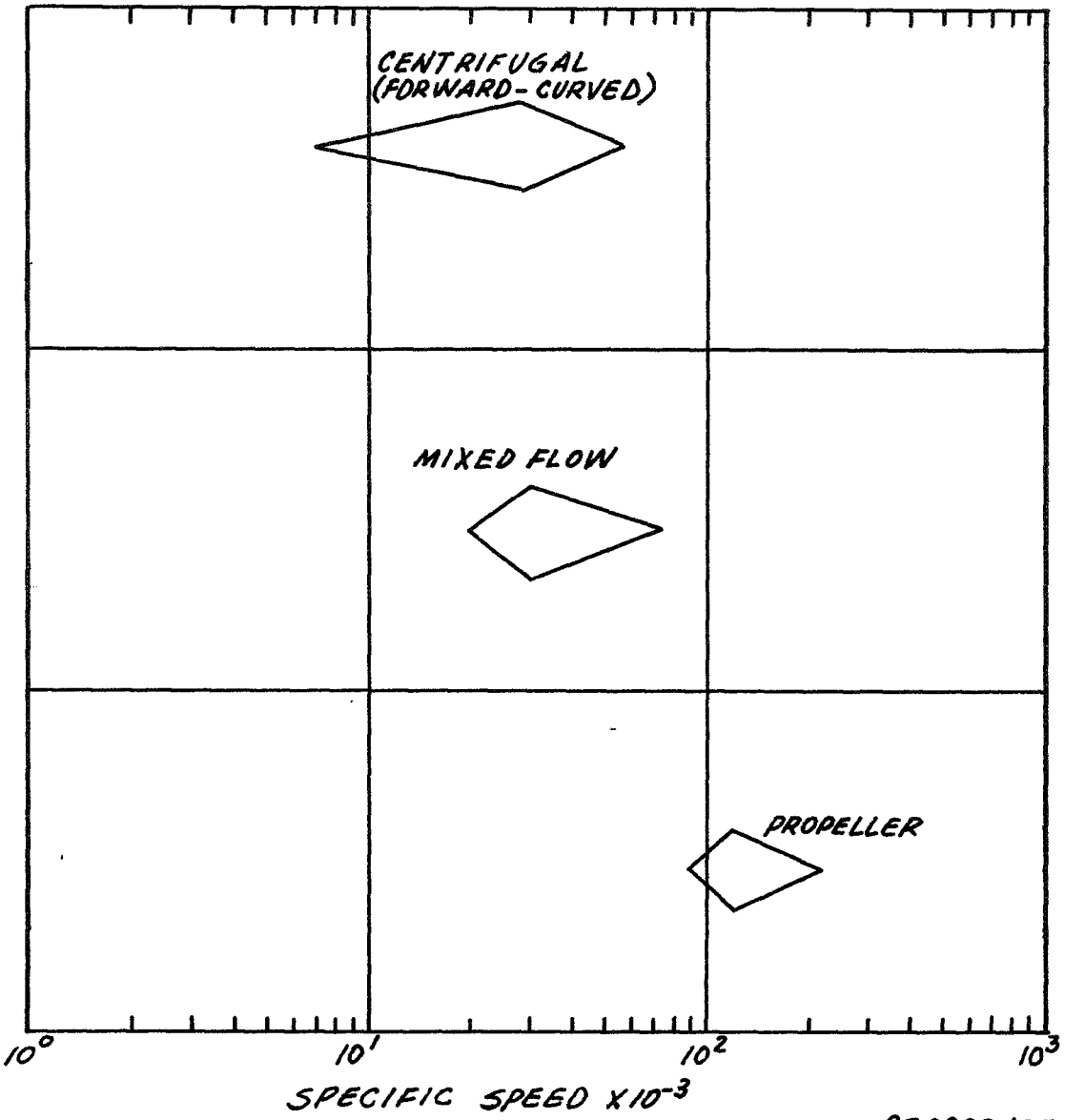

FIGURE 3.1.6

REPRODUCED FROM TORRINGTON
IMPELLER CATALOG
TORRINGTON MANUFACTURING CO.

Euqations 3.1.1.2 and 3.1.1.3. This chamber's pressure loss as a function of pumping speed (curve 2 in Figure 3.1.4) when compared to the fan properties (Figure 3.1.7) shows a relative improvement in required operating conditions. However the maximum motor speed is still in excess of 5000 rpm and there is still a large pressure loss at the higher motor speeds. It should be noted that the fan properties are for a 9" Torrington Company fan.

Further attempts to bring the chamber configuration into line with the fan capability can take several paths. The desired affects to be achieved are the reduction in the chamber pressure loss versus pumping speed and the reduction in the motor speed required to achieve 40 mph. One approach can be to continue increasing the chamber leg diameter. The approach however will lead to an unwieldly leglength since the criteria of $L \geq 7D$ for the test section must be maintained. For example, with a D = 12 inches, the length and height must be more than 7 feet. Such lengths will significantly encroach on the available laboratory space and cause the construction cost to continue to increase particularly with the construction of the three chambers required to meet the program schedule.

Another approach is to keep the test section diameter small and increase the diameter of the remaining three legs. This method permits the $L \geq 7D$ criteria to be met while minimizing pressure losses along a large fraction of the flow path. Furthermore, the overall envelope can be held to a reasonable size with only a moderate increase in construction complexity. The resulting geometry begins to approach the more

COMPARISON OF AVAILABLE 9" FAN CAPABILITY TO OPTIMUM CAPABILITY FOR THE 9.25" CHAMBER

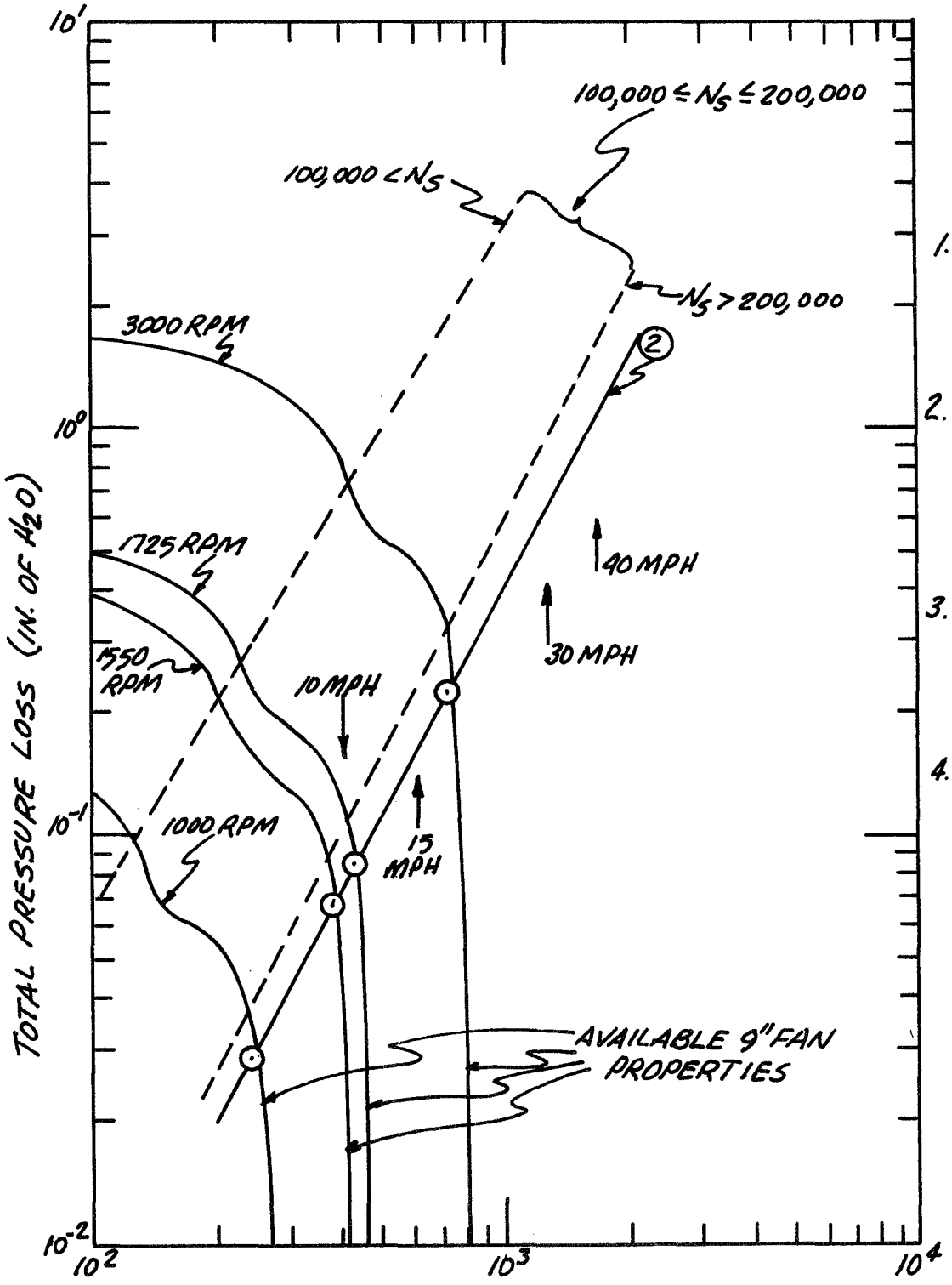

KEY

1. BOUNDARIES FOR ACCEPTABLE N_S ---- ($100,000 \leq N_S \leq 200,000$)
2. TORRINGTON FAN PROPERTIES
   9" DIAMETER
   26 DEGREE PITCH
   4 BLADES
3. FLOW CHAMBER REQUIREMENTS: CURVE ② FROM FIGURE 3.1.4
4. OPERATING POINTS FOR FAN ⊙

FIGURE 3.1.7

familiar shape of aerodynamic wind tunnels which consist of expansion, contraction, and transition sections. The evaluation of pressure losses requires the addition to Equations 3.1.1.1 to 3.1.1.3 of:

Expandor

$$K_o = \left[\frac{\lambda}{8\tan(\alpha/2)} + 0.6\tan(\alpha/2)\right]\left[1 - \frac{D_1^4}{D_2^4}\right]\left[\frac{D_o}{D_1}\right]^4 \quad (3.1.1.8)$$

and:

Contraction

$$K_o = 0.32\,\lambda\,\frac{L_c}{D_o} \quad (3.1.1.9)$$

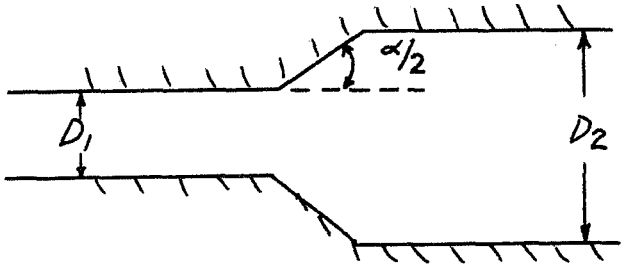

Several design variations were considered where trade-offs between leg length and leg diameter, fan capability and chamber loss characteristics, and construction complexity and flow properties were made. The final design is shown in Figure 3.1.8 and its associated pressure loss graph is shown in curve 3 of Figure 3.1.4. It can be observed that a reasonable reduction in the velocity dependence of the pressure drop has been

AMP FLOW CHAMBER DESIGN (HIGH SPEED)

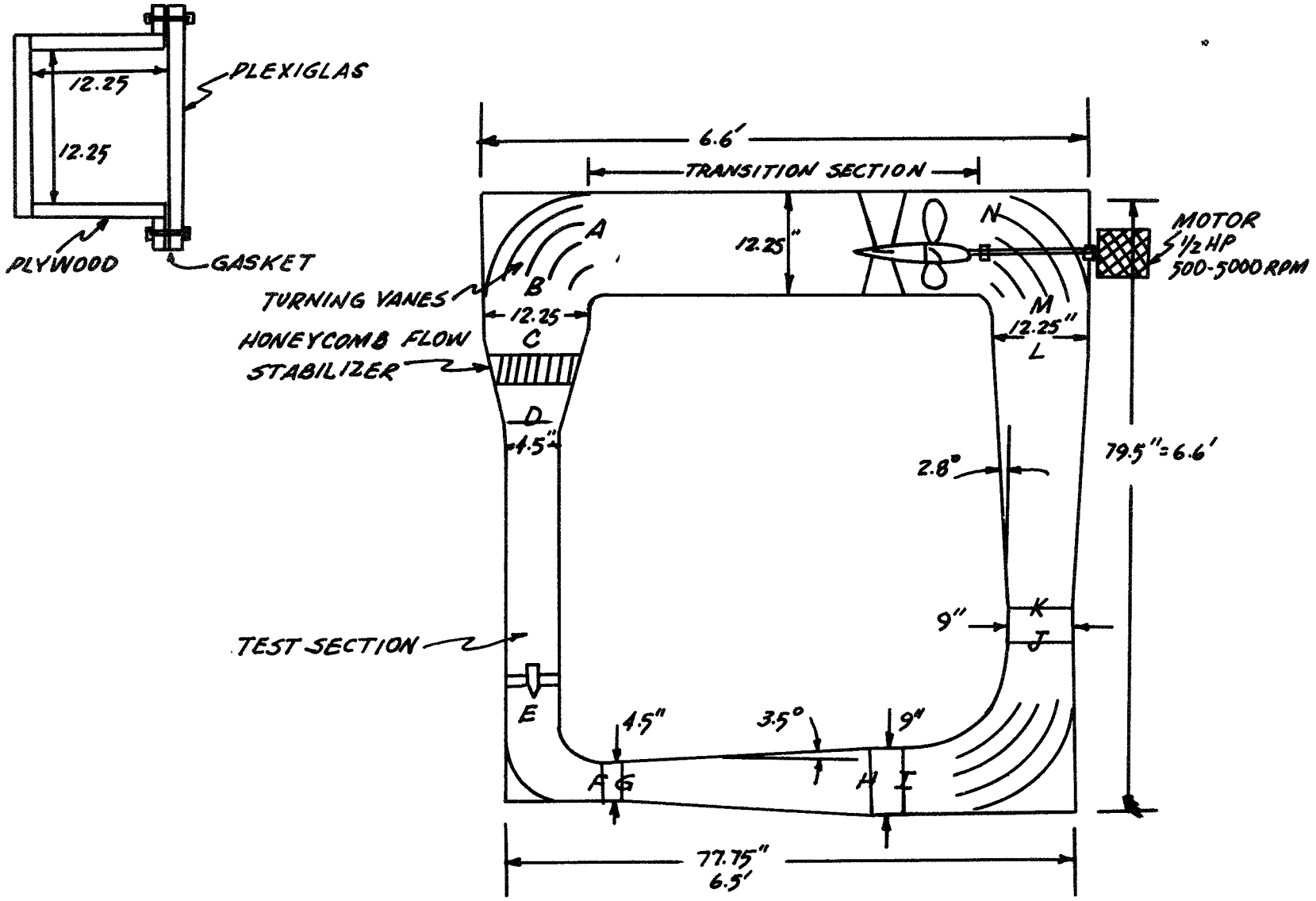

FIGURE 3.1.B

achieved. The impeller chosen is a 12 inch diameter, 16 degree pitch, 4 blade unit. Its operating characteristics (Figure 3.1.9) can be seen to be compatible with the chamber flow losses which has been superimposed in Figure 3.1.9 and labeled curve 3. While the system operating conditions are slightly outside the optimal operating regime for the impeller, the reduced motor speed (hence less noise) and the reduced wear on bearings are an acceptable trade-off. Emphasis has been placed on the latter two quantities since it was recognized early in the program that meeting the test schedule would permit very little down time on the test apparatus. The decrease in the operating effiency of the impeller can be readily overcome by using the motor at slightly higher speeds to achieve the desired flow speeds.

The final dimensions for the chamber were selected using not only the above mentioned criteria but attention was also paid to avoiding flow separation from the expansion section walls and to minimizing pressure losses in the contraction section. Past efforts in wind tunnel design have shown that at high speeds the expansion section angle (defined in Figure 3.1.10) should not exceed seven degrees if the possibility of flow separation is to be avoided.

COMPARISON OF AVAILABLE 12" FAN CAPABILITY TO OPTIMUM CAPABILITY REQUIRED FOR AMP FLOW CHAMBER

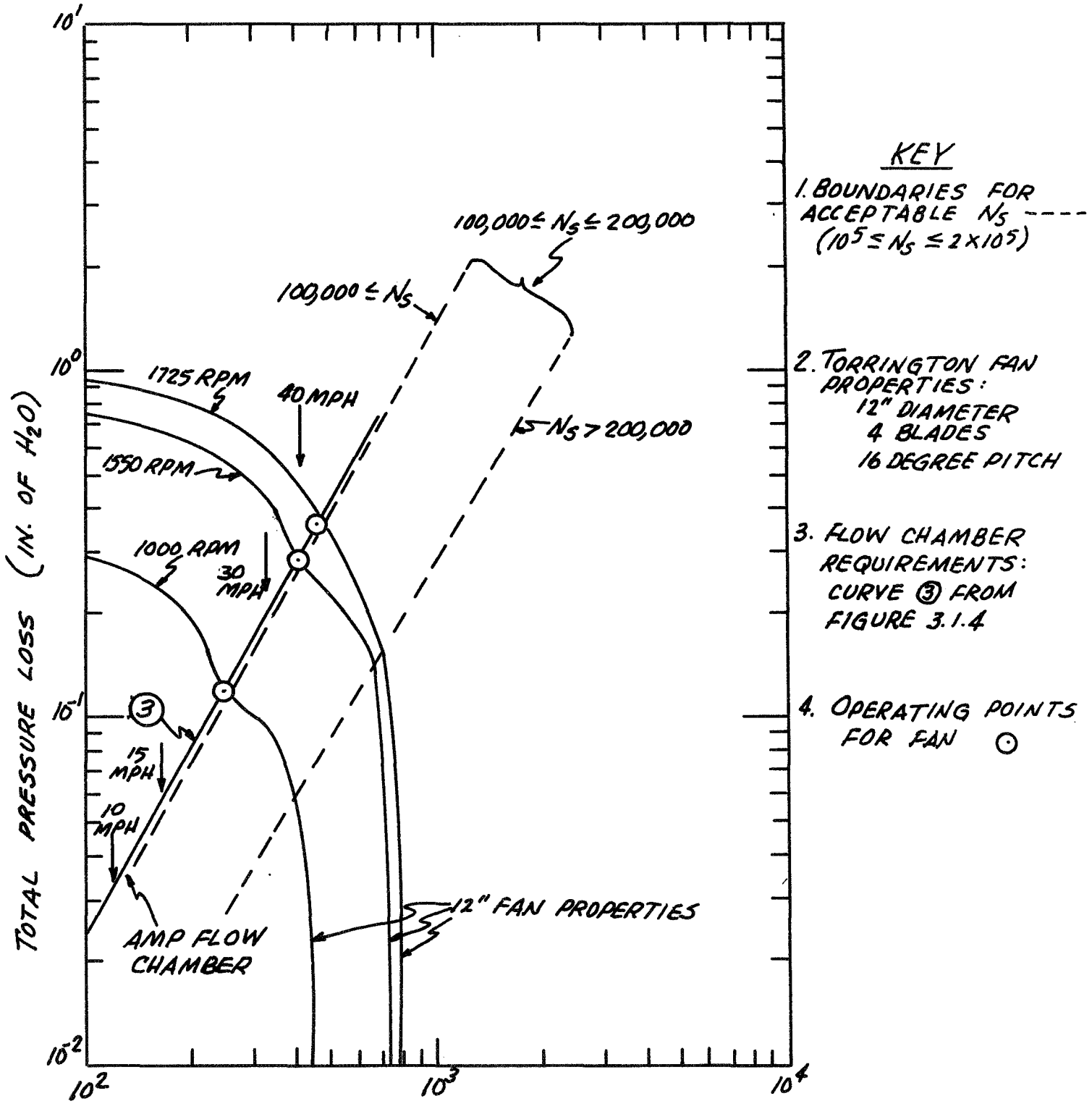

FIGURE 3.1.9

DEFINITION OF EXPANSION AND CONTRACTION ANGLES

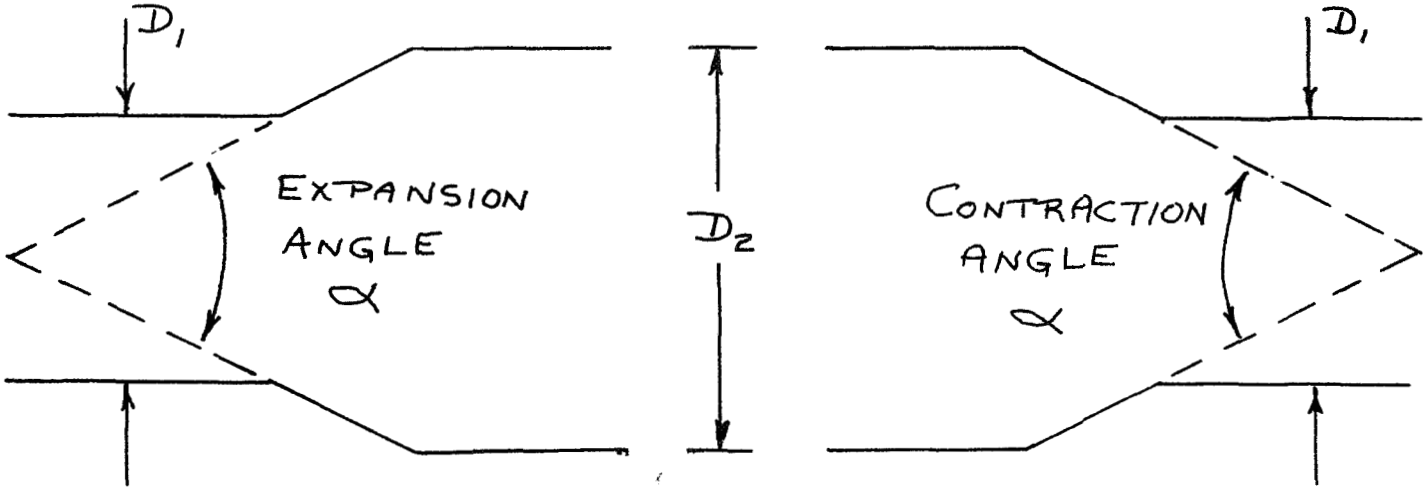

FIGURE 3.1.10

To maintain a space conserving design, it was decided that two of the flow chamber legs would be used to achieve expansion from the 4.5 inch diameter of the test section to the 12.25 inch diameter of the fan section. The resulting angles and leg dimensions are shown in Figure 3.1.8. In a similar manner, past experience was used to establish the dimensions for the contraction section. It is well established that at high speeds the losses encountered in a contractor are due only to friction and hence one desires a short contractor length. In opposition, the loss at low speeds are increased as the section's angle increases; thus dictating a long section

length. Clearly an analytical compromise was required and a section angle of 35^{o} (see Figure 3.1.10) was chosen; subject to change if empirical data indicated the tunnel was operating far off its design point. The contractor section length in going from 12.25 inches to 4.5 inches is then 12.3 inches.

The first unit to be built was intended to serve not only as a testing unit but also as a validation from which flow and structural modifications could be empirically derived. In order to facilitate the latter function, one side of the flow chamber was made of transparent plexiglass and screw mounted in eleven sections. This approach allowed not only for viewing of internal events but also for ready addition of new internal structures. The additions to the flow chamber once its configuration was selected (Figure 3.1.8) included: (1) turning vanes just prior to the test section; (2) inlet and outlet flow structure on the fan; (3) honeycomb structure after the vanes; and (4) structural weight and rigidizers near the fan assembly.

Turning vanes were factored into the original design of the chamber to minimize the pressure losses which occur as the flow turns the relative acute corners. If turning vanes were not used, the geometries needed to minimize such losses were anticipated to require turning radii which were imcompatible with the available laboratory space. The relationship between the vane hood length and its radius is $C_s = 2\pi\ r/N_s$ where N_s is the number

of vanes. Using $N_s = 4$, each vane will have a 90^o arc length (Figure 3.1.8). The vane as installed are shown in Section 4.2.2.

The fan assembly includes a structure before and after the impeller station. In the early design phases of the chamber, there was some concern over the possible occurrence of turbulence off the tips of the impeller. Such an occurrence would not only present an unstable flow to the membrane model but also introduce pressure losses which would worsen the chamber operating condition as given in Figure 3.1.9. Any significant perturbation would lead to a highly inefficient chamber and possibly a chamber re-design. To minimize this possibility, the internal volume of the chamber's transition section (see Figure 3.1.8) was configured to present a decreasing area as the flow approached the impeller and a gradually increasing area as the flow left the impeller. The analysis for the shaping was strictly geometric in nature and used as boundary conditions the transition section length, its 12.25 inch square cross-section, and the impeller position. The shaping permits a smooth flow to and from the impeller area and removes the square cross-sectional shape of the chamber which might impose unstable conditions.

The need for a flow straightener was determined empirically rather than analytically. Smoke tests to observe the chamber flow around the model clearly indicated the presence of unstable flow. Several honeycomb structures were readily installed and tested in the

position shown in Figure 3.1.8. Since an empirical approach was so easy to implement, no analyses were done and various structures were tried until a visually stable flow was obtained. The details and pictures of the selected structure are given in Sections 4.2.2 and 4.3.1.

The final phenomena which affected the configuration of the high velocity flow chamber was the occurrence of excessive heating and vibration in the impeller shaft area. A vibrational analysis was performed and led to the addition of rigidizing structure to alter the chamber's resonant frequency. The chamber's construction of plywood and plexiglass with demountable sections greatly facilitated the addition of the required structures. The analysis which led to the structure is given in the following subsection.

3.1.1.2 Vibration Analysis

The purpose of the analysis was to determine the cause of the significant vibrations occuring in the flow chamber fan system and to identify the corrective measures required to eliminate the vibrations. The main areas assessed were the shaft alignment in the bearings, the shaft critical frequency, and the support structure resonance. The maximum operating fan speed is 5000 rpm or an equivalent of 83.3 cps. The shaft and support structure resonant frequencies should be far removed from the fan operating speed. The following analysis assesses fan system as defined in Figure 3.1.11 for the above possible causes of vibration.

FLOW CHAMBER FAN SYSTEM

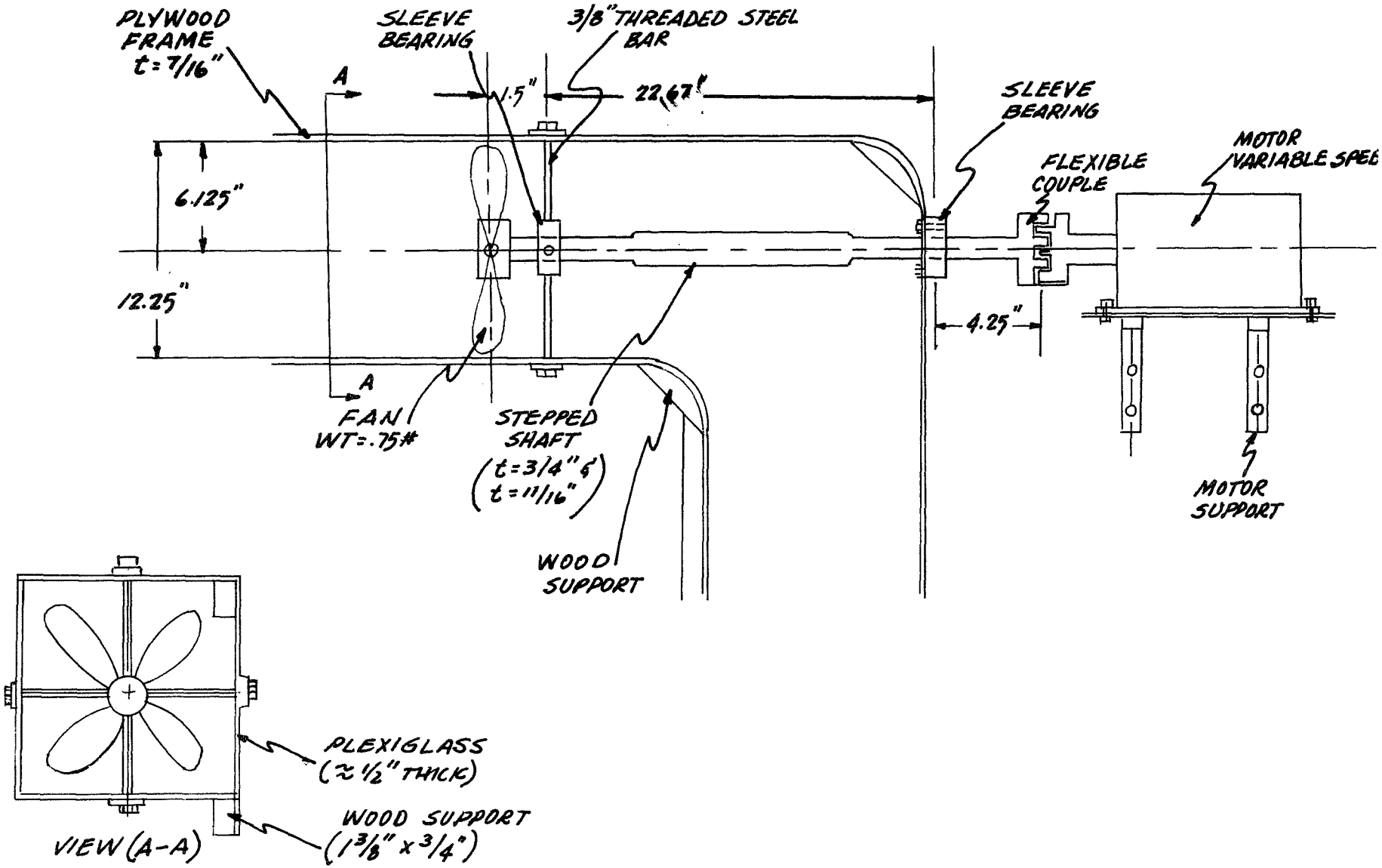

FIGURE 3.1.11

To determine the shaft critical frequency, the equation of motion $M\ddot{x} + Kx = 0$ was solved for the two shaft sections as depicted in Figure 3.1.12. The equation of motion after the introduction of the oscillation frequency $W = \sqrt{k/m}$ yields the expression:

$$-K^{-1}MX + \frac{1}{\omega^2}X = 0 \qquad (3.1.10)$$

which can be solved by the method of determinants for the two shaft sections (See Appendix B). The final equations to be enumerated are:

$$\frac{1}{\omega^2} = \frac{B \pm \sqrt{B^2 - 4C}}{2} \qquad (3.1.11)$$

where $B = a_{11}M_1 + a_{22}M_2$

$C = M_1 M_2 (a_{11}a_{22} - a_{12}a_{21})$

and $y_1 = a_{22}P_1 = \frac{b^3}{48EI}P_1$

$y_2 = a_{22}P_2 = \left[\frac{1}{3}\left(\frac{a^3}{EI} + \frac{a^2 b}{EI}\right)\right]P_2$

$y_{12} = a_{12}P_1 = -\frac{ab^2}{16EI}P_1$

$a_{12} = a_{21}$

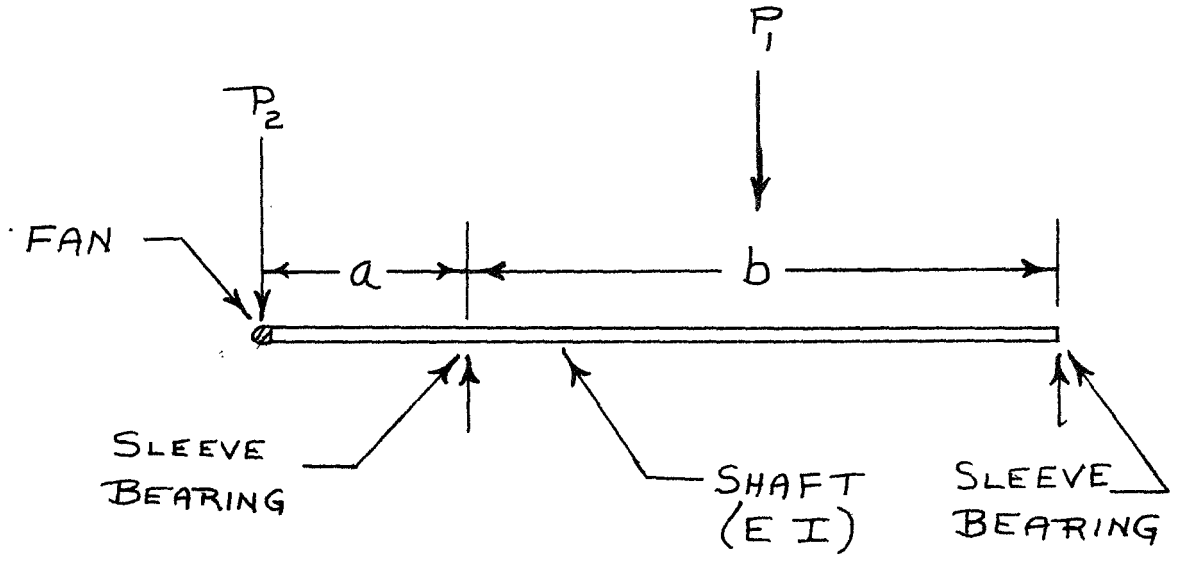

FIGURE 3.1.12

DYNAMIC MODEL OF FAN SHAFT

Definitions:

y_1 = Deflection of b due to load P_1

y_2 = Deflection of a due to load P_2

y_{12} = Deflection of b due to load P_2

y_{21} = Deflection of a due to load P_1

E = Young's modulus

I = Shaft Geometry Factor

The two solutions for the shaft frequency are found by inserting the shaft physical data from Table 3.1.1 into Equation 3.1.11. The values are 86 and 670 cps. Since the fan motor when driven at 5000 rpm is equivalent to 83.3 cps, one can expect severe vibrations in the fan system at the upper end of the motor's capability. The previous design analysis section indicated however that if the chamber operates close to its predicted conditions then the motor will never exceed 2500 rpm or 46.7 cps. Under this situation, there should be no significant vibrations caused by the primary frequency. This expectation is based on the rule-of-thumb from the Shock and Vibration Handbook which states the shaft critical frequency should be at least 20% removed from the operating speed. In the above cases, the shaft frequency is 100% removed. But with the fundamental frequency of the motor being a factor of two below the shaft resonant frequency, the motor's first harmonic could give rise to excessive vibrations. Stiffening of the shaft mount should reduce this possibility.

The next item to be investigated is the inner bearing support which consist of one vertical threaded bar mounted to plywood (See Figure 3.1.11). The expression for lateral frequency from Equation 3.1.10 is given by:

$$f_N = \frac{1}{2\pi}\sqrt{\frac{K_g}{W_T}} \qquad (3.1.12)$$

TABLE 3.1.1

IMPELLER AND SHAFT PHYSICAL PROPERTIES

ITEM IDENTIFICATION	PHYSICAL VALUE	ITEM IDENTIFICATION	PHYSICAL VALUE
Mass of Shaft (14 inch length)	4.5×10^{-3} lb-sec^2/in	Weight of Shaft (14 inch length)	1.74 lb.
Mass of Fan	1.95×10^{-3} lb-sec^2/in	Weight of Fan	0.75 lb.
Mass of Shaft (1.5 inch length)	0.48×10^{-3} lb-sec^2/in	Weight of Shaft (1.5 inch length)	0.187 lb.
Youngs Modulus E (steel)	3×10^7 psi	Shaft Lengths a b	 1.5 inch 14.0 inch

where W_T is the weight load of the fan, bearing, and shaft acting on the plywood surface. Taking the plywood surface on which the bearing is mounted to be 3" x 12.25" x 1/16" then the spring constant K is related to Young's Modulus by:

$$K = \frac{48EI}{L^3} \qquad (3.1.13)$$

$$I = 1/12\ bh^3 = 1/12\ (3.0)(7/16)^3; \quad b = 3.0 \text{ in.}$$

$$I = 2.07 \times 10^{-2} \text{ in}^4 \quad ; \quad h = 7/16 \text{ in.}$$

$$L = 12.25 \text{ in.} \quad ; \quad E = 2 \times 10^6 \text{ psi (wood)}$$

This yields from Equation 3.1.12, K = 1080 lb/in. which when substituted in Equation 3.1.12 gives

$$\underline{\underline{f_n = 57 \text{ cps}}}$$

for the bearing support lateral frequency. It is obvious that this critical frequency can present a problem when the fan motor is operating at its upper range of 2500 rpm. To correct this condition the plywood must be stiffened in the area of the threaded bar connections. The recommended solution is a channel section, as shown in the following sketch, attached to the plywood at the threaded bar attachment area. The bearing support threaded bars are bolted to these channels.

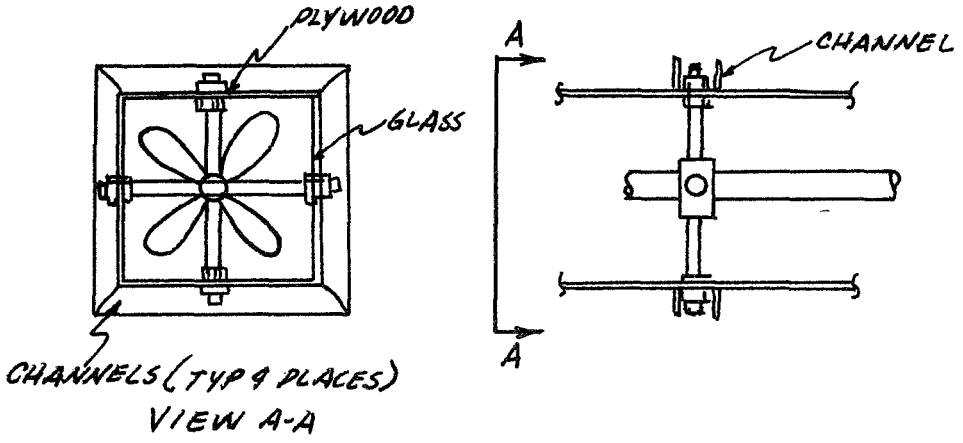

FIGURE 3.1.13

STRUCTURE MODIFICATION TO ALTER RESONANT FREQUENCY

In installing the channel stiffeners, the following criteria were obeyed:

1. Each channel was attached to the plywood or plexiglass structure;

2. they were also to be attached to one another forming a box structure;

3. the threaded bar was mounted with a nut on both the plywood (inner) and the channel (outer) side, enabling each bar to act in both tension and compression;

4. the minimum channel dimensions to increase the frequency of the support structure to greater than 150 cps was set as follows:

Material Aluminum

$I_{total} > 0.04\ in^2$ (Plywood & Channel)

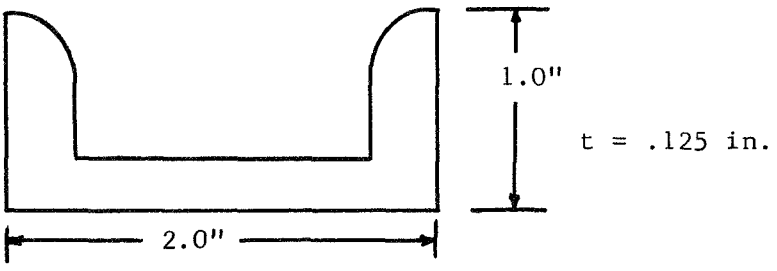

5. the channel box section was also utilized in the area of the additional inner bearing rod support location.

The final items examined as a possible source of vibration were the shaft bearings. It was determined after visual inspection that the original sleeve bearings were unacceptable because of the critical alignment requirements. The present fan system utilizes two (2) sleeve bearings. A small misalignment of the shaft through the bearings could cause a moment at the bearings and during fan operation severe vibrations could occur. It was decided to install self-aligned bearings and eliminate the problem.

The incorporation of the stiffener channels and the self-aligned bearings reduced the vibration levels to acceptable levels and virtually eliminated the shaft heating problem. As mentioned at the beginning of the analysis section, the resulting design was sufficiently conservative to permit five months of steady operation on the three chambers with no time lost for maintenance.

3.1.2 Experiment Test Parameter Analysis

A qualitative theoretical study followed by a dimensional analysis was performed to facilitate and systemize the experiment. By dimensional analysis it is found that the minimum pressure drop required to prevent

penetration can be described by a relations of the form:

$$\frac{g_c \Delta P}{\rho V_\infty} = f\left(\frac{\rho d_s V_\infty}{g_c \mu}, \frac{n_s m_s}{\rho}, \frac{D_h}{L_h}, \frac{d_s}{D_h} \right)$$

where consideration is limited to spores and fluid medium of fixed properties. The notation is given in Table 3.1.2. If penetration is insensitive to n_s and L_h seems plausible, and also to D_h as indicated in previous experiments (Reference 3.1), then a simpler relation of the form

$$\frac{g_c \Delta P}{\rho V_\infty^2} = f\left(\frac{\rho d_s V_\infty}{g_c \mu} \right)$$

is adequate.

3.1.2.1 Physical Considerations

Before proceeding with the analysis, a model of the problem must be formulated. This is illustrated in the figure below. The membrane is represented by a flat surface having a thickness L_h and a hole of diameter D_h. The membrane is exposed to an ambient current of steady uniform velocity $\vec{V_\infty}$ and a body force field with gravitational acceleration g. Orientation of the velocity and force fields relative to the membrane is arbitrary. Spherical spores of diameter d_s, mass m_s and number density n_s are carried by the ambient current and are assumed to have a velocity approximately equal to that of the current. A pressure drop Δ P

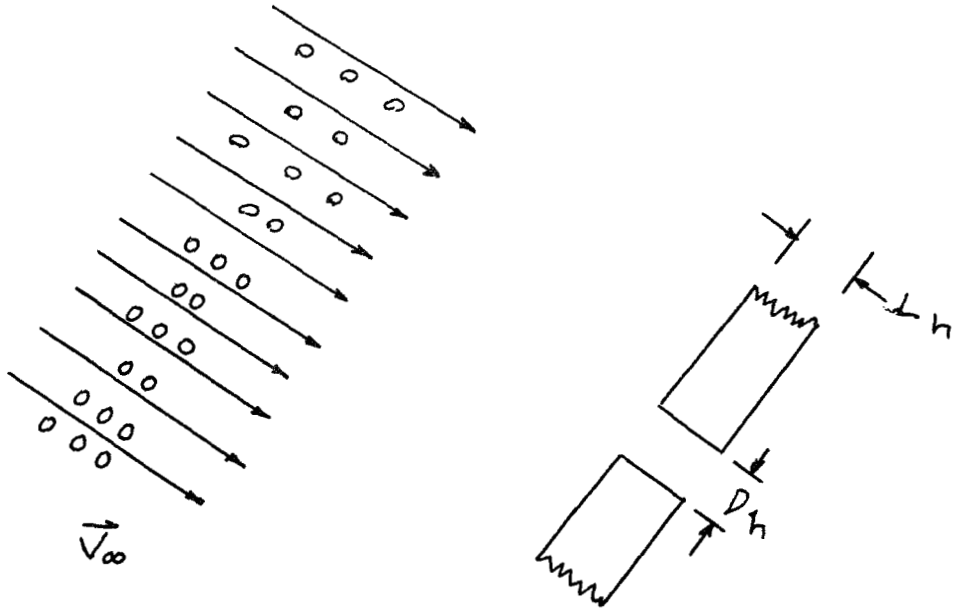

FIGURE 3.1.14 CHALLENGE GEOMETRY

is imposed across the membrane to prevent penetration of spores through the hole.

A point of interest is the nature of flow through the hole and about a spore. Are they continuum or free molecular flow? For this purpose the Knudsen number K

$$K = \frac{\text{mean free path}}{\text{characteristic length}}$$

is evaluated. Assuming the fluid to be air at standard temperature and pressure, the mean free path is approximately 6×10^{-6} cm. The smallest diameter holes to be considered are about 20 microns while the spore diameters are from 1 to 100 microns. Thus the Knudsen number for the hole and spores are respectively:

$$K_H = 3 \times 10^{-3} \ll \quad 1 \qquad 20 \text{ micron}$$

$$K_S = 6 \times 10^{-2} \ll 1 \qquad 1 \text{ micron}$$

$$K_S = 6 \times 10^{-4} \ll 1 \qquad 100 \text{ micron}$$

Since the calculated values are much less than 1, the flow is in the continuum regime. The following arguments, therefore, have been developed with this in mind.

Now to determine the parameters affecting hole penetration, look first at the motion of a single spore. Initially it has a velocity $\vec{V_\infty}$ with a component of momentum toward the membrane hole. This momentum component must be reversed in direction before the inside of the membrane is reached, if penetration is to be prevented. In this case, the velocity $\vec{V_\infty}$ defines the initial conditions while the spore momentum is related to its mass m_s and its motion. Body forces are characterized by the gravitational acceleration g. Drag is dependent upon spore size d_s, density ρ and viscosity μ of the fluid, and the fluid velocity relative to the spore. Because of drag the flow field in the membrane hole and existing jet is important. This flow is determined by the hole dimensions D_h and L_h, the fluid properties ρ and μ, the pressure drop Δ P across the hole, the gravity field g, and the ambient current velocity $\vec{V_\infty}$. Summarizing the above, it is expected that the following parameters will influence penetration:

$$\vec{V_\infty}, m_s, g, d_s, \rho, \mu, D_h, L_h, \Delta P$$

Another possibly important factor is wall roughness within the hole. This may affect penetration either indirectly by altering the flow field, or by direct interaction between spore and roughness elements. Based on the range of hole configurations under consideration and pressure drops up to about 5 inches of water, as investigated in past experiments (Reference 3.1), flow through the hole will always be laminar and therefore, unaffected by roughness. By direct interaction with roughness elements the inward movement, as well as the outward movement, of spore should be somewhat retarded. The tendency thus appears to be a minor one of collecting spores in the hole, but not of enhancing their ability to penetrate. Assuming smooth holes will be investigated, a roughness parameter is not included here. This should lead to conservative, if not accurate, results for the Δ P required to prevent penetration regardless of roughness. In the event that holes being investigated are not smooth, an additional parameter such as roughness height may be necessary.

Also affecting penetration is the alignment of the membrane relative to the gravity and ambient flow fields. This is indicated above by the vectorial nature of $\vec{g}$ and $\vec{V_\infty}$. The most serious threat of penetration, however, occurs when both gravity and velocity are directed towards the hole and along its axis. Therefore, it is suggested that the experiment be so aligned and only the magnitudes of velocity V_∞ and gravitational acceleration g need be included in the analysis.

Up to this point, discussion has been limited to a single spore in a fluid flow field. In reality there are many such spores as determined by the number density n_s. For a sufficiently large number of spores, penetration may be aided by diffusion. In such cases they diffusion coefficient $\mathcal{D}$ and the number density n_s enter into the analysis. Besides it relationship to diffusion, n_s is a further indication of the challenge to sterility, since penetration should be more probable for larger values of n_s.

The terms n_s and $\mathcal{D}$ are now added to the above list of parameters. In addition, because Newton's second law is involved in the physical phenomena, the gravitational constant g_c should be included. The complete list of all parameters believed to influence penetration is given in Table 3.1.2. Also given are the dimensions of each term with F, M, L and T representing force, mass, length and time respectively.

3.1.2.2 Dimensional Analysis

By dimensional analysis the above list of terms has been cast into an equivalent set of dimensionless groups. This is according to the Buckingham pi theorem (see Reference 3.2). The number of such groups necessary to completely describe the system is fewer than the number of dimensional parameters. Consequently a relatively simple, but complete, empirical relationship can be obtained with a minimum number of experimental measurements. By rearrangement of terms, infinitely many set of non-

TABLE 3.1.2

PHYSICAL PARAMETERS GOVERNING MICROBIAL PENETRATION

Parameter	Description	Dimensions
ΔP	pressure drop across membrane	(FL^{-2})
V_∞	ambient velocity of fluid approaching membrane	(LT^{-1})
n_s	spore population density	(L^{-3})
m_s	spore mass	(M)
d_s	spore diameter	(L)
$\mathscr{D}$	diffusion coefficient	(L^2T^{-1})
D_h	hole diameter	(L)
L_h	membrane thickness	(L)
ρ	fluid density	(ML^{-3})
μ	fluid viscosity	(FTL^{-2})
g	acceleration of gravity	(LT^{-2})
g_c	gravitational constant	$(MLF^{-1}T^{-2})$

dimensional groups can be obtained. Any such set is correct if it contains the proper number of groups and involves all of the parameters from the original dimensional list. In the present case, to facilitate experimentation, the dimensionless groups have been arranged such that parameters which are to be varied over the widest range (such as V_∞ and Δ P) appear in the fewest number of groups. At the same time other groups have been arranged to contain only terms which will not be varied in the proposed experiments. Thus, the following complete list of eight non-dimensional terms is obtained:

$$\pi_1 = \frac{g_c \Delta P}{\rho V_\infty^2} \qquad \pi_2 = \frac{\rho d_s V_\infty}{g_c \mu}$$

$$\pi_3 = \frac{n_s m_s}{\rho} \qquad \pi_4 = \frac{D_h}{L_h}$$

$$\pi_5 = \frac{d_s}{D_h} \qquad \pi_6 = \frac{g_c \mu}{\rho \sigma}$$

$$\pi_7 = \frac{m_s}{\rho d_s^3} \qquad \pi_8 = \frac{m_s^2 g}{\mu^2 d_s^3 g_c^2}$$

The above results may be written in functional form as:

$$\frac{g_c \Delta P}{\rho V_\infty^2} = f\left(\frac{\rho d_s V_\infty}{g_c \mu}, \frac{n_s m_s}{\rho}, \frac{D_h}{L_h}, \frac{d_s}{D_h}, \frac{g_c \mu}{\rho \mathcal{D}}, \frac{m_s}{\rho d_s^3}, \frac{m_s^2 g}{\mu^2 d_s^3 g_c^2}\right) \quad (3.1.13)$$

where ΔP is the minimum pressure required to prevent penetration and the form of f is to be obtained by experiment. Since the proposed experiments will be conducted with air at standard temperature and pressure, and with spores of fixed properties, all parameters in the last three groups are constant. There is also suspicion that penetration is insensitive to variations of n_s over its range of typical values. This might be true if n_s is small enough that diffusion is not a factor, but still large enough that variations in n_s do not determine if penetrations occur, only how many occur in a given time period. It must be emphasized that the above remarks are only speculation. They should be verified experimentally. This can be accomplished with a minimal effort by investigating $\frac{g_c \Delta P}{\rho V_\infty^2}$ at a few values of the terms $n_s m_s/\rho$, d_s/D_h and D_h/L_h, including especially the limits of their ranges. If it is shown that effects of changing n_s and L are weak then the terms $n_s m_s/\rho$ and D_h/L_h may be eliminated also from the empirical function f and thus a relationship of the following form will be sought:

$$\frac{g_c \Delta P}{\rho V_\infty^2} = f\left(\frac{\rho d_s V_\infty}{g_c \mu}, \frac{D_h}{L_h}, \frac{d_s}{D_h}\right) \quad (3.1.14)$$

In previous experiments with quiescent air (Reference 3.1) it was indicated that penetration is not sensitive to the hole dimensions D_h and L_h. This is surprising in the case of D_h, but perhaps plausible with respect to L_h. As L_h alone increases, the outward flow velocity in the hole is reduced, thus tending to make penetration easier. However, because L_h is greater, spores must move against this lower velocity flow for a greater distance. As a result the net effect of variations in L_h may be slight. In case of the possible situation that penetration is also insensitive to D_h, then the experiment can be conducted to determine a very simple relationship of the form:

$$\frac{g_c \Delta P}{\rho V_\infty^2} = f\left(\frac{\rho d_s V_\infty}{g_c \mu}\right) \qquad (3.1.15)$$

With ρ, g_c, and μ constant values, it becomes apparent that the collection of data for Δ P versus V_∞ (for a given spore population) with hole size as a parameter should suffice to test the adequacy of Equations 3.1.14 and 3.1.15. In the event neither equation adequately describes the experimental data, the effects of a varying microbial diameter, number density, and membrane will be investigated in their stated order. Any dependence on hole diameter will most probably manifest itself through a variation in spore particle size population.

3.1.2.3 Minimum Pressure Requirements

The analysis includes approximate calculation of pressures required to maintain sterility together with experiment design specifying parameters to be measured and estimating parameter values near which penetration can first be expected to occur. (Reference 3.6)

The analysis is intended to approximate the pressure required to prevent penetration. Application is made to the configuration shown in Figure 3.1.15. A spore of diameter, d_s, moves with velocity V_s through a membrane hole which has an outward flow velocity V_h.

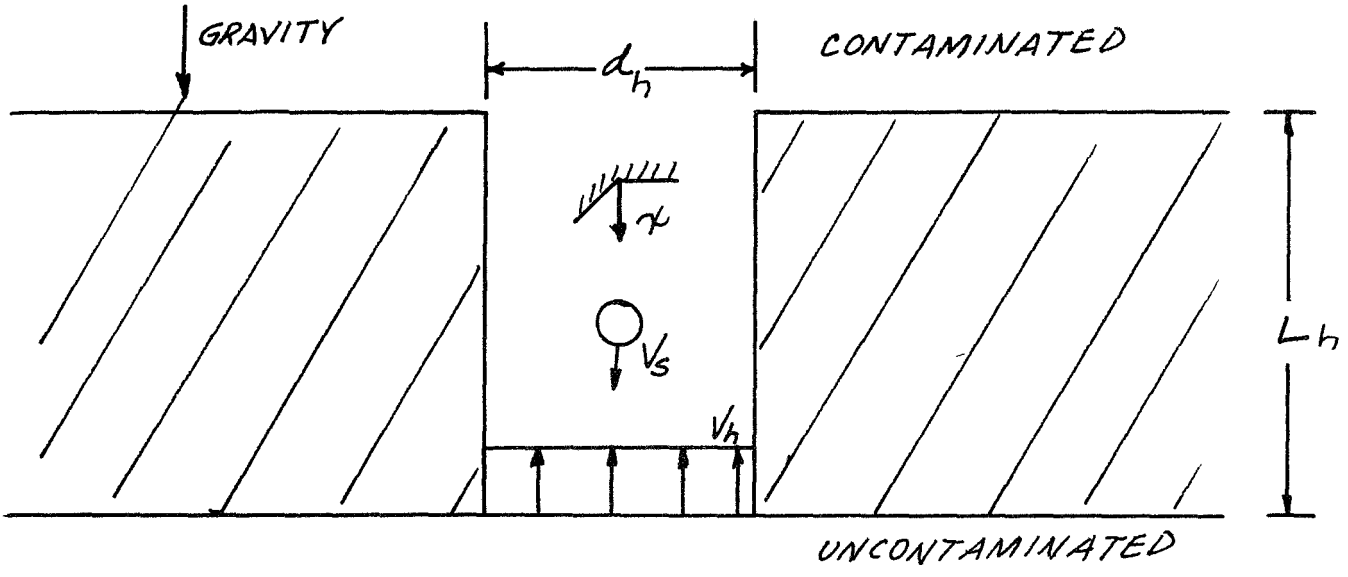

FIGURE 3.1.15

VISUALIZATION OF SPORE MOTION

A force balance give

$$\frac{1}{g_c}\frac{dV}{dt} = \frac{F_g}{m_s} + \frac{F_o}{m_s}$$

$$\frac{V}{g_c}\frac{dV}{dx} = \frac{g}{g_c} - \frac{3\pi\mu d_s}{m_s}(V_h + V)$$

where Stokes' law has been assumed for the drag. Letting

$$U = \frac{V}{\sqrt{g d_s}}, \quad X = \frac{x}{d_s}, \quad \alpha = \frac{3\pi\mu d_s^2 g_c}{m_s\sqrt{g d_s}}$$

the force balance takes the form

$$U\frac{du}{dx} = (1 - \alpha V_h) - \alpha U \qquad (3.1.16)$$

The spore velocity at the hole entrance (X = 0) is specified as U_i, i.e.,

$$U(0) = U_i \qquad (3.1.17)$$

Specific values of U_i are difficult to determine and in some cases will be conservatively assumed to equal the free stream velocity. It must be noted from Equation (3.1.16) that unless

$$(1 - \alpha V_h) < 0 \qquad (3.1.18)$$

a spore with initial inward velocity cannot decelerate to zero velocity and thus the above requirement is a necessary condition for sterility to be maintained. In other terms this condition can be written as

$$V_h > V_{set} \tag{3.1.19}$$

where V_{set} is the spore settling velocity. It will be assumed here that penetration occurs or does not occur depending upon whether the spore velocity is greater or less than zero at the hole exit plane (X = L), i.e.

$$V(L) = 0 \tag{3.1.20}$$

Solutions of Equation (3.1.16) satisfying the conditions from Equations (3.1.17) and (3.1.18) lead to the Equation

$$(1-\alpha V_h)\left\{\log|1-\alpha V_h| - \log|1-\alpha V_h - \alpha V_i|\right\} = \alpha V_i - \alpha^2\left(\frac{L_h}{d_s}\right)$$

This is an implicit relationship for the minimum velocity V_h required to maintain sterility in terms of the parameters of the problem. Assuming Poiseuille flow this velocity is related to the required pressure drop across the hole according to the relationship

$$\Delta P = \frac{32\mu V_h L_h}{d^2} \tag{3.1.21}$$

where μ is the fluid viscosity.

Values of ΔP calculated for various cases of interest are given in Table 3.1.3.

TABLE 3.1.3

Minimum Pressure Drop ΔP Required to Prevent Penetration in a Sea-Level and Gravitational Field

d_s (microns)	V_i (mph)	L (microns)	ΔP (in H_2O)
1	30	300	10^{-4}
1	30	800	10^{-4}
15	30	300	100
15	30	800	100
15	3	300	0.4
15	3	800	0.2

The above results are for d_s= 20 microns. Calculations for larger d_s give larger ΔP. For extremely large d_s however, the calculations are not necessarily applicable since assumptions such as Poiseuille flow may no longer be valid. The Reynolds number R_e for the case of d_s = 15 microns and V_i = 30 mph is 13. Stokes' law therefore still gives a reasonable order of magnitude estimate for the drag. Since it underestimates the drag it is a conservative approximation. For the other cases in Table 3.1.3, $R_e \lesssim 1$ and Stokes' law is quite accurate.

As the above calculations indicate, penetration of small spores is prevented by extremely small pressure differentials ΔP. Experiments might therefore be intended to verify this result. Unfortunately, measurements of ΔP across the hole is impractical. It is more feasible to measure pressures in the free-stream and within the membrane. For cases of small outward flow velocities, pressures in the hole as well as that within the membrane (P_m) should be very nearly equal to the ambient stagnation pressure. The stagnation pressure is in turn related to the free-stream velocity (V_∞) and static pressure (P_∞) by the following equation from inviscid theory:

$$P_o = P_\infty + \frac{\rho g}{g_c}\left[\frac{V_\infty^2}{2g} + Z_\infty\right] \qquad (3.1.22)$$

as illustrated in Figure 3.1.16. It follows that cases of $\Delta P \cong 0$ correspond to $P_m \cong P_o$ or approximately

$$P_m - P_\infty = \frac{\rho g}{g_c}\left[\frac{V_\infty^2}{2g} + Z_\infty\right] \qquad (3.1.23)$$

Thus it is suggested that this relationship for membrane pressure in terms of measurable free-stream properties be used as a baseline near which experimental tests should be conducted. Values of Z_∞ in the test facility will cause negligible pressure differences and so it is sufficient to consider

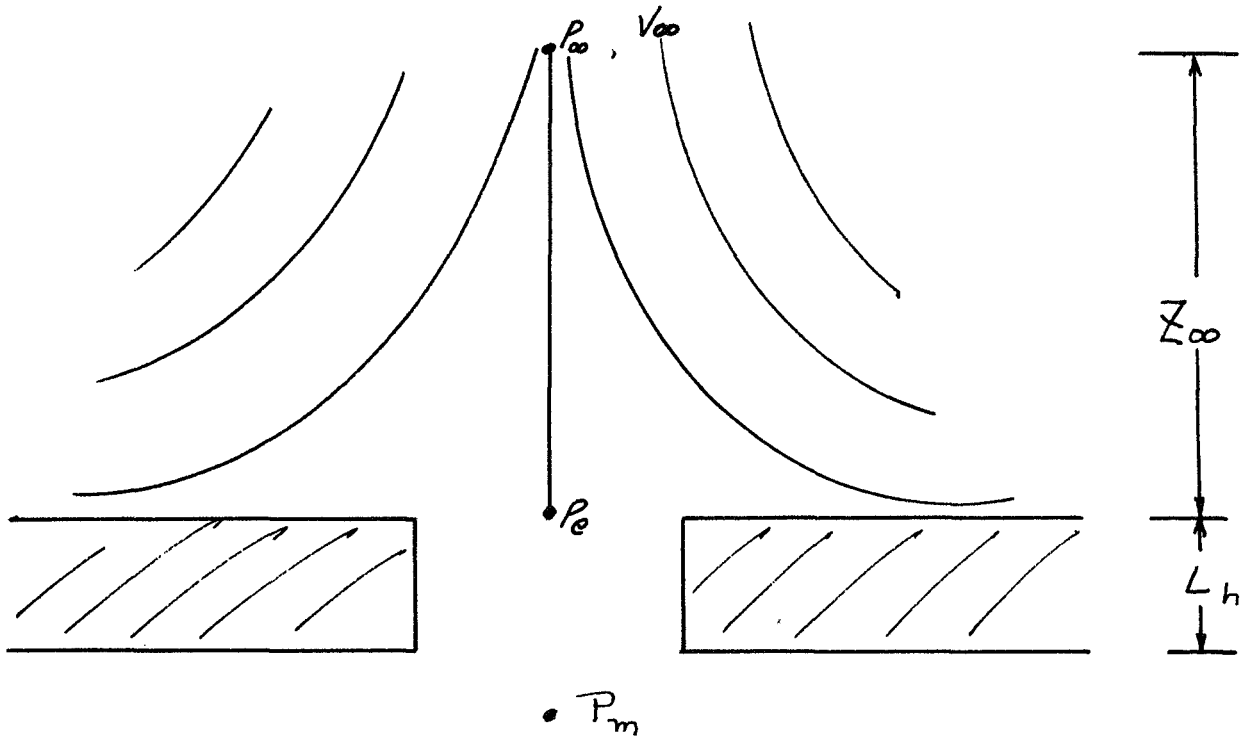

FIGURE 3.1.16

RELATIONSHIP OF P_∞ TO P_m

$$P_m - P_\infty = \frac{\rho V_\infty^2}{2g_c} \qquad (3.1.24)$$

This pressure difference is illustrated in Figure 3.1.17 as a function of the free-stream velocity.

The following conclusions now can be made based upon the above analysis:

EFFECT OF IMPINGING AIR STREAM VELOCITY ON MICROBIAL PENETRATION THROUGH MICROSCOPIC HOLES IN MEMBRANES - THEORETICAL

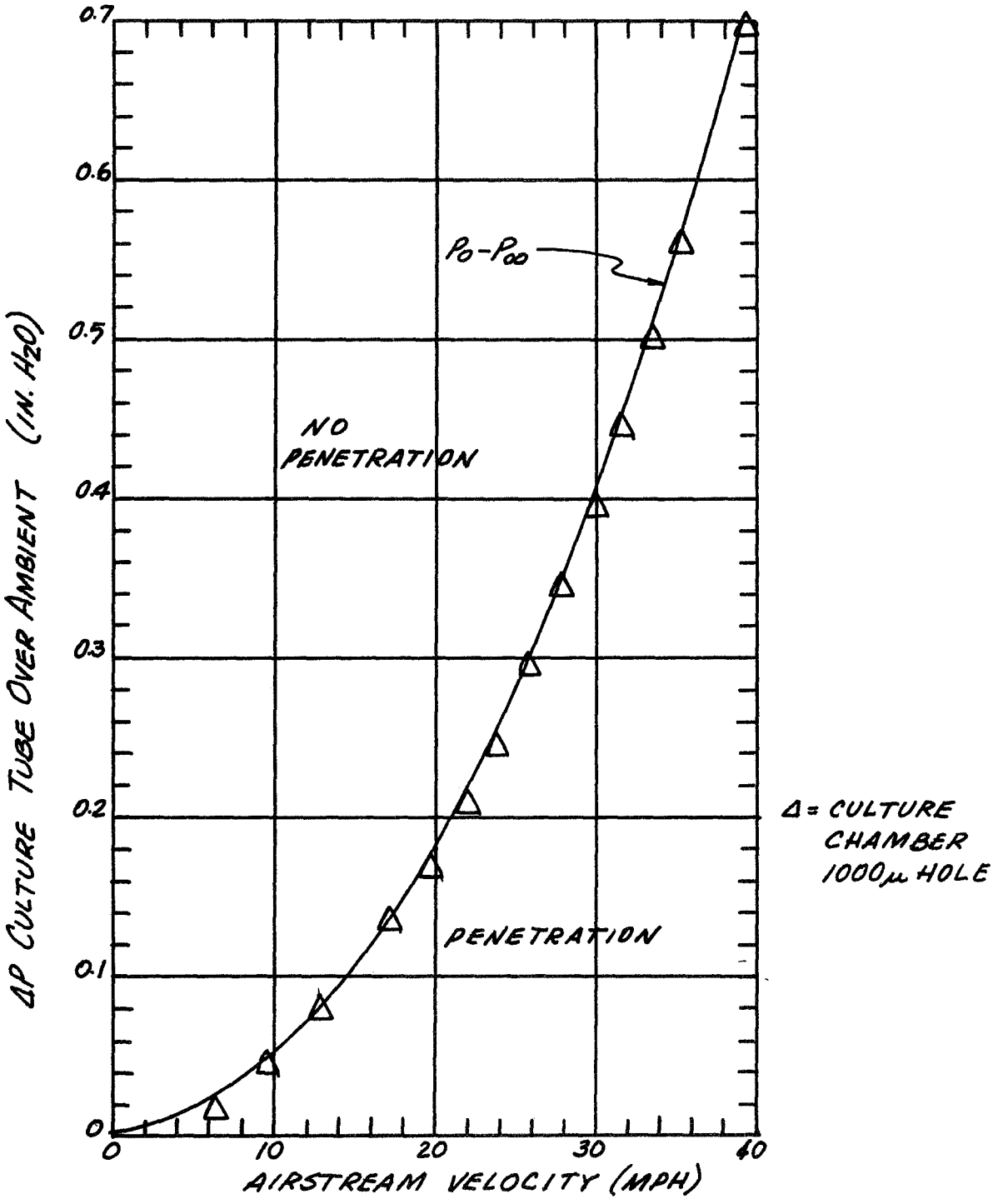

FIGURE 3.1.17

(1) For small spores of the order of 1 micron in diameter calculations indicate that penetration is prevented if outward gas flow in the hole is equal to or greater than the spore settling velocity. It then follows for small spores in the hole configurations of interest and ambient flows up to 100 mph that the minimum pressure required within the membrane must be approximately equal to and slightly greater than stagnation pressure of the ambient flow.

(2) For small spores it is seen that ΔP is insensitive to hole dimensions d_h and L_h. This supports the results of earlier quiescent tests, where such a behavior was observed.

(3) For 15 micron diameter spores it is estimated that $\Delta P \leq 1/2$ in H_2O above ambient is required to prevent penetration under quiescent conditions.

(4) The stagnation pressure curve is therefore suggested as a baseline for membrane pressure near which experimental tests should be conducted. This baseline pressure as a function of ambient velocity is displayed in Figure 3.1.17.

3.2 MICROBIAL MOTION ON FLOW FIELDS

3.2.1 Response to Turbulent Flow

The dimensional and pressure analysis studies reported in Section 3.1.2.2 and 3.1.2.3 are summaries of the many variables important to the AMP

program. However, while it is helpful to have such an analyses to guide in organizing the test program, it is still difficult to visualize in detail the problem of the drift motion of particles ranging from 1 to 100 microns in size. It is the objective of this analysis to examine their motion in somewhat greater detail with emphasis on turbulent flow.

First let us examine some motion histories, assuming that we can set such a small object in motion in still air. We imagine that we can shoot an individual spore at an initial velocity in a horizontal direction, and then see how it decelerates. The derivation of the spores motion is given in detail in Appendix A and follows the same procedure used in Section 3.1.1 for the flow chamber design. In Section 3.1.1, it will be remembered that the equations of motion expressed the spore motion relative to fixed spatial axes. This was necessary to establish the minimal lengths for the flow chamber legs. The primary interest in the present analysis is to investigate the dynamic response of a spore relative to the flow acting on it. For this situation, the equation of motion are:

$$V_s = -V_\infty e^{t/\tau} \tag{3.2.1}$$

and

$$S_s = V_\infty \tau \left(1 - e^{t/\tau}\right) \tag{3.2.2}$$

where V_s is the spore velocity relative to the flow and S_s is the spore displacement relative to its original position. Equation (3.2.2) contains a very curious result: the particle never moves beyond the distance it would traverse in a time τ if it maintained its initial velocity. To represent this result graphically, we plot the ratio $S/V_o\tau$ against t/τ. Figure 3.2.1 shows the results for the particle moving with respect to the fluid. This also shows the displacement of the particle from its original position in the moving fluid, but with the particle initially at rest and the fluid in motion. In this particular case of impulsive Stokesian motion it is impossible to cause a particle to move in the fluid beyond the distance $V_o\tau$.

SPORE MOTION RELATIVE TO FLOW

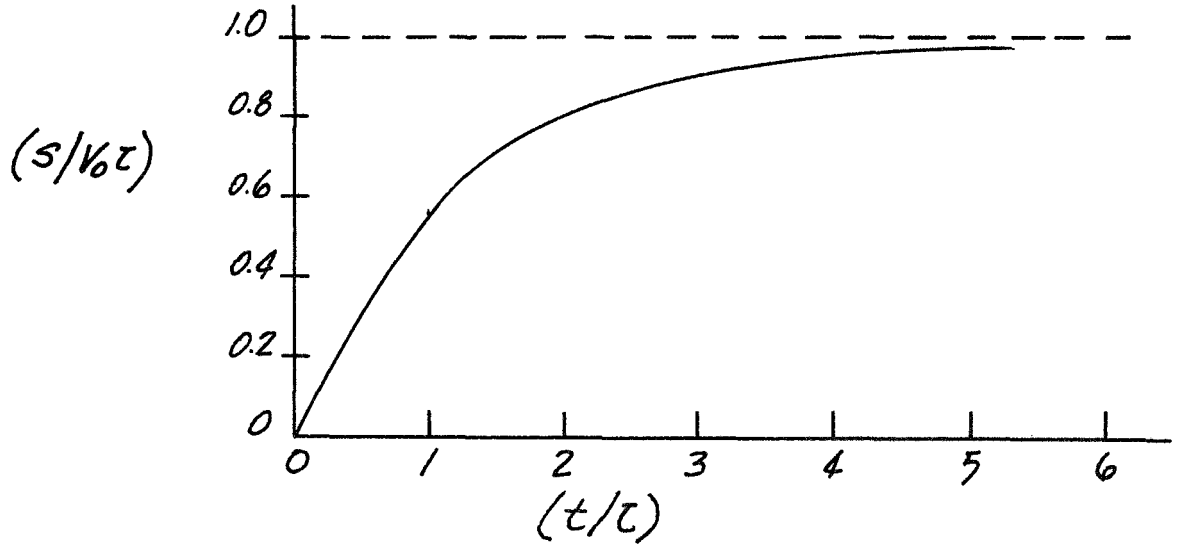

FIGURE 3.2.1

Let us see what effect a sharp turbulent fluctuation in the flow would have on the path of the particle. For simplicity, let us assume (1) that the droplet is initially moving with the fluid and (2) there is an instantaneous 10% increase in the velocity in its original direction. This corresponds to our impulsive velocity step. We see that the response of the particle is described by $V = (V'(t) - 1.1\ V_\infty)$, where again V is the velocity relative to the fluid, V' is the particle velocity in space, and $1.10\ V_\infty$ represents the fluid velocity after the instantaneous turbulent fluctuation. Now the only difference from the previous example is that at $t = 0$, $V' = 1.0\ V_\infty$ so that $V = 0.1\ V_\infty$ at $t = 0$, and the function relations become $V = (-0.1V)\ e^{-\alpha t}$, from which

$$V' = 1.1\,V_\infty + V = 1.1\,V_\infty - 0.1\,V_\infty e^{-\alpha t} \qquad (3.2.3)$$
$$= V_\infty + 0.1\,V_\infty\,(1 - e^{-\alpha t})$$

Similarly, the lag of the particle behind its original position in the fluid is

$$S = 0.1\,V_\infty\,\tau\,(1 - e^{-\alpha t}) \qquad (3.2.4)$$

The relative drift between the particle and the fluid thus cannot exceed 0.1 $V\tau$; for a 1 micron diameter spore and for V_∞ = 1790 cm/sec, this amount to 5.6 microns. Approximately 95% of this drift has been accomplished in about 9 microseconds. If we wish to have on the average only 5% of the droplets in the turbulent fluid element left behind (i.e., move out of the fluid element), and if we assume the element is a small spherical volume, it can be shown from geometric considerations that the diameter of this element must be approximately 25 times this lag distance, or about 140 microns (0.14 mm). Now, it is very difficult to associate a physical length with a turbulent fluid element. Hinze (Reference 3.3) gives for subsonic flow of velocity of the order of 100 m/sec an estimate of the "smallest" eddy size of about 1 mm. We see that we can expect the 1 micron droplets to follow the turbulent flow fluctuations with considerable exactness.

In the case of the 100 micron diameter spore particles, a close response to turbulent flow is not likely. If we again assume the worst case condition (as we did in Section 3.1.1) by taking the drag coefficient C_D as given by Stokes' law, we get the dependence of τ, the time constant, on the spore diameter going as the inverse square. Hence the relative drift in Equation (3.2.4) becomes 5.6 cm and the turbulent fluid element required for a 5% loss of particles becomes about 1.4 meters. The likelihood of encountering such elements of this size is extremely small and one can expect 100 micron particles to be somewhat insensitive to fluid turbulence.

It is apparent therefore that turbulence in the test section lag could lead to an unpredictable velocity spread in the spore particles impinging on the membrane. Since the control of spore size population is not planned, steady "laminar" flow over the four feet upstream of the membrane plane must be achieved. The direct dependence of the spore motion on the velocity perturbation dictates the close control of flow velocity to an accuracy compatible with the experiment requirements.

3.2.2 Penetration by Large Contaminants

In Section 3.1.2.2, a general analysis was made on the problem, and it was concluded that the experiments very probably could be adequately characterized by two parameters.

$$\pi_1 = \frac{g_c \Delta P}{\rho V_\infty^2} \qquad \text{and} \qquad \pi_2 = \frac{\rho d_s V_\infty}{g_c \mu}$$

Expressed in a more direct manner, one could expect that ΔP, the pressure increment required to maintain sterility would be given by

$$\Delta P = \frac{\rho V_\infty^2}{g_c} f\left(\frac{\rho d_s V_\infty}{g_c \mu}\right)$$

i.e., that it would be proportional to the free-stream dynamic pressure and to a function of the Reynolds number based on the spore diameter and

the properties of the air stream in which is is suspended $\left(\rho d_s V_\infty / g_c \mu\right)$.

On the basis that there is a 1 micron particle, it was concluded that the Reynolds number would always be less than unity.

In Section 3.1.2.3, some particular examples of particle motion were studied under this limitation. These preliminary analyses showed that for the nominal contaminant (a spore of 1 micron diameter) there was no possibility of contamination unless there was a flow of air from outside into the cavity, or unless the settling velocity of the spore was not counteracted by an efflux of air. If one considers the possibility of contamination by clumps consisting of thousands of individual spores, then the motion of such relatively massive particles cannot be described by the simple relations of Section 3.1.2.2. In fact, the simple analysis becomes the optimal boundary case and one can expect the experimental data to show a deviation from the results of Section 3.1.2.3. To enhance our understanding of penetration by large contaminants, it becomes necessary to re-examine the problem and produce quantitative predictions which will serve to limit the experimental tests to a minimum level.

For simplicity, we represent the conditions we wish to discuss as shown in the sketch. We have a cylindrical collector, with a thin membrane forming a flat surface normal to the test facility flow. A small orifice of known diameter is located in the center of this surface. The alignment

is vertical, so that we do not need to consider any gravitational drift of particles across the flow. The flow velocity is known; it is steady in time and uniform in magnitude at least over the collector surface. A uniform pressure can be maintained in the collector.

MEMBRANE HOLDER VISUALIZATION

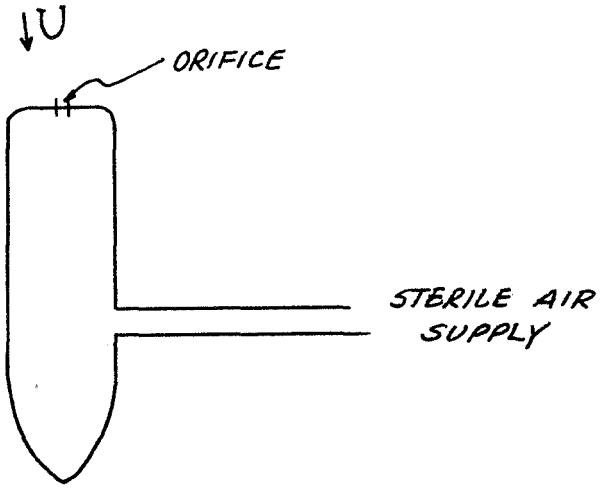

FIGURE 3.2.2

We look first at the problem of a 15 micron particle entrained in an air flow. The flow impinges on a flat surface with a perforation, and there is a pressure differential across the surface so that there is a flow through the orifice opposite to the external flow. Note that this is a much more specific problem than that stated in Section 3.1.2.2.

In the discussions of Section 3.1.2.3, we assumed that the particles arrived at the orifice possessing the free-stream velocity.

The situation with larger spores is more complicated than this. The flow is decelerated, the central part being essentially brought to rest by the normal surface, and turned so as to flow around the obstacle. In addition, at the orifice itself the flow from within the collector tube exits into this stagnation region.

Let us separate the analysis into two portions. First, we will describe the flow of the air up to and around the collector tube. This was completely ignored before. Next we will follow the motion of the entrained particles.

For the description of the flow, it is suggested that the collector tube be represented by a sphere generated by a doublet in a uniform flow. While this does not produce the flat surface that is present in the actual collector, it does permit the flow to escape around the body and flow downstream. If we try to utilize stagnation flow against an infinite flat plate, we cannot satisfy this condition, nor can we accommodate the essentially uniform flow velocity upstream. The source-sink doublet in a uniform potential flow defines a sphere. As a start, it is suggested that the doublet be chosen to give a sphere 0.75" in diameter, as more nearly representing the plane surface of the collector tube than a sphere with diameter equal to that of the tube.

The potential function for the doublet (sphere) in a uniform stream is

$$\phi = \frac{Ua^3}{2r^2} \cos\phi + V_r \cos\phi$$

where ϕ is the angle off the free stream flow direction and from which the velocity along the stream line to the stagnation point can be obtained.

For the second part of our problem, we allow a heavy particle to move along this decelerating streamline and approximate its deceleration by a step-by-step computation procedure. We neglect the direct effect of the pressure gradient on the volume of the particle and determine the drag on the particle due to its relative motion with respect to the decelerating air stream. The corrections to this potential flow due to the restraints of the tunnel walls can be ignored since we are not working at this level of certainty.

We note in passing that the measure of the flow path during the deceleration process is the radius of the sphere. This is extremely large in comparison to the penetration distance considered before (the skin thickness). Accordingly, we expect this step in refining the analysis to be quite significant.

With respect to the actual deceleration of the particle, one must test the growth of the Reynolds number as defined by

$$R_e = \frac{(v_f - v_p)ds}{\nu}$$

As long as $R_e \leq 1$, the drag will be given by Stokes' law; if $R_e \rightarrow 10$, the actual drag coefficient will be almost double that computed by Stokes' law. Thus for values of R_e greater than say 2 or 3, it will be necessary to use experimental drag data. The velocity of the contaminant particle was assumed to be equal to free stream velocity at a distance of 10 radii upstream, and the relative velocity between the particle and the decelerating flow along the stagnation stream line was calculated step-by-step. Initially this relative velocity is small, so that the resistance (and deceleration) is obtained from Stokes' law. As the particle nears the sphere the Reynolds number based on the particle size and the relative velocity becomes large enough to require the use of experimental drag coefficients. The particle velocity at the stagnation point on the sphere is taken to be a reasonable estimate of the velocity of the contaminant as it approaches the orifice exposed to the flow. No allowance is made for the flow of the jet of air outside of the pressurized culture tube. Also no correction was made for tunnel wall effects; i.e. the flow field was computed as if the test stream was infinite.

After the particle arrives at the orifice, its depth of penetration in a uniform efflux velocity is determined. If this penetration depth exceeds the skin thickness (taken to be 300 microns) the efflux velocity

will not maintain sterility. Since it is somewhat difficult to solve explicitly for the efflux velocity required to limit the penetration to the skin depth, penetration depth was found for a range of velocities, and the required velocity estimated from this series of results. For these computations, the deceleration for a given particle size was expressed as an exponential, thus

$$\frac{dV_p}{dt} = -\frac{DRAG}{MASS} = -aV^n$$

and the coefficient a and exponent n determined from experimental C_D data. It was found that such an expression served very well over the particle sizes investigated, and for the range of efflux velocities required. Since the depth of penetration is given at the time when the particle velocity v_p becomes zero, the relative velocity which determines the deceleration never drops below the efflux velocity. Thus there is no need to consider very large ranges of Reynolds number; this is what makes practical the use of simple exponential expressions.

Tables 3.2.1 and 3.2.2 give penetration depths for 15 and 20 micron particles as a function of efflux velocity. Note that the initial particle velocity, the end result of the computations of the velocity of the particle as it approaches the collector tube, is given as 10 mph for the 15 micron particle, and 14.8mph for the 20 micron particle. From

TABLE 3.2.1

PENETRATION DEPTHS AS A FUNCTION OF EFFLUX VELOCITY FOR 15 MICRON PARTICLES IN 30 MPH TEST FLOW, V_{P_o} = 10 MPH

V_e fps	ΔP Inches of Water	Depth of Penetration Microns
10	.023	816
20	.092	457
30	.206	308
40	.366	225
ΔP in inches of water $= \frac{\rho V^2}{2} \cdot \frac{12}{62.4}$		

TABLE 3.2.2

PENETRATION DEPTHS AS A FUNCTION OF EFFLUX VELOCITY FOR 20 MICRON PARTICLES IN 30 MPH TEST FLOW V_{P_o} = 14.8 MPH

V_e fps	ΔP Inches of Water	Depth of Penetration Microns
50	.57	549
60	.82	439
70	1.12	396
80	1.46	317
90	1.85	295
ΔP in inches of water $= \frac{\rho V^2}{2} \times \frac{12}{62.4}$		

Table 3.2.1 it is seen that an efflux velocity of 30 fps would limit the penetration of the 15 micron particle to 308 microns; the different approximations in the method do not justify any more accurate interpolation between the tabular values. From Table 3.2.2, an efflux velocity between 80 and 90 fps is required to decelerate the 20 micron particle to zero velocity within the 300 micron distance.

It is of course necessary to go from these velocities to the pressure differential required. This raises some very interesting points. Thus, if we consider the flow set up in a 1000 micron orifice through a 300 micron skin, we expect the velocities to be given quite accurately by

$$v = \sqrt{\frac{2\Delta p}{\rho}}$$

From this relation, very modest pressure differentials are required, 0.2" of water and between 1.5 and 1.8 inches of water respectively. However, if we look at the calibration curve for the flow through such an orifice (Figure 4.11), we find that Δ P values of about 0.6 and about 4 inches of water are indicated, if we wish the average velocity in the orifice to be the magnitudes given in Tables 3.2.1 and 3.2.2. On looking at the calibration curves, it is found that the data is consistent with discharge coefficient of about 0.6, typical for conventional sharp-edge orifices. A review of these data indicates that this is caused mostly by

the contraction of the flow, velocity coefficients (ratio of measured velocity to $\sqrt{\frac{2\Delta P}{\rho}}$) are very close to unity. Thus an essential element of the maintenance of sterility by pressurization for large orifices is the mixing and enlargement of the jet beyond the orifice, rather than simply generating a flow in the opening. Of course, these observations would not hold for small orifices, those where the thickness of the skin is say three or four times the hole size, so that the flow becomes attached to the surface of the orifice.

Tables 3.2.1 and 3.2.2 represent useful results and since it becomes apparent that the pressure differential required for aseptic maintenance is a function of both particle size and orifice dimension, through basic flow parameters.

3.2.3 Behavior at Reduced Ambient Pressures

It is required to investigate the manner in which the analysis of spore penetration can be extended to other ambient conditions. For example, during launch a spacecraft passes through the complete range of atmospheric pressure, from sea-level pressure to the vacuum of deep space. It is desired to look at the effects of this range of conditions on Aseptic Maintenance by Pressurization capabilities.

We assume that the differential pressure within the membrane can be maintained constant. For the sake of arriving at definite numbers, we

also assume that the interior of the pressurized chamber remains at constant temperature. The analysis will consider only nominal particle size - one micron diameter. This permits a much more definitie discussion, and the method of extending the analysis to a range of particle sizes, and the results to be expected can be more clearly explained.

We recognize that as the density of the gas within the membrane decreases the flow conditions about a tiny sphere may range from continuum flow at sea-level to what may become free-molecular flow when the ambient pressure is essentially zero and the pressure within the membrane is correspondingly low. We look first at the problem of a small particle being carried at a definite velocity and the pressure differential set equal to the flow stagnation pressure; i.e. $\Delta P = 1/2 \rho v^2$. If the penetration is less than the membrane thickness, we need not conduct any further analysis. If it is greater, we must try to evaluate the flow through the orifice and determine the effect on the particle motion more exactly.

To cover the wide range of flow conditions we make use of three different formulations for the drag on a sphere:

Stokes' Law: $F = -6\pi\mu r V$ (3.2.5)

Millikan's empirical modification of Stokes' Law

$$F = -\frac{6\pi\mu r V}{1 + \frac{L}{r}\left[A + B\exp(-cr/L)\right]} \qquad (3.2.6)$$

Epstein's relation:

$$F = -k\vec{V}_M \rho r^2 V \qquad (3.2.7)$$

We note that the drag is independent of the density, except in free molecular flow, and since the viscosity is also independent of the density (nearly proportional to the product of density and mean free path) we expect our simple estimation of penetration capability to be quite useful for a range of ambient pressures. Stokes' Law Equation (3.2.5) has been demonstrated to hold for continuum, low Reynolds number flows ($R_e \lesssim 1$), and is appropriate for our one micron spheres at sea-level pressures for velocities below 40 mph (58.6 fps). Epstein's relation, Equation (3.2.7) is appropriate for free-molecular flow. We will use the constants A, B, and C in Equation (3.2.6) which were determined for Milliken's oil droplets; it may be noted that measurements of the constant k in Equation (3.2.7) for oil droplets and for small glass spheres differed by less than 1%. Since Stokes' Law has also been verified for oil droplets and for tiny glass spheres, one expects that empirical formula should not be especially

sensitive to the actual surface material.

Table 3.2.3 exhibits computations for a range of altitudes and hence atmospheric pressures (Reference 3.4). The equations of motion used for the table are those derived in Appendix A where the basic force equation if $F/M_s = -\alpha v$. The expressions for α follow from re-arrangements of Equations (3.2.5) to (3.2.7). It was also shown in the appendix that the maximum distance that a particle can traverse in a gas under such laws of force is given by

$$S_o = \tau V_o$$

where τ is a characteristic time equal to $1/\alpha$ and v_o is the initial velocity of the sphere in the gas. This parameter is the "Penetration Distance" given in Table 3.2.3. This concept of "penetration distance" is valid provided there exists a ΔP across the membrane that slightly excees the flow stagnation pressure (see Section 3.1.2.3). Since the ΔP required to produce a low-velocity flow in a nozzle or orifice is proportional to the density and the square of the velocity, or: $\Delta P = 1/2 \rho V^2$, we must note that at high altitudes it will be much reduced from the sea-level value for a given velocity. The ΔP required for this case are given in Table 3.2.3.

We see from the tabular results that for a very large range of

TABLE 3.2.3 PENETRATION DISTANCE FOR ONE MICRON PARTICLE AS A FUNCTION OF ALTITUDE WITH ΔP EQUAL TO STAGNATION PRESSURE

ALTITUDE (KFT)	AMBIENT PRESSURE (ATM.)	AMBIENT PRESSURE (INCHES OF H_2O)	ATM. DENSITY (SLUG/FT^3)	MEMBRANE ΔP (IN OF H_2O)	PENETRATION DISTANCE (MICRONS)
0	1.0	407	2.38×10^{-3}	0.78	56.0
21.9	0.5	203	1.19×10^{-3}	0.37	74.3
44.2	0.2	81.2	4.76×10^{-4}	0.16	105
52.8	0.13	54.2	3.16×10^{-4}	0.11	135
58.8	0.10	40.7	2.38×10^{-4}	0.078	162
67.2	0.067	27.0	1.58×10^{-4}	0.052	222
75.6	0.044	18.0	1.05×10^{-4}	0.035	312
77.6	0.040	16.3	9.52×10^{-5}	0.031	324
81.4	0.033	13.5	7.90×10^{-5}	0.026	403

ASSUMPTIONS:

1. SPORE INITIAL VELOCITY = 40 MPH = 1788 CM/SEC
2. TEMPERATURE IN MEMBRANE CONSTANT AND = $288^{\circ}K$
3. ρ_L IS CONSTANT AND = 5.17×10^{-10} SLUG/FT^3
4. MEMBRANE THICKNESS = 300 MICRONS

ambient pressures the general conclusions drawn in the previous analytical sections for one micron particles still apply. In particular, the penetration threshold curve derived in Section 3.1.2.3 can be adjusted to any altitude by adjusting the Δ P in direct proportion to the ratio ρ (at altitude)/ ρ (sea-level).

However, if we go to ambient pressures less than 0.044 atmospheres or correspondingly above an altitude of 75,000 feet, we must go beyond the above simple, "penetration distance" concept and take into account the required overpressure to adequately decelerate the incoming particles. It must be noted that this limiting value for ambient pressure occurs because of the assumption that the membrane has a 300 micron thickness. For this case, we still wish to use a simple analysis, without solving the problem exactly. We assume for the next step that there is an overpressure of 2" of water within the barrier; thus, in Table 3.2.4 we tabulate ambient pressures from 60 psf down to 0 psf, and internal pressure of 2" of water (10.4 psf) higher than these. Again, we assume that the internal temperature is constant ($288^{o}K$). The altitudes corresponding to this ambient pressure are given in Column 1. From the ratio P_i/P_∞ , we can find the velocity developed in the orifice; this is tabulated conveniently in Reference 3.5. For altitudes above 119 kft., the ambient pressure is low enough that sonic flow develops in the orifice; since we assume a constant

TABLE 3.2.4 PENETRATION DISTANCE FOR ONE MICRON PARTICLE AS A FUNCTION OF ALTITUDE WITH ΔP EQUAL TO TWO INCHES OF H_2O

ALTITUDE (KFT)	AMBIENT PRESSURE (PSF)	AMBIENT PRESSURE (INCHES OF WATER)	INTERIOR MEMBRANE PRESSURE (PSF)	EFFLUX GAS VELOCITY (FPS)	PENETRATION DISTANCE (MICRONS)
79.5	60	11.8	70.4	526	41
88.0	40	7.85	50.4	631	52
103	20	3.92	30.4	835	77
119	10	1.97	20.4	1020	111
132	6	1.18	16.4	1020	163
157	2	0.39	12.4	1020	202
180	1	0.20	11.4	1020	267
198	0.5	0.098	10.9	1020	303
220	0.2	0.039	10.6	1020	313
	0	0	10.4	1020	321

ASSUMPTIONS:
1. SPORE INITIAL VELOCITY = 40 MPH = 1788 CM/SEC
2. TEMPERATURE IN MEMBRANE CONSTANT AND = $288^{o}K$
3. MEMBRANE THICKNESS = 300 MICRONS
4. ρL IS CONSTANT AND = 5.17×10^{-10} SLUG/FT^3

reservoir temperature, the efflux velocity is constant above this altitude, although the density of the flow decreases in proportion to the decrease in reservoir pressure.

We next assume that the spore approaches the orifice at the velocity of 58.6 fps, and as it starts to enter the orifice, the relative velocity between it and the gas flowing out is $V_s + V_e$. We assume that V_e, the efflux gas velocity, is constant through the orifice. Now we find the time required to decelerate the particle to the efflux velocity, i.e., to annul V_s. This comes from the relation

$$V_s = V_o e^{-\alpha t}, \qquad \text{where } V_o = V_s + V_e$$

This point in space represents the deepest penetration of the particle; if the velocity relative to the gas becomes less than V_e, the particle is being swept out of the orifice. There are analytical relations to give the depth of penetration, but we compute the product $v_s t$, which is a conservative penetration distance, if this is less than the thickness of the membrane, we know penetration cannot occur.

The particle deceleration for Table 3.2.4 are computed by the Epstein free-molecular flow relation (Equation 3.2.7), except that for

the first row of figures, which are given by the Milliken formulation. It is seen that a 2" water pressure differential prevents penetration of one micron particles with velocities of approach of 40 mph for altitudes up to 198,000 feet. If one resolves the above equations for the vacuum of space, it is readily determined that 5.0 inches of water will stop a one micron particle approaching at 40 mph from penetrating through a hole in a 300 micron thick membrane. The velocity dependent penetration threshold curve for the vacuum case which corresponds to Figure 3.1.17 for the sea-level case is given in Figure 3.2.3.

FIGURE 3.2.3 PENETRATION THRESHOLD FOR ONE MICRON PARTICLE IN VACUUM CONDITION

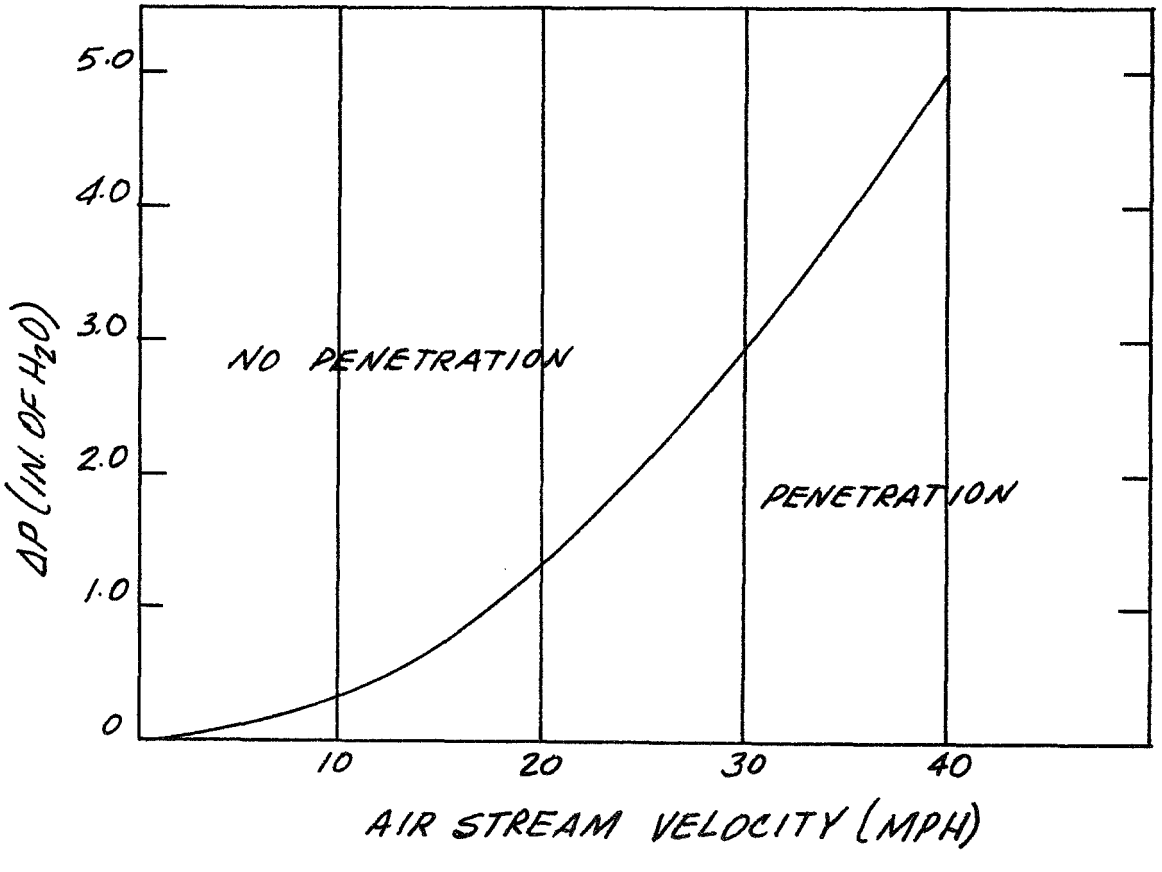

If one extends this analysis to larger particles, we note immediately that the ratios of molecular mean free path to particle radius, L/r, will decrease to the point where within the orifice, the ratios will be < 10. Since the value of m_s will increase as the diameter cubed, the magnitudes of α will be greatly reduced. Thus if we take a 20 micron particle, the L/r for zero ambient pressure will be ~ 2 instead of 40, and the value of α then will be roughly that corresponding to L/r $\sim$ 4 (top row) divided by $(20)^3$ or $(4.6/8000) \times 10^4$, or an exponent of only -6, instead of -46,000. For such a case the above simple techniques are inadequate and it will be necessary to investigate the deceleration of the particle by the flow after it passes through the membrane. Moreover, the expanded jet acts on the particle for a long time, relative to those shown in Table 3.2.4 and since the gas is continuously expanding, the value of α is changing during the particle approach. A numerical integration of the particle path seems to be the best method of study with particle size as a parameter. A more complete evaluation requires an effort beyond the time and funding available on this current program. It seem obvious, however, that like the sea-level conditions the penetration significantly increases with particle size.

REFERENCES

3.1 NASA CR-66548, 1 March 1968: "A Study of Aseptic Maintenance by Pressurization".

3.2 Kline, Stephen, J.: Similitude and Approximation Theory, McGraw-Hill Book Company, New York, 1965.

3.3 Hinze: Turbulence, McGraw-Hill Book Company, Inc., (see p.7).

3.4 Long, M.E., "Extension of AMP Analysis to Different Ambient Conditions"; GE PIR 9522-AMP-113 ; January 23, 1970.

3.5 Kuethe, A. M. and Schetzer, J. D.: "Foundations of Aerodynamics"; John Wiley and Sons, Inc., 1950. See Table 1, p. 140 and following.

3.6 Sontowski, J., "Dimensional Analysis and Experimental Design for Aseptic Maintenance by Pressurization"; GE-PIR 9522-AMP-086; 6/12/69.

3.7 Sontowski, J., "Calculation and Experiment Design"; GE PIR 9522-114; 1/27/70.

4.0 EXPERIMENTAL PROGRAM

4.1 APPARATUS DESCRIPTION

4.1.1 Quiescent Test

A laboratory apparatus for determining the flow of microorganisms through various microscopic holes in membranes, and for controlling a range of differential pressures was designed and four such units were fabricated. Each apparatus consists of the following materials assembled as shown in Figure 4-1 and P-0.

Aerosol Chambers - Twenty-two liter Glass Reaction flasks, Catalog No. K61240, Kontes Glass Company, Vineland, New Jersey.

Chamber Clamps - Reaction Flask Clamp, Catalog No. 61375, Kontes Glass Company, Vineland, New Jersey.

Membrane Holders - The membrane holders were machined from aluminum. The top piece was 0.6 cm thick and the bottom piece was 1.9 cm thick. Both were 19 cm in diameter and were machined to fit the chamber clamp. A 2.54 cm diameter hole was drilled centrally in each piece to hold the Viable Culture Detector Tube. Additionally, the 1.9 cm bottom piece had a 1.5 mm hole drilled on its horizontal plane through the center and entire diameter of the piece. This was adapted to provide a source of air pressure on the membrane, and a port for attachment of the manometer.

EXPERIMENTAL APPARATUS

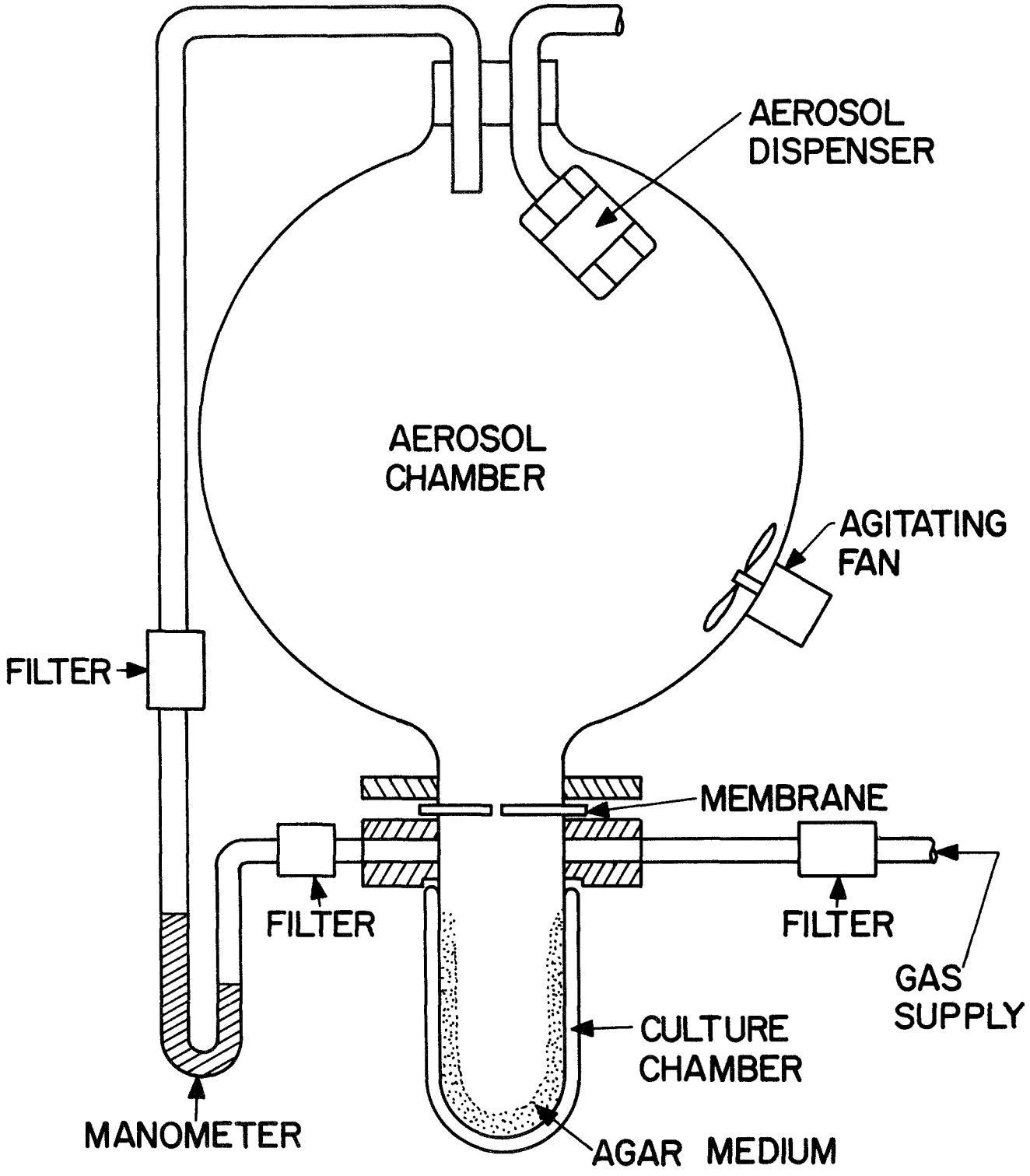

FIGURE 4.1

Quiescent Test Chamber

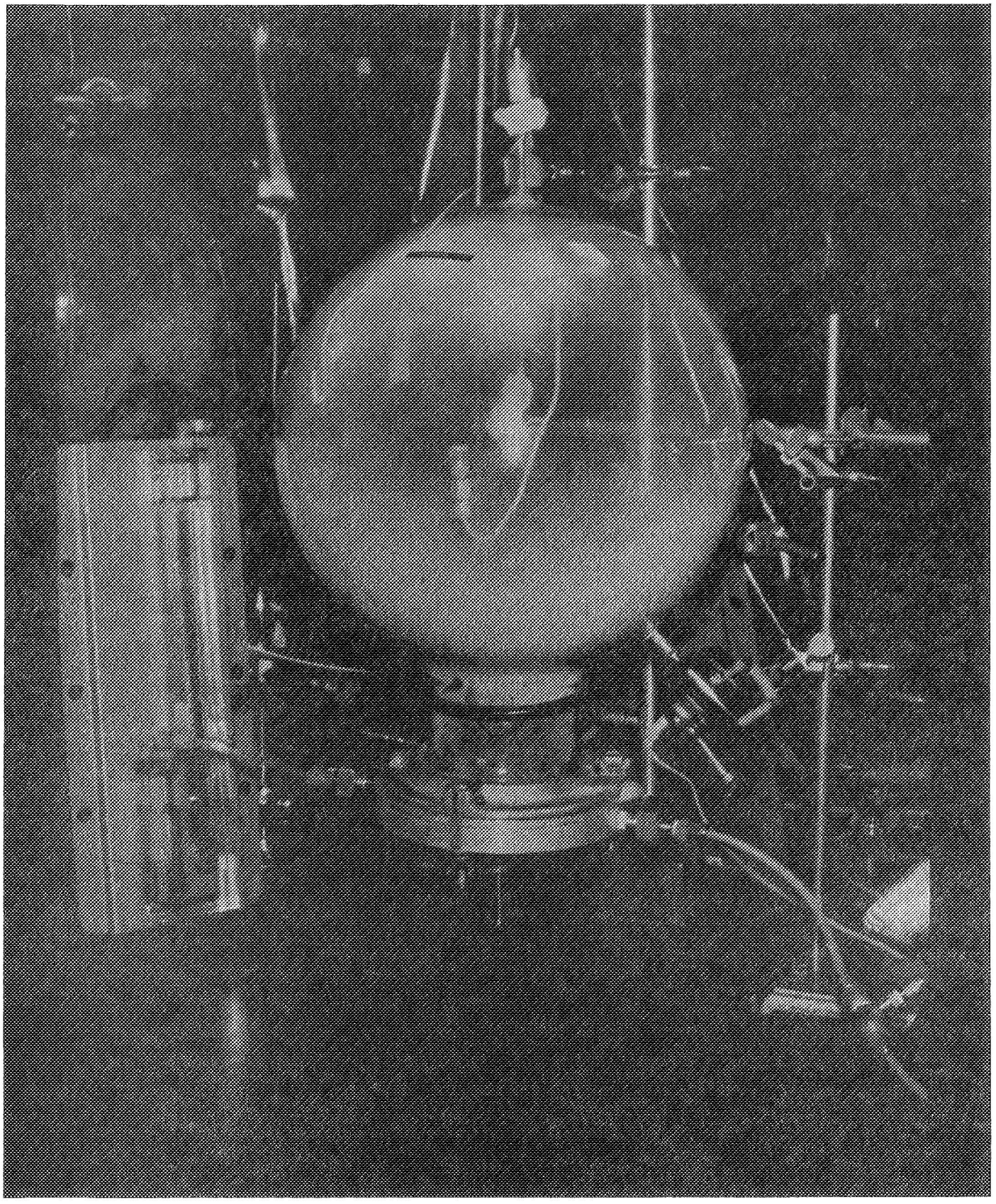

Figure P-0

Agitating Fan - The fan employed was A Sears Roebuck Company two speed defroster type fan. Catalog No. 28A78528, with three-four inch rubber blades.

Air Filter Holders - The air filter holders used were Millipore Gas Line filter holders, Catalog No. XX40 025 00, Millipore Corporation, Bedford, Massachusetts.

Air Filters - The air filters used in the filter holders were Millipore HABG with a mean pore size of 0.45 microns.

Manometers - Solid plastic, vertical style with a range of 0-10" of water. Model #310, F. W. Dwyer Manufacturing Company, Inc., Michigan City, Indiana.

Pressure Regulator - Range 0-60 psi Model No. 40, The Matheson Company, East Rutherford, New Jersey.

Aerosol Dispenser Head - The aerosol dispenser head was fabricated from standard brass tubing connections. Figure 4-2 shows the aerosol dispenser with one end fastened to a 1/8" stainless steel tube. The dispenser functions when a pressure of approximately 100 psi is applied to the dispenser. Both aluminum foil seals rupture and an aerosol is discharged explosively into the chamber. The design for this aerosol head was furnished by Mr. Carl Depeople of the U.S. Army Chemical Corps at Fort Dietrick, Maryland.

AEROSOL DISPENSER

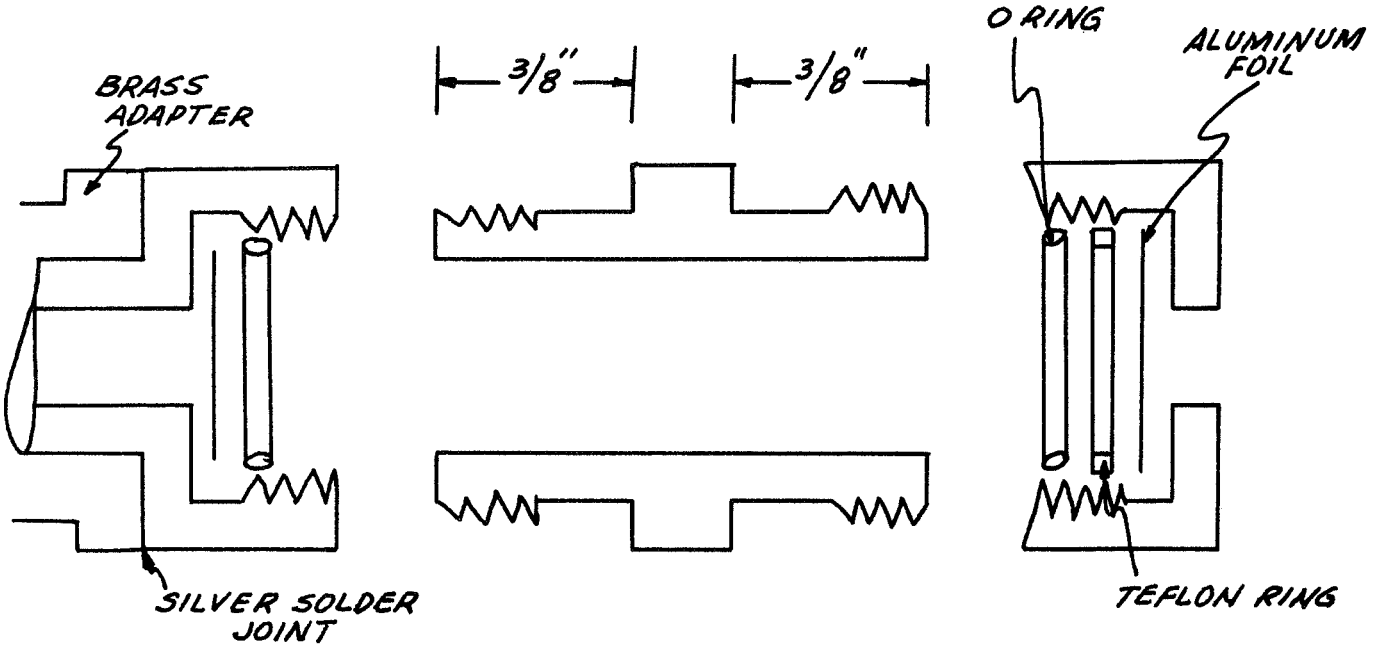

FIGURE 4.2

Membranes - The membranes used were fabricated from .012 inch aluminum stock. Holes of 20, 200, 1000 and 1800 micron diameter were used. The 20 micron and 200 micron diameter holes were drilled using a Lear-Siegler LW-212 metal working laser with a Nikkon Compariton, using a 6 millisecond pulse at 4 kilowatts, 2 pulses per hole.

Holes varying in size from 19 to 232 microns were produced for our determinations. Because 2 pulses were required, some holes were oval, and cone shaped in cross-section. Such holes were dimensioned by their maximum and minimum dimensions. The 1000 and 1800 micron diameter holes were machine drilled.

Micrometer calipers were used to determine the thickness of each membrane. The lateral dimensions of the membrane holes were determined by light microscopy using a standardized ocular micrometer. The cross-section dimensions were measured using a destructive technique. This technique is described in detail in the Section 4.3.2., Hole Characterization.

Viable Culture Detector Tubes - Twenty-five by seventy-five millimeter culture tubes which are washed, sterilized, filled with agar, and capped, are installed on the membrane holder assembly as shown in Figure 4.1. The tubes are prepared several days in advance of their intended use so that they can be carried through a sterility assurance test (see Section 4.2.1.2).

Aerosol Sampling Apparatus - An aerosol sampling apparatus as shown in Figure 4-3 was fabricated out of the following pieces to effectively quantitate the bacterial air count within the aerosol chambers: a 50 ml sterile disposable syringe, Catalog No. 14-823-200 Fisher Scientific Company, King of Prussia, Pennsylvania, was attached to a 15" sterile French Feeding Tube, Catalog No. K-32, Joseph E. Frankle Company, Philadelphia, Pa. The feeding tube was in turn passed through a flexible tube guide located within a rigid sampling tube guide. This introduced the sampling tube into the chamber where air was removed via the sampling ports.

4.1.2 High Velocity Tests

Three high velocity wind tunnels were designed and fabricated to determine the differential pressures, at various wind velocities, required to prevent microbial penetration through microscopic holes in membranes. Each apparatus consists of the following materials assembled as shown in Figures 3.1.8 and 3.1.11 and in photographs P-1 and P-2.

High Velocity Wind Tunnels - Three high velocity wind tunnels were fabricated out of 1/4" and 3/4" plywood and 1/2" plexiglass. Each apparatus consisted of the following materials:

Reversible Motors - The fan motors used were 1/2 hp variable speed reversible motors Catalog No. 6K011, W. W. Granger, Inc.

AEROSOL SAMPLING APPARATUS

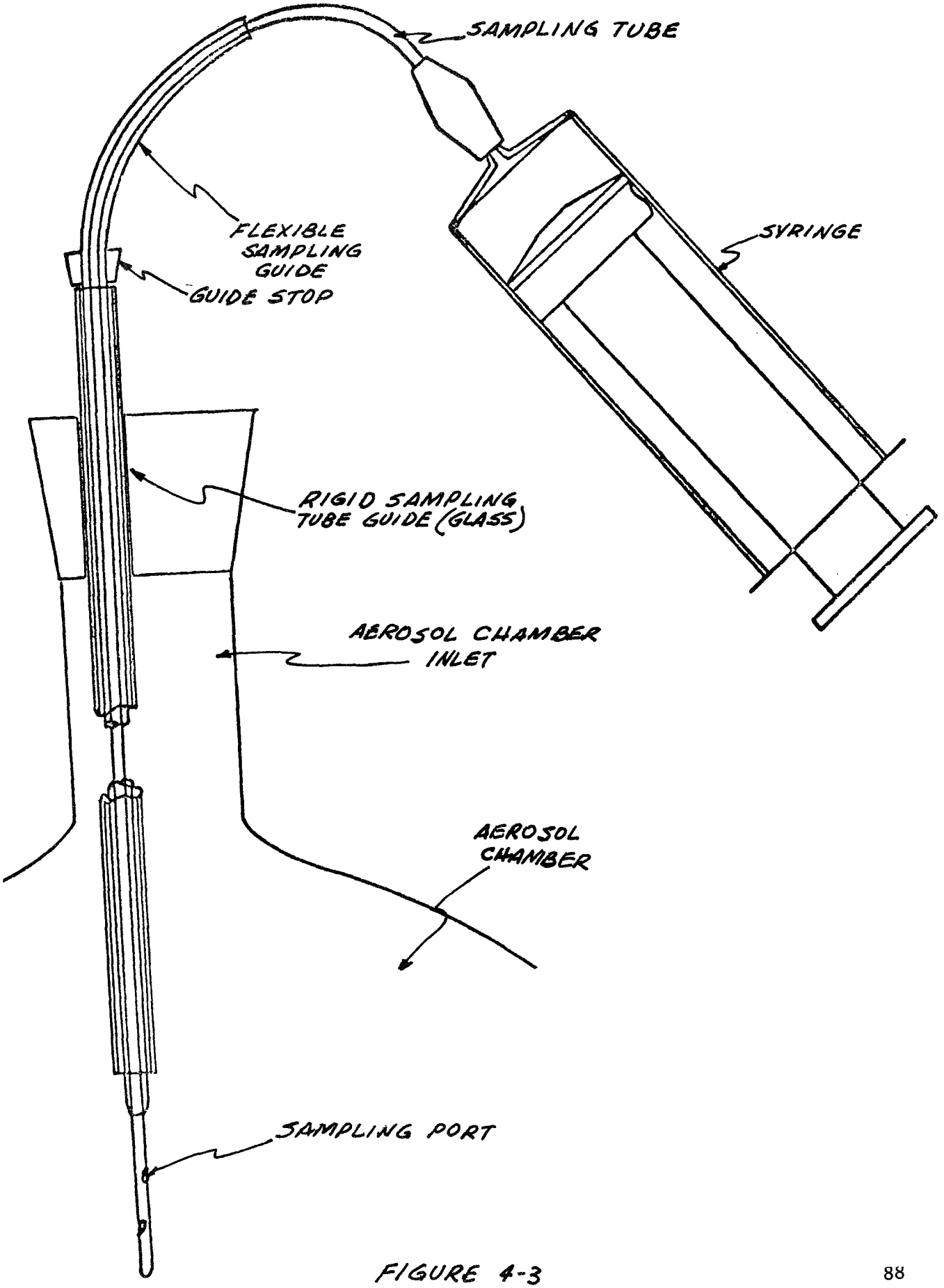

FIGURE 4-3

High Velocity Wind Tunnel

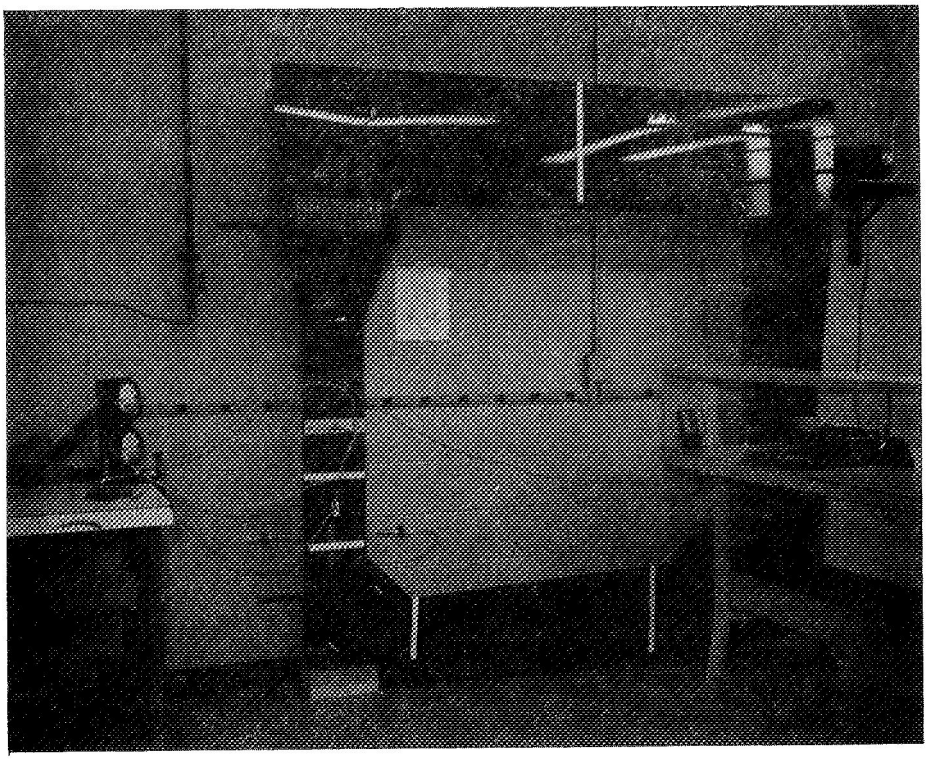

Complete Tunnel

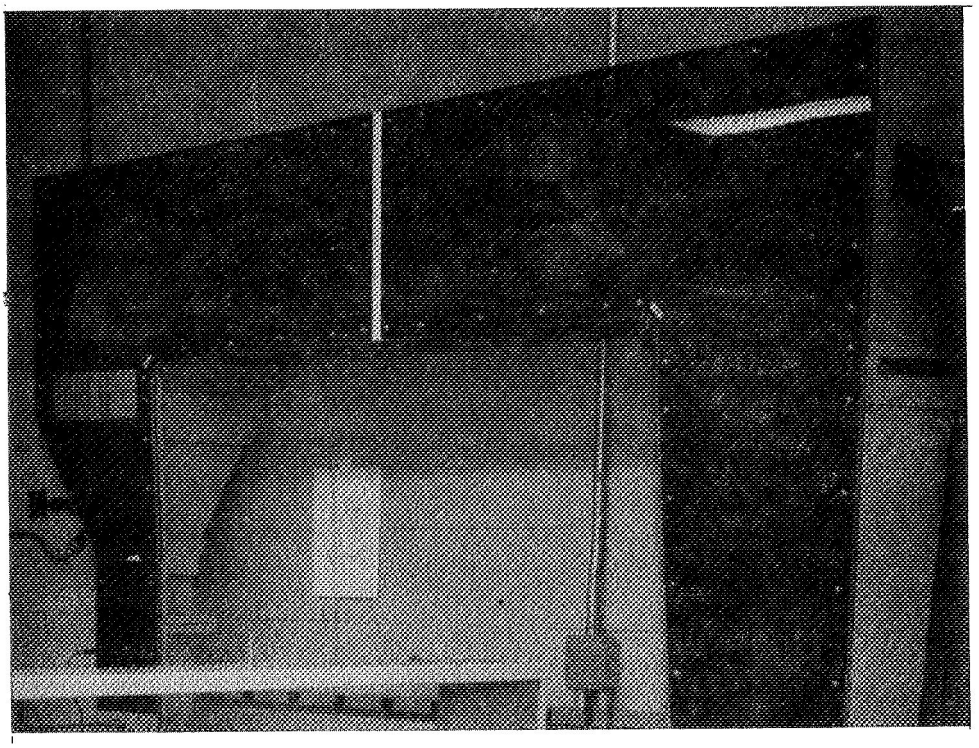

Fan and Stabilizing Vanes

Figure P-1

Wind Tunnel

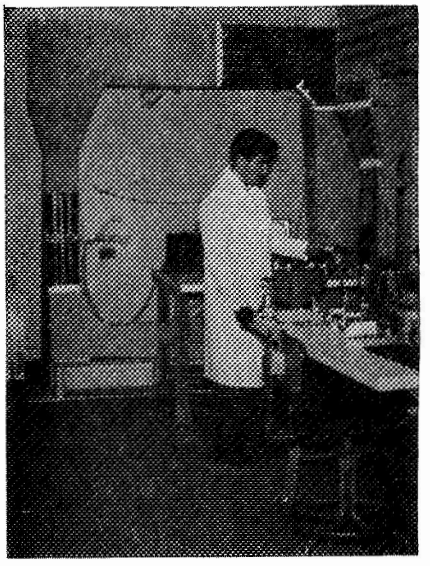

Complete Set Up

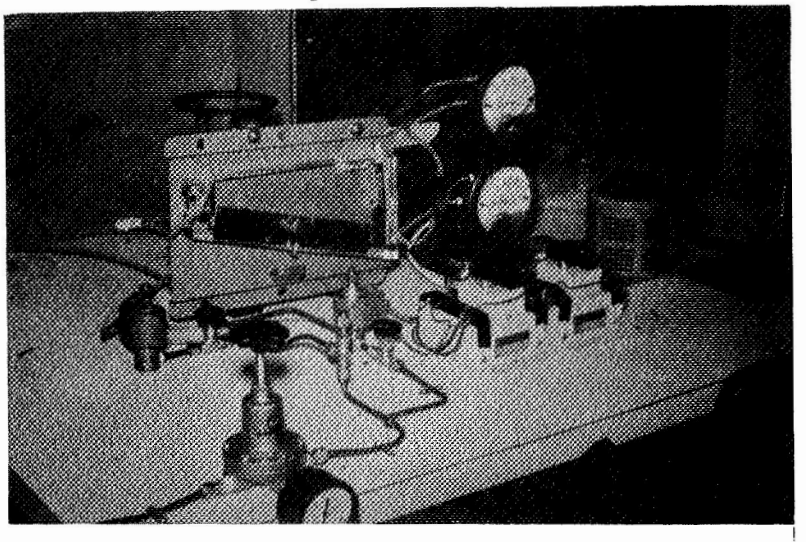

Control Apparatus

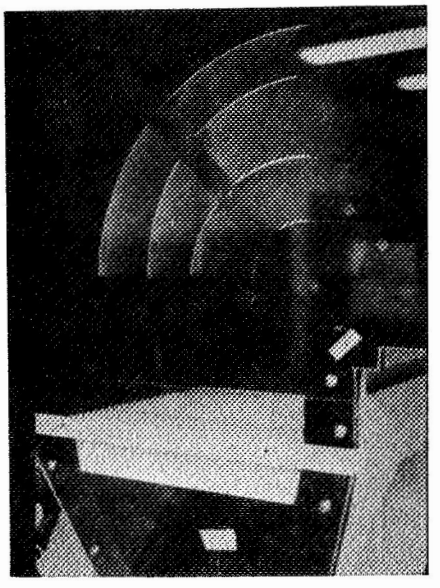

Wind Stabilizing Vanes

Figure P-2

Fan Blades - Twelve inch aluminum fan blades Catalog No. H-1240-4, Torrington Company, Doylestown, Pa.

Pitot Tubes - The 5/16" pitot tubes used to measure the wind velocity within the wind tunnel were Catalog No. 160-18P with packing gland, F. W. Dwyer Manufacturing Inc., Michigan City, Indiana.

Pressure Transducer Gages - The pressure transducers gages used in conjunction with the pitot tubes were Catalog No. 6003-A-02-A22X, Differential Pressure Transducer Gages, H. H. Barnum Company, Brighton, Michigan.

Relay Controllers - On-off solid state relay controllers, Catalog No. 6182D-A-01-X, Automatic Timing and Control Inc., King of Prussia, Pa.

Inclined Manometers -

0.0 to 0.25 Range No. 215

0.1 to 1.0 Range No. 200.5

0.2 to 2.0 Range No. 202.5

F. W. Dwyer Manufacturing Inc., Michigan City, Indiana

Presure Gages - Magnehelic - The Magnehelic Pressure Gages used to measure the Δ P across the membranes were Catalog No. 2005-2010-0 - 10"; No. 2005-2030-0 - 30"; F. W. Dwyer Manufacturing Inc., Michigan City, Ind.

Solenoid Valves -

a. Normally closed, 120V 60 cycle

b. Normally open, 120V 60 cycle

General Controls ITT, Capp Supply, Inc., Philadelphia, Pa.

Needle Valves - Hoke Brass needle valves, No. 1325H4B, Shelby Jones Company, Inc., Havertown, Pa.

Aerosol Dispenser - Same as that used during Quiescent Tests (Figure 4-2).

Filter Holders and Filters - Same as those used for Quiescent Tests.

Membranes - Same as those used for Quiescent Tests.

Membrane Holder Assembly - The membrane holder assembly used to hold the membrane holders were machined in two sections from brass as shown in Figure 3.1.3 and the photograph P-3.

Membrane Holders - The assembly utilized to hold the viable culture detector tube was designed and fabricated out of stainless steel as shown in Figure 4.4 and photograph P-3. The tubing used for the transport of the sterile air across the membrane was 3/16" OD stainless steel.

MEMBRANE AND VIABLE CULTURE TUBE HOLDER

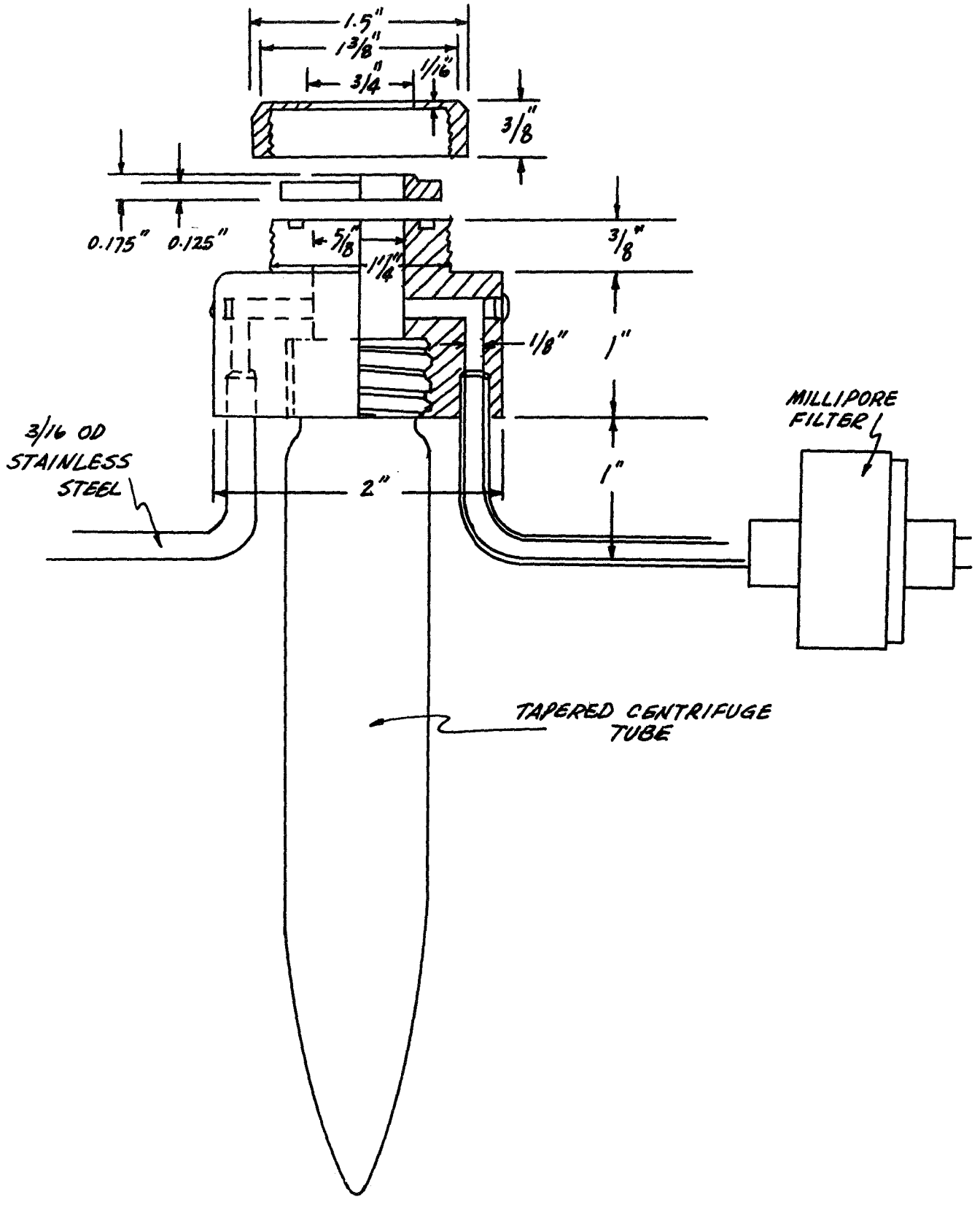

FIGURE 4.4

High Velocity Apparatus

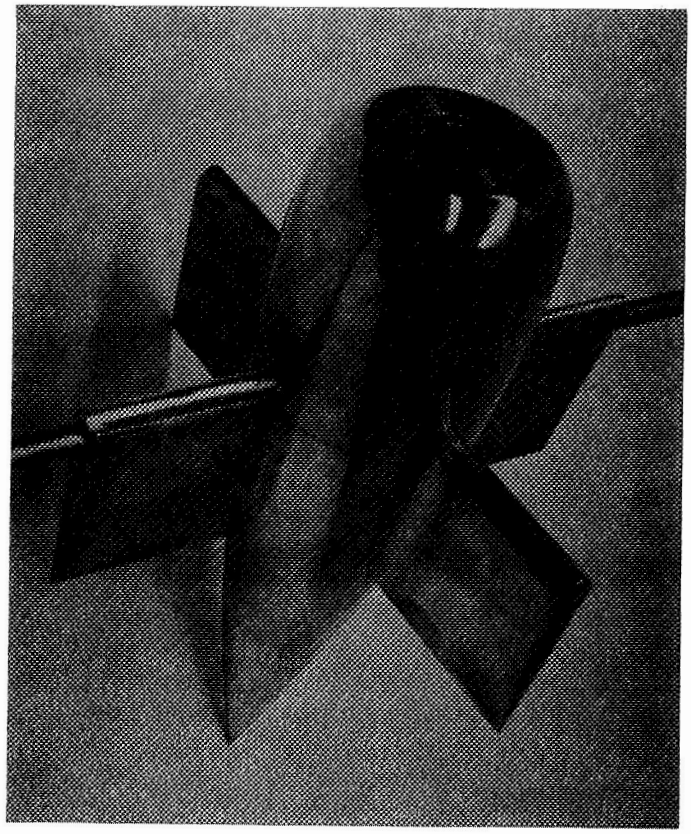

Test Membrane Assembly Holder

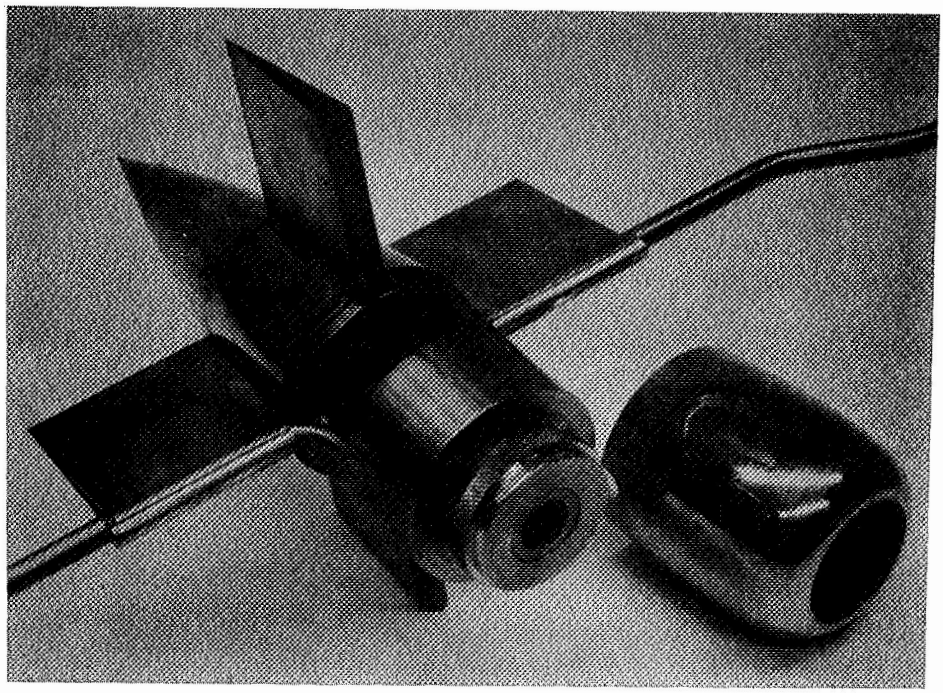

Holder with Test Assembly

Figure P-3

Viable Culture Detector Tubes - Forty-five ml capacity centrifuge tubes, Catalog No. 5-538-30, Fisher Scientific Company, King of Prussia, Pa., are washed, sterilized, filled with agar, and capped. The tubes are carried through the same sterility assurance tests as those used for quiescent testing.

4.2 TEST PROTOCOL

4.2.1 Test Procedures - Quiescent

The test procedures used for the quiescent testing program are shown in Figure 4.5. The check-out sheet used to record the set-up of any given run is given in Figure 4.6 and was completed for each test case. A description of the procedures followed in each case is given below.

4.2.1.1 Preparation of the Experimental Chamber

Twenty-five by seventy-five millimeter culture tubes were washed in an aqueous solution of alconox, rinsed in deionized water and sterilized. Ten milliliters of previously sterilized nutrient Agar, fortified with .0001% $MnSO_4$ was placed in each tube, and the tubes were capped. The capped tubes were then rotated manually at an approximate 80^{o} angle until the medium hardened. The tubes were then cooled additionally by placing them in a refrigerator for approximately one hour to set the agar. They were then placed in an incubator for 48 hours at $37^{o}C$ to assure sterility.

TEST PROCEDURE - QUIESCENT TESTS

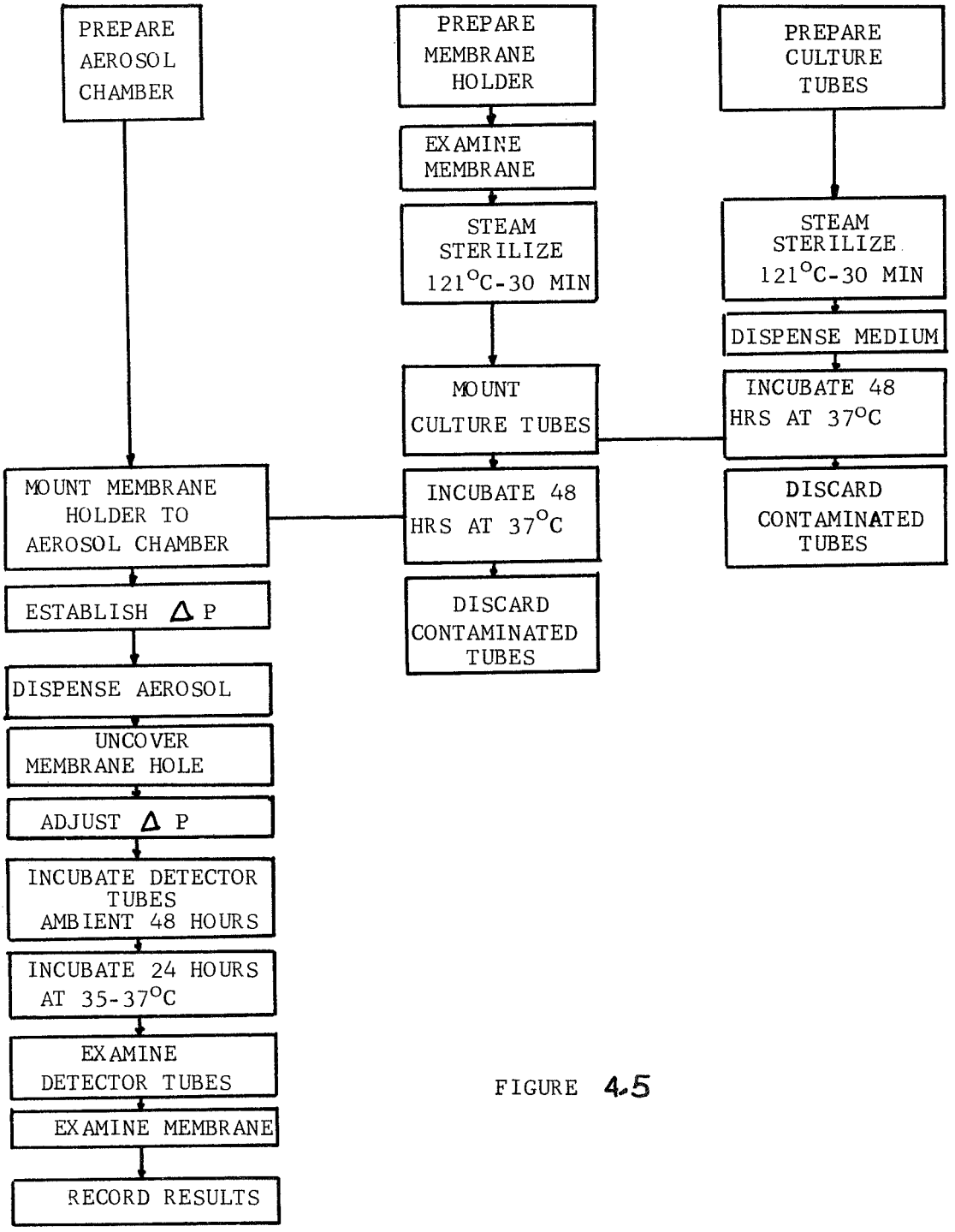

FIGURE 4.5

QUIESCENT TEST PROCEDURE CHECKOUT SHEET

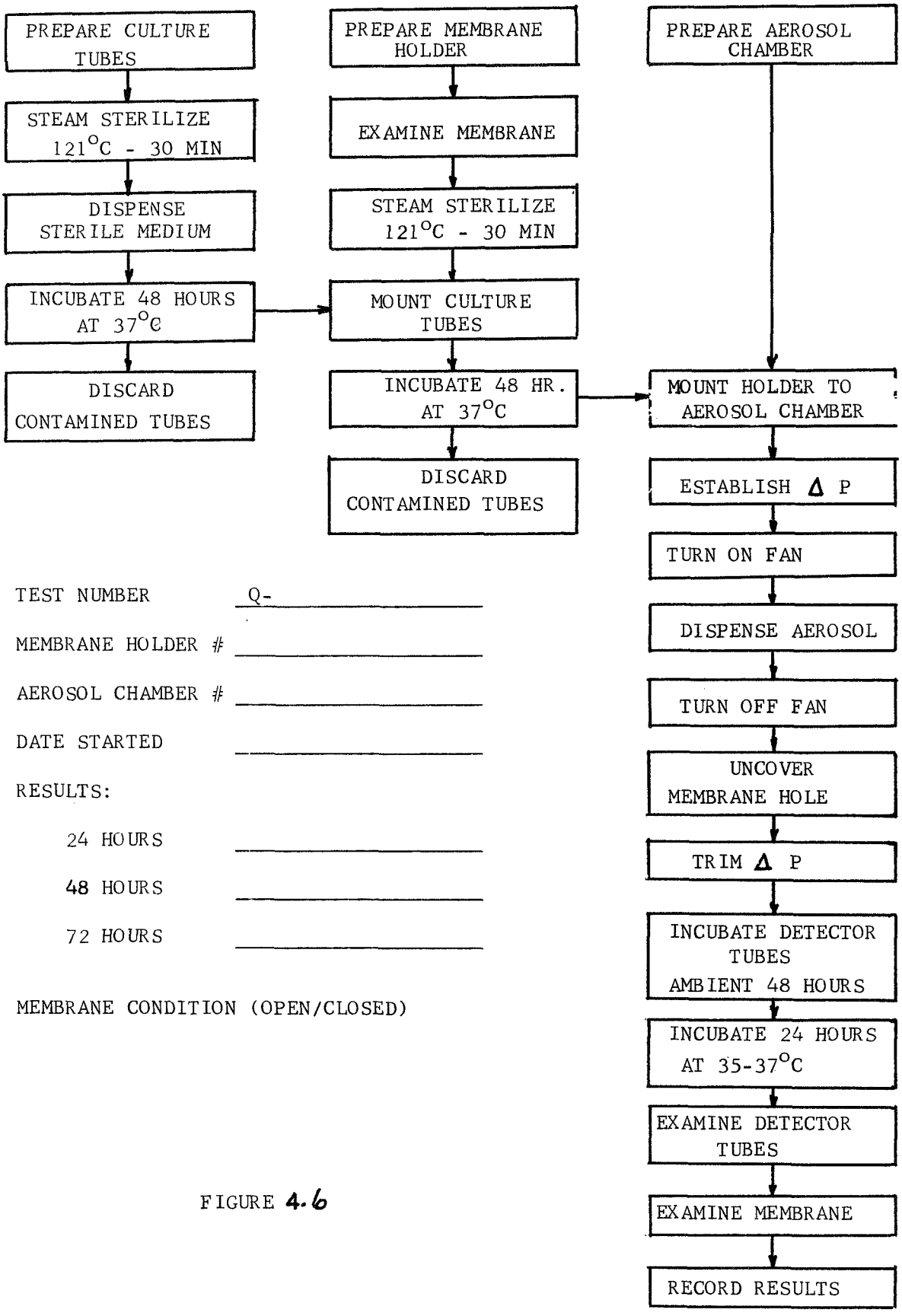

TEST NUMBER Q-_____

MEMBRANE HOLDER # _____

AEROSOL CHAMBER # _____

DATE STARTED _____

RESULTS:

24 HOURS _____

48 HOURS _____

72 HOURS _____

MEMBRANE CONDITION (OPEN/CLOSED)

FIGURE 4.6

The membrane selected for test was examined microscopically to verify that the hole was open, and to measure the hole diameter. It was then installed in the membrane and culture tube holder. A small square of teflon tape was placed over the hole and held in place with a piece of autoclave tape with a string stapled to the tape. An empty 25 x 75 mm test tube was mounted to the lower side of the membrane holder. Two millipore filters (0.25 micron pore size) were placed in each gas line filter holder and hand tightened. Aluminum foil was then wrapped around each filter holder. The assembled membrane holder with the attached filters and empty test tube, were autoclaved at 121°C and 15 psig for 30 minutes, then subjected to a 15 minute vacuum drying cycle.

Following the autoclaving and cool down of the empty test tube mentioned above, it was removed and the viable culture detector tube was carefully inserted in a laminar flow bench. The complete assembly was then incubated at 37°C for 48 hours to insure sterility of the test assembly.

During the sterility test for the culture tube assembly, the aerosol dispenser was opened by removing the nut at the exit end holding the aluminum foil in position. 50 mgs of lyophilized B. subtilis var. niger spores, having a viability of 1.7×10^8 bacteria per mg, were placed in the dispenser. The dispenser was introduced into the chamber through the bottom opening and drawn into position by raising the steel tubing through the

rubber stopper located at the top of the chamber.

After incubation, the culture tube assembly was removed and checked for the presence of contaminants. If found to be free from contamination, the assembly was placed into position beneath the opening of the aerosol chamber. The string attached to the tape covering the membrane hole was fed up through the top opening of the chamber. A rubber gasket was inserted between the assembly and the chamber, and the holder was clamped into position and hand tightened.

The filter, manometer, and associated tubing were connected, and an external pressurized nitrogen source was connected to the upstream side of the aerosol dispenser as the final step in the equipment set-up.

4.2.1.2 Aerosol Generation and Maintenance

After assembly as described above, the fan was activated and pressurized nitrogen gas was introduced into the aerosol dispenser at 100 psi. The aluminum foil sealing both ends of the dispenser ruptured under gas pressure, and the stored spores were ejected into the aerosol chamber. The resulting aerosol was agitated by the fan for a period of 5 minutes before the fan was shut down. Additional 15 minute settling period was incorporated into the test procedure to remove the larger particles, which might clog the membrane hole, from the air.

After the fan shut-down and 15 minute settling period, the air supply to the culture chamber was activated and adjusted to approximately 10 inches water pressure. The tape blocking the topside of the membrane hole was then removed by pulling the string passing through the top of the aerosol chamber. The air input was then trimmed as necessary to achieve the differential pressure required across the membrane.

The purpose of initially adjusting the pressure to 10 inches water pressure, is to prevent the sudden drop in pressure from falling below the ΔP required,when the tape is removed from the hole. Even a momentary drop in pressure could theoretically cause a bacterial particle to transgress the opening if it were indeed challenged.

The test was then allowed to run for a period of 72 hours. During the last 24 hours the temperature of the culture chamber was raised to 37°C by placing a beaker of water around the viable culture tube, and placing an asbestos heating jacket around the beaker. The temperature was then regulated to 37°C by means of a Variac voltage regulator.

Upon completion of the test period the culture detector chamber was removed from the assembly and observed macroscopically for evidence of microbial growth. Following this, the membrane was removed from the apparatus and examined microscopically to insure that the hole had remained open.

Before this experimental phase was initiated, the question arose as to the reliability of the millipore filters in stopping any bacterial particles which may be picked up in the air stream approaching the membrane.

In an effort to determine whether or not this was of significant importance, a series of tests were devised as following to check the reliability of the millipore membranes.

Air containing bacterial spores was removed from the aerosol chamber by means of a vacuum pump,and filtered through an air filter holder containing a 0.45 micron pore size millipore filter membrane. The air passed through the filter and into a water impinger containing 10 mls of a 1% peptone solution. After a period of five minutes, the apparatus was removed and the peptone solution and filter were bioassayed. Ten experiments were performed with the results shown in Table 4.1

The data from the 10 tests performed indicated that the millipore membranes used to filter the incoming air were indeed removing the bacterial spores from the air. The investigators realize that ten tests do not represent an exhaustive study, but they do indicate that the method in which the filters are used is acceptable for the program under study. At no time during the experiments would the air filters be challenged by bacterial spores of the magnitude encountered during these tests.

In a further effort to minimize the remote possibility of bacteria entering through the air filter, two membrane filters were incorporated into each holder during the test runs.

TABLE 4.1

PERFORMANCE OF MILLIPORE FILTERS

Experiment No.	Counts/cc 1% Peptone	Total Filter Counts
Experiment 1	0/cc	3200/10 mls
Experiment 2	0/cc	1200
Experiment 3	0/cc	6300
Experiment 4	0/cc	700
Experiment 5	0/cc	3100
Experiment 6	0/cc	4400
Experiment 7	0/cc	2700
Experiment 8	0/cc	1600
Experiment 9	0/cc	19000
Experiment 10	0/cc	100

Finally, a phenomena occurred with the testing of the 1000 micron holes which forced a slight deviation from the above test

protocol. Because of excessive dehydration of nutrient agar in the culture tubes associated with the 1000 micron holes, the amount of dry powder used to make the agar preparation for these holes was reduced to 1/2 the recommended amount. The resulting agar maintained its firmness and was less sensitive to dehydration during the 72 hour run.

4.2.2 Test Procedures - High Velocity

4.2.2.1 Development of Test Apparatus

During the early testing of the High Velocity Wind Tunnels, modifications were made as required to given maximum efficiency to the test program.

Initial smoke tests in the chamber indicated a high degree of turbulence which started in the fan area and persisted to the culture tube area. A successful solution to the problem was found in the use of 1/2 inch square plastic grid material, 2-1/2 inches thick. This was placed in the chambers between the turning vanes and culture tube, to stabilize the air flow approaching the test assembly.

Manometers were incorporated into each apparatus to supplement the Magnahelic gages by serving as a more accurate pressure measurement, whenever low pressures - between 0 and 0.25 inches water pressure - were required.

Pressure regulators were incorporated into the air supply line, in series with the micrometer valves, to assure a stable and trouble free air supply.

In addition, strips of aluminized Mylar tape were placed on the inside surfaces of the plexiglas plates, and connected to a common ground, in an effort to reduce the electrostatic charge-build-up within the chamber (Reference 4.2.6.3).

Once these changes were incorporated into the test procedure, the test phase began. No additional changes were needed, or incorporated, during the experimental investigation. The test procedures used are given in Figures 4.7 and 4.8 and are described in the following sections.

4.2.2.2 Preparation of the Experimental Apparatus

Forty-five ml capacity centrifuge tubes, Catalog No. 5-538-30, Fisher Scientific Company, King of Prussia, Pa., were washed in aqueous solution of Alconox and rinsed in deionized water and sterilized at 121^{o}C for 15 minutes. 35 mls of sterile nutrient agar at 45^{o}C, fortified with .0001% $MnSO_4$, was added to each tube. The tube was then rotated and placed at an angle of approximately 70^{o} to solidify. After solidification, the tubes were incubated at 37^{o}C for 48 hours to insure sterility.

TEST PROCEDURE - HIGH VELOCITY

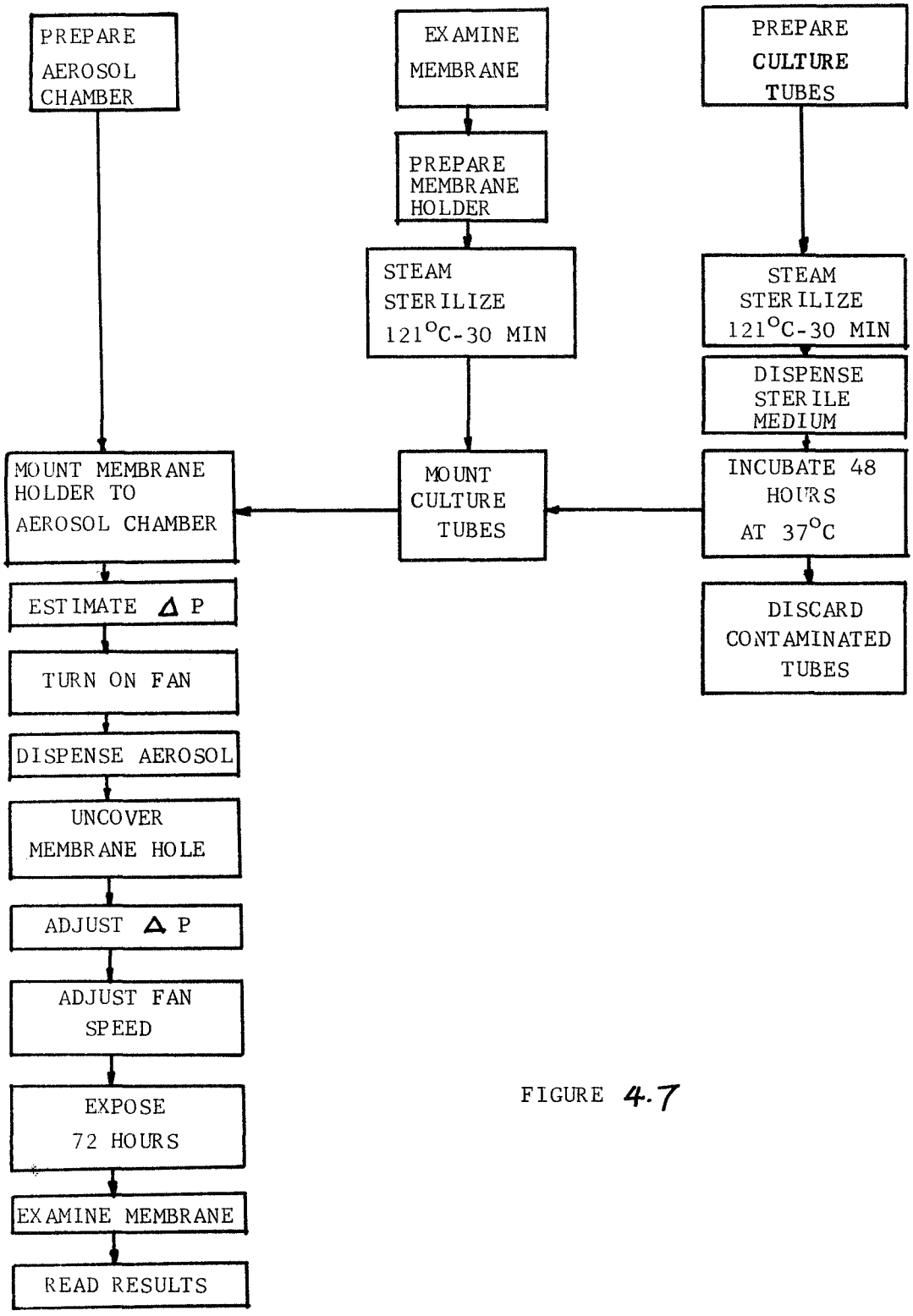

FIGURE 4.7

HIGH VELOCITY TEST PROCEDURE CHECKOUT SHEET

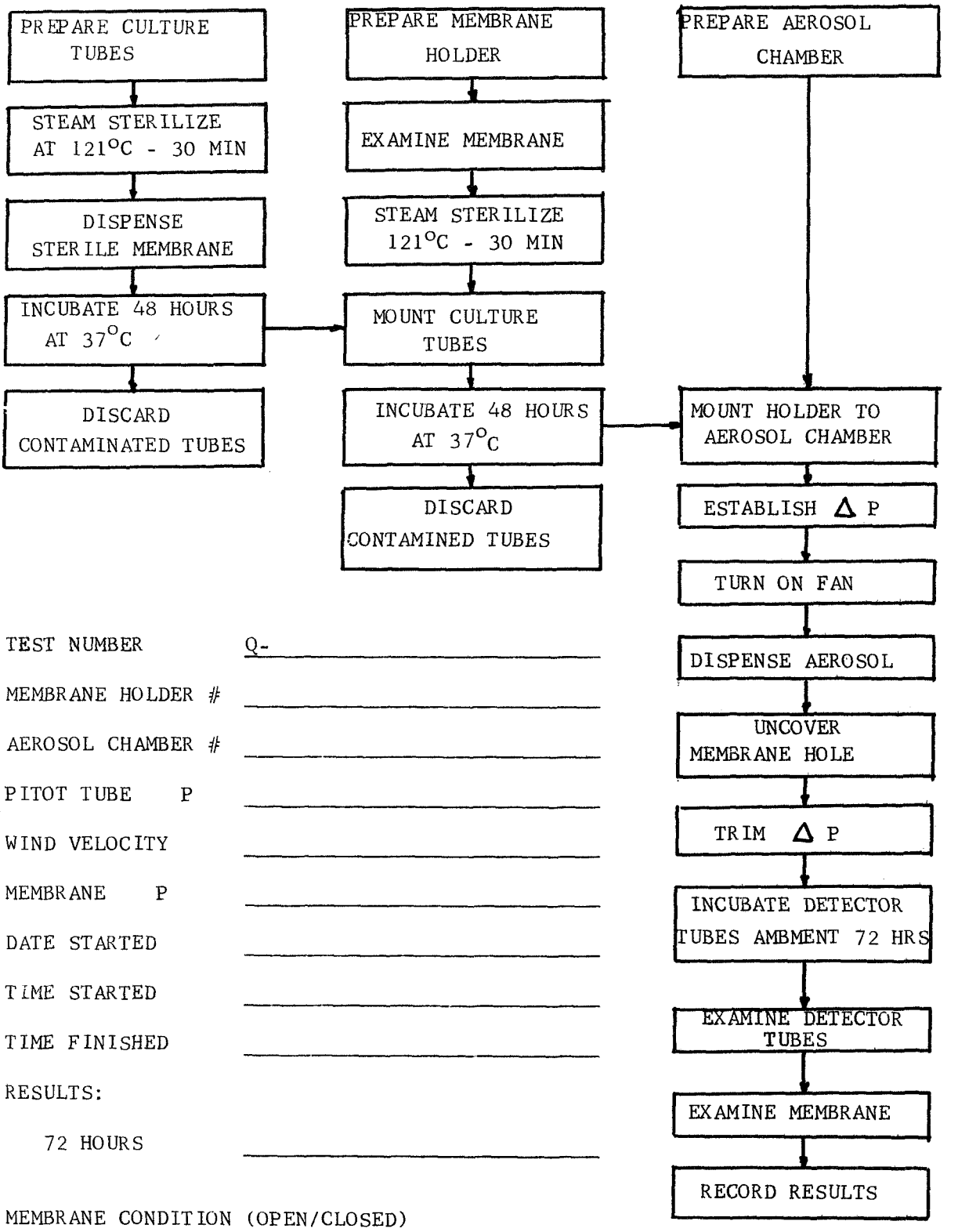

TEST NUMBER Q-_____

MEMBRANE HOLDER # _____

AEROSOL CHAMBER # _____

PITOT TUBE P _____

WIND VELOCITY _____

MEMBRANE P _____

DATE STARTED _____

TIME STARTED _____

TIME FINISHED _____

RESULTS:

72 HOURS _____

MEMBRANE CONDITION (OPEN/CLOSED)

COMMENTS:

FIGURE 4.8

The membrane selected for the test run was examined microscopically to determine if the hole was open, and to measure the hole diameter. It was then installed in the membrane holder, with the smaller opening towards the aerosol. A small square of teflon tape was placed over the hole and held in place by a piece of autoclave tape. A piece of string was stapled to this tape for subsequent removal from the membrane. An empty 12 x 75 screw top test tube was affixed to the bottom of the membrane holder and tightened into position. Two 0.45 micron millipore filter membranes were placed in each gas line filter located on either side of the membrane holder. These were tightened into place and the whole assembly was checked for leaks as follows:

The inlet gas line air filter holder was attached to a small tank of pressurized freon 12. The outlet air filter was connected to a Dwyer calibrated 10 inch manometer. The pressurized freon tank was then opened and the gas flow adjusted to 10 inches water pressure. The assembly was then checked for gas leaks with a G.E. Halogen detector. This instrument is capable of detecting a leak as small as 5×10^{-5} cc/second.

After checking and tightening if necessary, the air filters were covered with aluminum foil and the assembly was then autoclaved at $121^{\circ}C$, 15 psi for 30 minutes then subjected to a 15 minute drying cycle.

After cooling the empty test tube was removed in a laminar flow hood, and the viable culture tube was aseptically inserted and tightened into place. The assembly was then incubated at 37°C for 48 hours to ensure sterility before placing in the test apparatus.

After incubation, the test apparatus was then inserted into the wind tunnel as follows:

The two side ports on the wind tunnel were removed and the test membrane inserted into the stationary brass membrane assembly holder. The string was passed up through the brass cap, and the cap put into place over the upper portion of the membrane assembly. The string was then attached to a line that ran up the wind tunnel a distance of two feet, then out through a hole in the plexiglas. The side port and plexiglas hole were then sealed. The apparatus was now positioned for test.

The air pressure line to the assembly and the air line away from the assembly were put into place and tightened. The pressure was then regulated and stabilized by means of a needle valve to some point above that required for the test.

4.2.2.3 Aerosol Generation and Maintenance

50 mg B. subtilis var niger spores were placed in the aerosol dispensing head in the same manner as with the quiescent tests and

positioned so that the explosive blast would be propelled directly into the front of the fan and thereby swept around the wind tunnel in a counter-clockwise motion.

The fan was then activated and adjusted to a pitot tube Δ P of 0.30 inches of water - corresponding to a wind velocity of 25 mph. (All tests were initiated at 25 mph for uniformity.)

The B. subtilis spores were then aerosolized into the chamber by means of a sudden blast of air pressure regulated to deliver 80 psi. The fan circulated the aerosolized spores for a period of 5 minutes before the fan speed was cut to zero and the tape covering the membrane hole was removed. The Δ P across the membrane (culture chamber pressure - stagnation pressure) was now trimmed to the test requirements as the fan speed was slowly increased to the desired speed.

The automatic Relay Controller was adjusted so that the normally closed solenoid valve allowing air into the membrane assembly would be activated by the on-off controller when the Δ P across the membrane dropped to a point .01 inches below the adjusted pressure.

In a similar manner, the relay controller regulating the "over pressurization" of the assembly was adjusted so that the normally

closed solenoid valve would activate and reduce the air pressure when a point approximately .05 inch above the required pressure was reached. The automatic relay controllers then regulated the Δ P across the test assembly for the duration of the test.

At the conclusion of the 72 hour test run, the membrane assembly was removed from the wind tunnel and the viable culture tube examined macroscopically for evidence of growth. The membrane hole was then examined microscopically to determine whether or not the hole was clogged. The results were then recorded and the assembly was cleaned and assembled for additional tests.

Aerosol particle distribution and stability determinations were made at various times during the course of the contract, and are recorded in Section 4.3.3 of this report.

4.2.3 Spore Preparation and Biological Materials

Viability of the culture through preparation and aerosol production is critical to the Viable Culture Technique. For this purpose, it appeared suitable to employ spores of a species of Bacillus subtilis var. niger. This was a logical choice because of its characteristic cultural morphology, stability of drying and storage, and general ease of handling. Spores used for this purpose were thoroughly cleaned to reduce clumping. The spores

were then freeze dried in order to provide uniform distribution in an aerosol.

The lyophilized spores of B. Subtilis used during the AMP II contract were from the same lot that was prepared for the AMP I contract. Information pertaining to spore preparation and particle sizing can be obtained from pages 37 and 38 and Appendix A of the AMP I Final Report.

4.3 APPARATUS VALIDATION

4.3.1 Flow Characterization

4.3.1.1 Flow Stability

The flow characteristics in the wind tunnels were determined by means of a smoke screen test. Initial tests indicated a high degree of turbulence which started in the fan area and persisted to the culture tube area. A successful solution to the problem was the use of 1/2 inch square plastic grid material about 2.5 inches thickness. This material, which was placed immediately after a set of turning vanes, sufficiently straightens the flow so that a stable condition was established in the culture tube area.

4.3.1.2 Flow Rates

Air flow through the 20 micron, 200 micron and 1000 micron holes were determined by either the Gow-Mac Flow-Mate Meter, a Wet test Meter*, or a conventional soap film flow meter, as in the case of the 20 micron hole, and the results tabulated in Figures 4.9, 4.10, and 4.11. The data points were obtained over a range of 20 inches of water pressure to 0.05 inches of water differential pressure.

Each membrane to be tested was installed in a membrane and culture tube holder without the air filters. An empty 25 x 75 mm test tube was mounted to the lower side of the membrane holder and leak checked. One side of the 1/4" OD S.S. tube was attached to a Dwyer manometer to regulate the ΔP across the membrane. The other side of the tubing was attached to an air supply regulated by means of a pressure regulator and a needle valve. A special conical cap containing a teflon O ring was screwed down on top of the membrane sealing the membrane within the membrane holder. A 1/4" OD stainless tube protruded from the top of the conical "cap" and was in turn connected to the appropriate measuring device.

For the 20 micron hole the cap was connected to a 1.0 cc

---

*Gow-Mac Flow-Mate Meter, Gow-Mac Instruments Company, Madison, New Jersey
Wet Test Meter - Precision Scientific Company, Chicago, Illinois

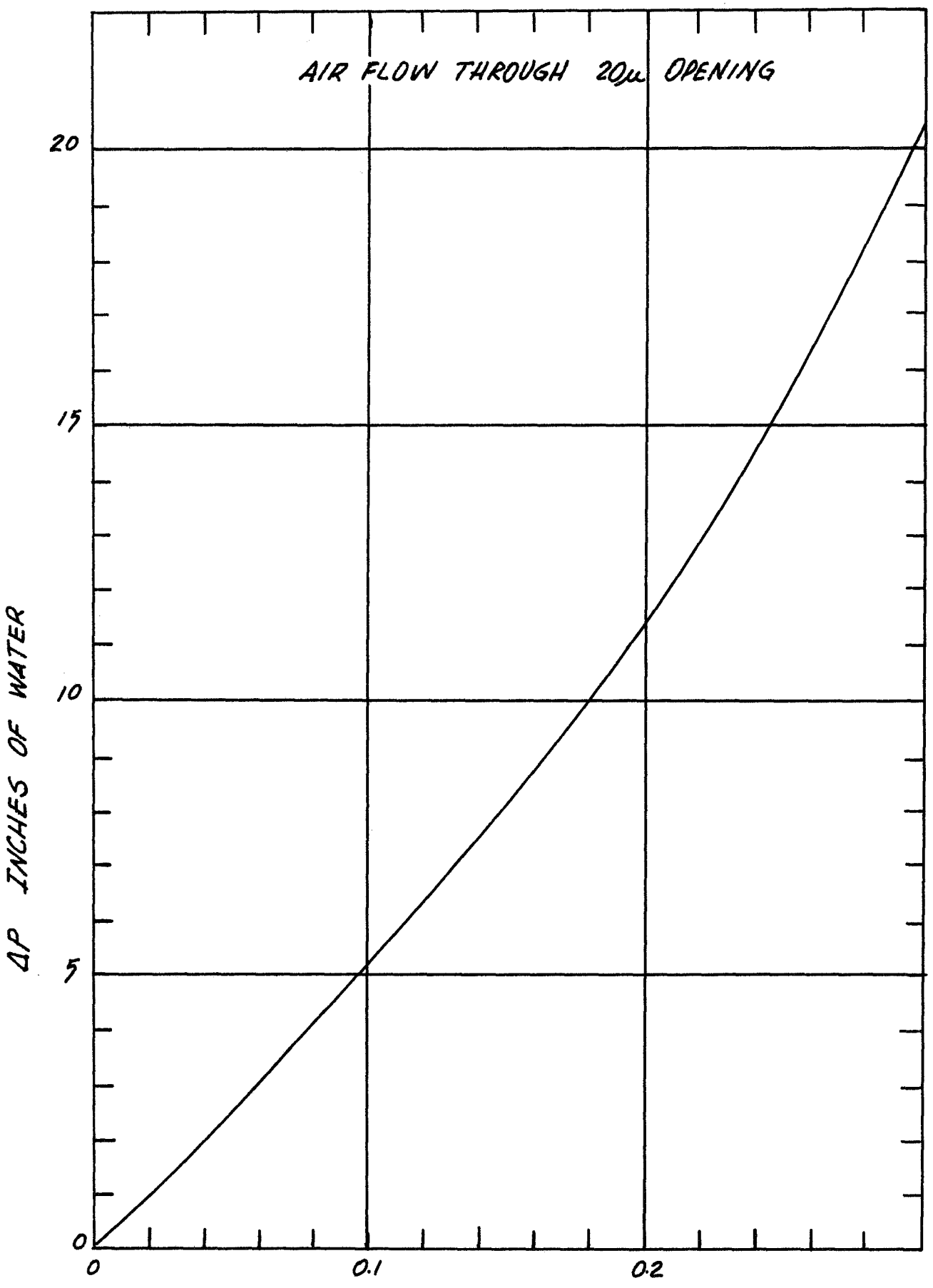
AIR FLOW THROUGH 20μ OPENING
20
15
10
5
0
ΔP INCHES OF WATER
0
0.1
0.2
CC's N2/MIN.

FIGURE 4.9

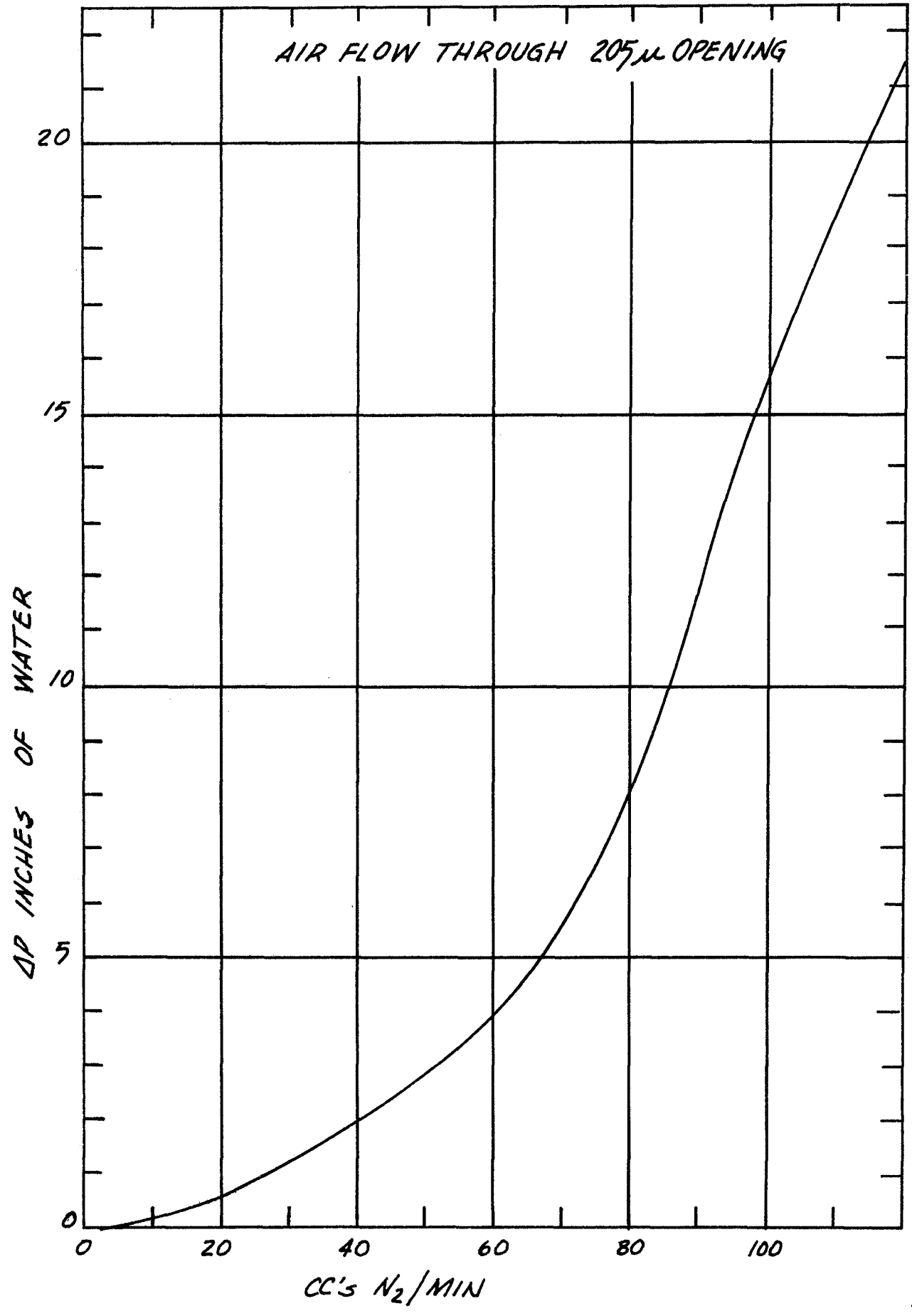
AIR FLOW THROUGH 205μ OPENING
ΔP INCHES OF WATER
0
5
10
15
20
0
20
40
60
80
100
CC's N_2/MIN

FIGURE 4-10

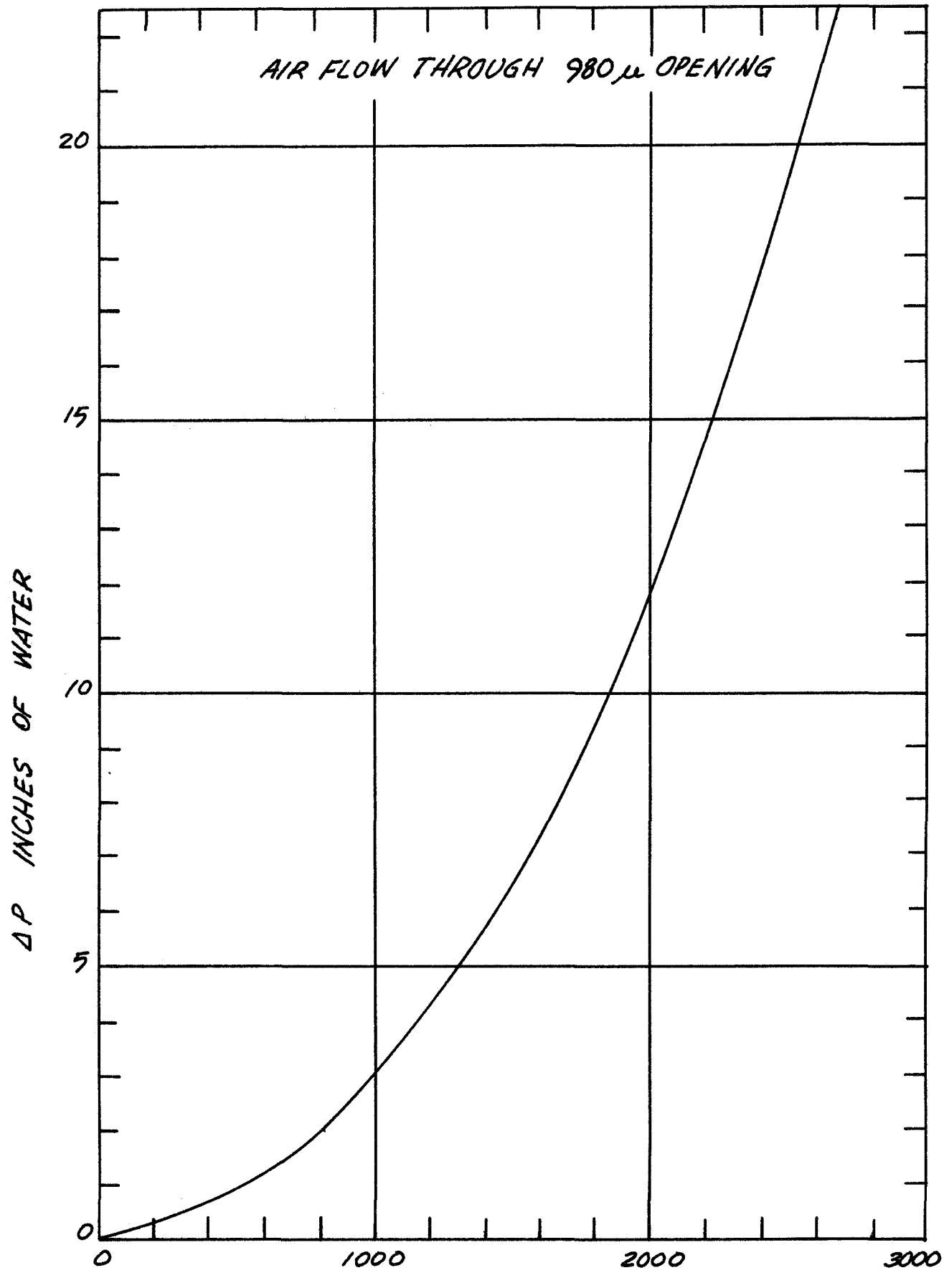
AIR FLOW THROUGH 980 μ OPENING
ΔP INCHES OF WATER
0
5
10
15
20
0
1000
2000
3000
CC's N2/MIN.

FIGURE 4-11

pipet graduated in .01 cc units. The air flow through the 20 micron hole was so small that it could not be measured on either of the other two instruments. A small drop of water was placed at the tip of the pipet and the flow rate determined. The results of this experiment are shown in Figure 4.9.

To measure the flow rate through the 200 micron holes and through the 1000 micron holes, a Gow-Mac Flow-Mater meter and a Wet test meter were used respectively. The use of the particular instrument was governed by the rate of air flow through the membrane hole. Figures 4.10 and 4.11 show the results of the 200 micron and 1000 micron flow rates.

4.3.2 Hole Characterization

Each membrane was examined microscopically and the hole characteristics and size observed.

Those membranes considered too large or too small in each size group were discarded. The 20 micron size holes included membranes with hole sizes ranging from 17 to 27 microns. The 200 size from 180-227 microns and the 1000 micron from 980-1020. Since the 20 and 200 micron diameter holes were drilled with a laser, the hole size top and bottom were of different dimensions.

To characterize the microscopic holes in the aluminum membranes,

Hole Characterization

150 x 170 Micron Hole

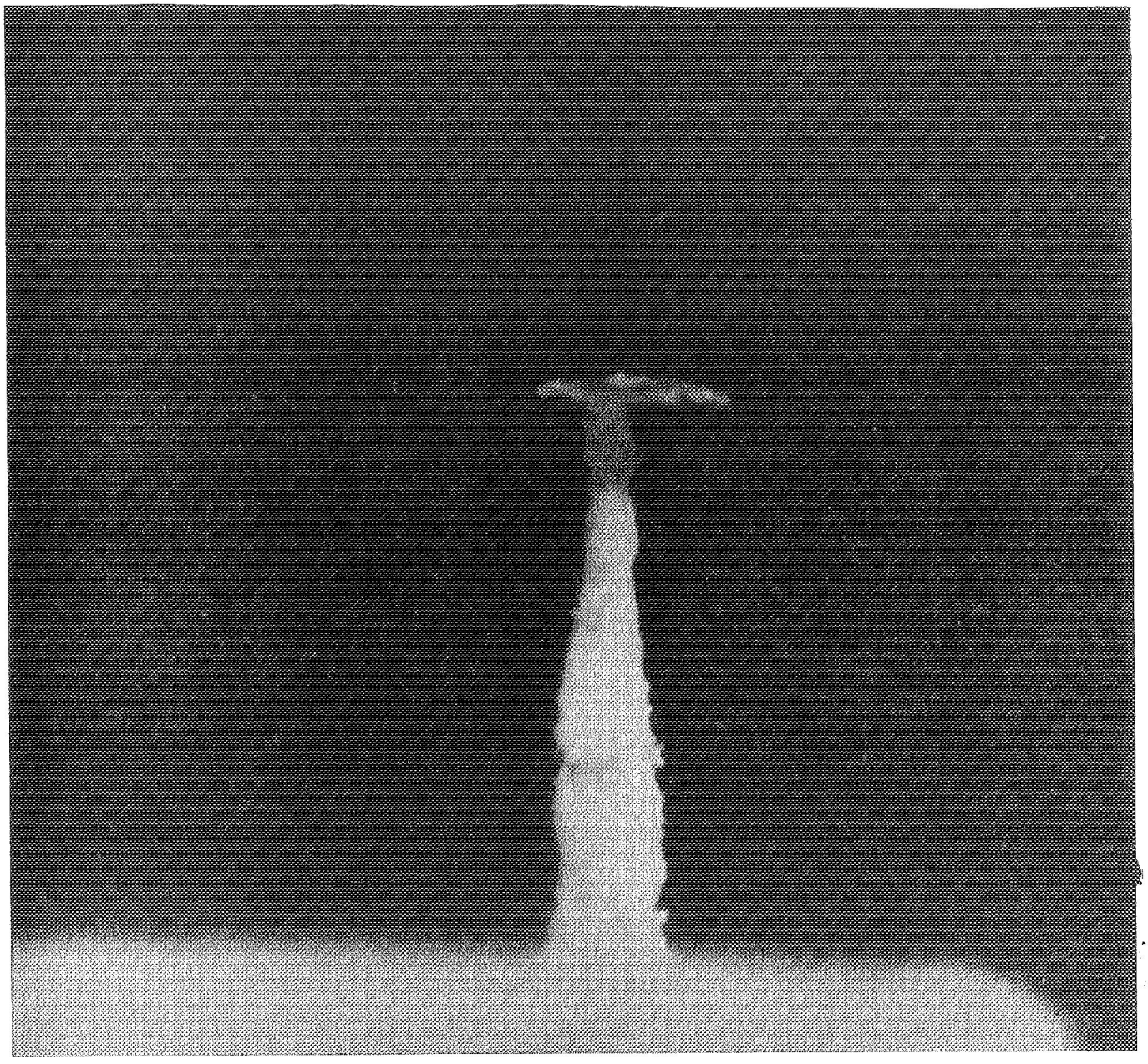

Figure P-4

a destructive technique was developed. This technique employed an epoxy resin to form a cast of the hole which is cured in place. The aluminum is then etched away with a 5 to 10% solution of hydrofluric acid and the remaining resin cast was photomicrographed and measured by means of an ocular micrometer. Photograph P-4 is a representative casting of a laser-drilled hole.

Measures by ocular micrometer and by construction on copies of the silhouettes show the casting to measure 802 micron in length, inclining 5^{o} from the vertical. The base of the casting measure 151 micron x 170 microns on the two diameters photographed while the opposite end measured 51 microns x 54 microns. The idealized geometry of the casting is that of a truncated cone with a 4^{o} half cone angle, the cone axis included 5^{o} from the normal to the base. Further detail can be obtained from the casting and the photographs to characterized roughness of the walls of the hole from which the casting was made.

E-63 epoxy resin (Techkits, Demarest, New Jersey) was prepared by mixing 3 parts of Part A with 2 parts of Part B. The mixture was then forced through the membrane hole with a spatula until the resin appeared on the opposite surface of the membrane. Particular care was required to avoid mixing air bubbles in the resin. A base of epoxy was then laid down on the side of the membrane on which the epoxy was applied to provide

Hole Characterization

200 Micron Hole

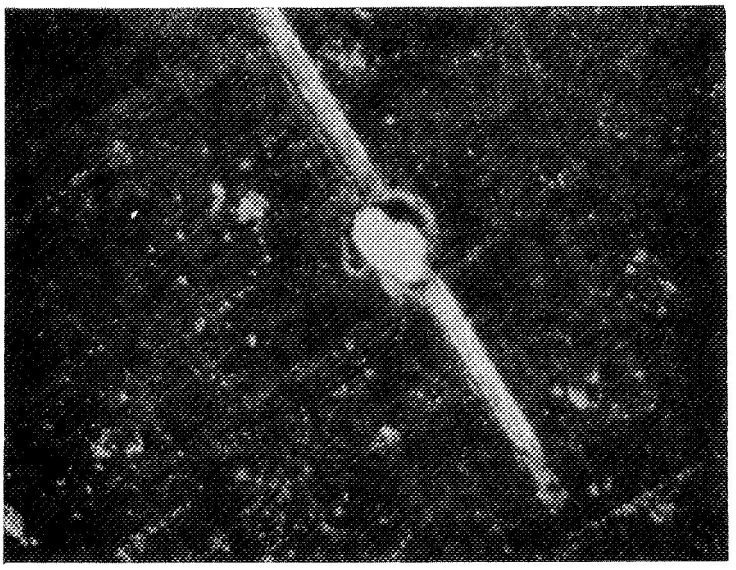

Hole Photomicrograph 100X

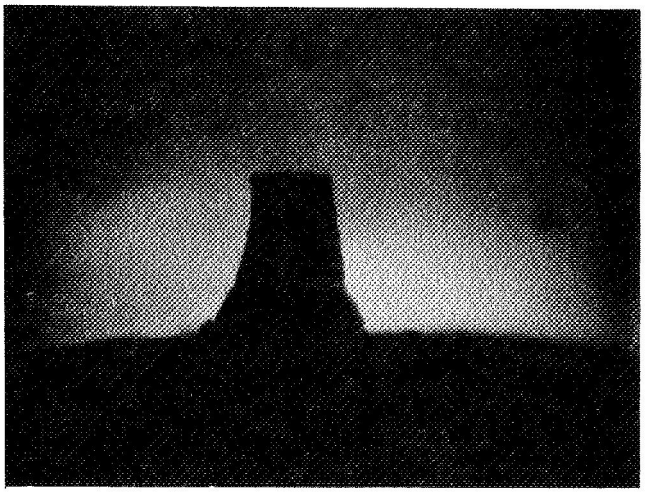

Casting - Silhouette

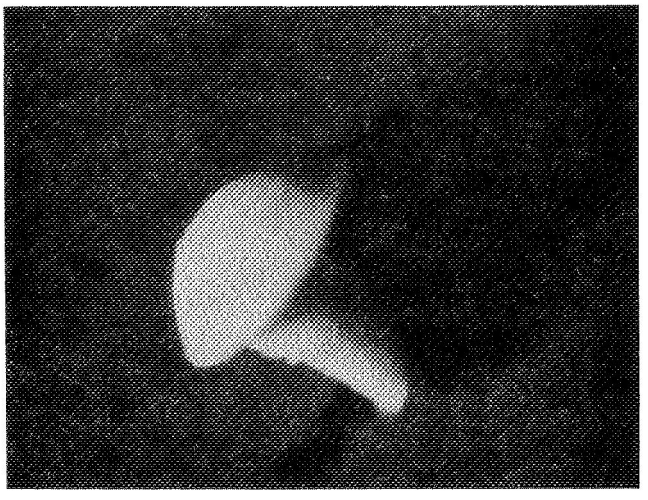

Casting Front Lighted 1 cm = 200 Microns

Figure P-5

Hole characterization

1000 Micron Hole

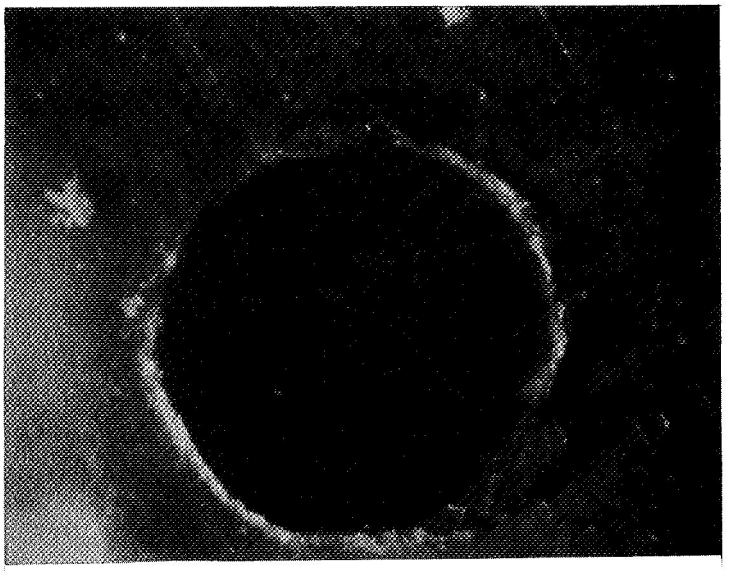

50X Enlargement

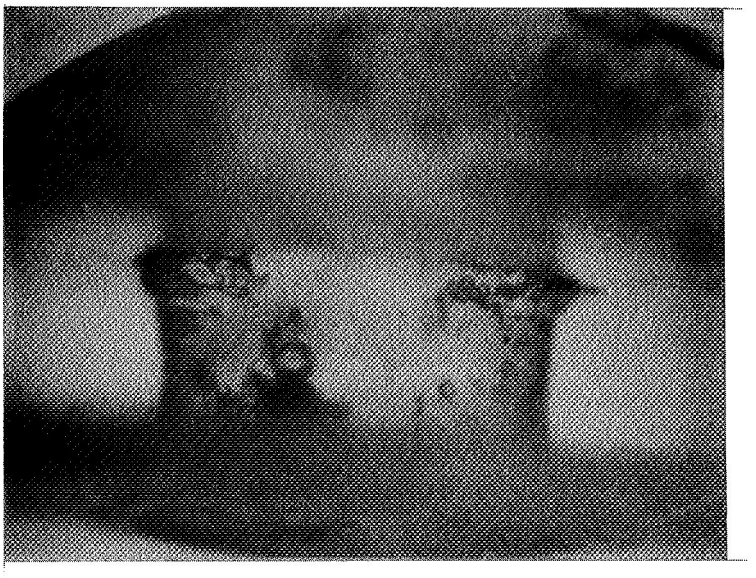

Epoxy Casting of Hole

1 cm = 200 Microns

Figure P-6

structural support to the casting. The epoxy was then cured for 10 minutes at 300°F. After trimming to about 3/8" square, the section containing the hole and casting was then immersed in a 5 to 10% HF solution until no metal remained. The casting was then rinsed, dried, trimmed and mounted for microscopic examination.

Figure P-5 is a photomicrograph of Membrane #23. One centimeter is equal to approximately 230 microns. These pictures are typical of the smaller size holes drilled by laser in that they are conical in configuration.

Figure P-6 is a photomicrograph of a 1000 micron diameter hole. This hole was made with a drill and bit and is more cylindrical in appearance than those drilled by laser.

Several different attempts were made to cast a 20 micron hole but all failed. The various epoxy resins and cements used would not penetrate the holes to give a cast. From the numerous microscopic examinations made with the 20 micron holes it is safe to assume that they are characteristically conical in configuration as are the 200 micron holes.

4.2.3 Aerosol Particle Distribution

4.2.3.1 Quiescent Chamber

Glass slides 1 x 3 inch in size were placed in an

aerosol chamber and covered with an aluminum shroud. The fan was activated and 50 mg of lyophilized B. subtilis spores were exploded into the chamber and allowed to circulate for a period of 5 minutes. The fan was then shut-off and the aerosol allowed to settle for a period of 15 minutes before the shroud was removed. The slides were then exposed for a period of one hour before removal and microscopic examination.

The particle sizes listed in Table 4.2 represent the maximum dimension, in microns, of the particle.

TABLE 4.2

PARTICLE DISTRIBUTION - QUIESCENT CHAMBER

Particle Size	Number Counted	Accumulative Total	% of Total
1 micron	188	188	35.2
2-5	246	434	46.2
6-10	81	515	15.2
11-15	11	526	2.1
16-20	3	529	0.6
21-25	2	531	0.3
26-30	1	532	0.1
30-35	2	534	0.3

The results of Table 4.2 indicate that approximately 99% of the particles falling on the glass slides after a 15 minute settling period, are 20 microns or less in diameter. The largest particle observed on the glass slide, was in the range of 30 to 35 microns.

4.3.3.2 Particle Distribution - High Velocity

Several experiments were performed on particle distribution in the high velocity-wind tunnels. These experiments were not as detailed as with the quiescent chambers, but were designed to serve as an indicator of the number of particles greater than 15 microns, to which a given area would be subjected in a given period of time.

The first of these experiments was carried out in the wind tunnel at a wind velocity calculated to be 30 mph. A black grid millipore filter (each grid was 9 mm^2) was covered during the aerosolization and for a 5 minute period before being exposed for 15 minutes to the chamber particles.

10-9 mm^2 grids were examined microscopically and the particles larger than 15 microns in diameter recorded in Table 4.3.

A second and similar experiment was performed with a glass slide. The set-up was similar to that of the quiescent chamber

experiment described above. The wind velocity in the tunnel was 30 mph and the exposure time 15 minutes.

TABLE 4.3

PARTICLE DISTRIBUTION - 30 MPH
(COLLECTOR - MILLIPORE FILTER)

Grid #	Particles $\geq$ 15 microns
1	10
2	6
3	13
4	7
5	19
6	4
7	21
8	16
9	7
10	27
Average No. Particles/grid = 13.0	
Average No. Particles/mm^2 = 1.44	

An Area 13.75 cm^2 was scanned under the microscope and all particles greater than 80 microns in diameter recorded. The total

number of particles observed on the slide (13.75 cm^2) was 1070. Table 4.4 represents the total number of particles (10) greater than 80 microns and their diameter.

TABLE 4.4

PARTICLE DISTRIBUTION - 30 MPH
(COLLECTOR - GLASS SLIDE)

Particle No.	Diameter
#1	233 microns
#2	213
#3	202
#4	200
#5	153
#6	133
#7	120
#8	100
#9	98
#10	80

Microscopic scanning of the membranes after test runs revealed that for tests run at 30-35 mph, particles as large as 230 microns in diameter are capable of remaining airborne, whereas at 15 mph, the largest particle observed was approximately 27 microns in diameter. The

wind velocity then becomes a significant factor in determining the size of the particles which may challenge the membrane holes. Photograph P-7 reveals the difference in particle sizes between a 25 mile run and 15 mile run.

4.3.3.3 Aerosol Stability - High Velocity

An experiment was conducted to determine the stability of the aerosol within the High Velocity Test Chamber. 50 mg. B. subtilis var niger spores were aerosolized into the wind tunnel with the air speed regulated to 15 mph - based on a water pressure of 0.14 inches of water (See Appendix C). Periodic air samples were taken by means of a 50 ml syringe and assayed for viable bacteria.

During the course of these early studies, it became apparent that the spores were adhering to the plexiglass walls of the wind tunnel due to a rapid build-up of electrostatic charge within the chamber.

To alleviate this build-up, aluminized mylar tape was affixed to the inside surfaces of the wind tunnel and grounded along with all metal pieces in the tunnel. The inside wooden surfaces were also treated with an antistatic solution in an effort to reduce the charge build-up. Table 4.5 shows the results before and after reduction of electrostatic charge.

High Velocity Aerosol Deposition

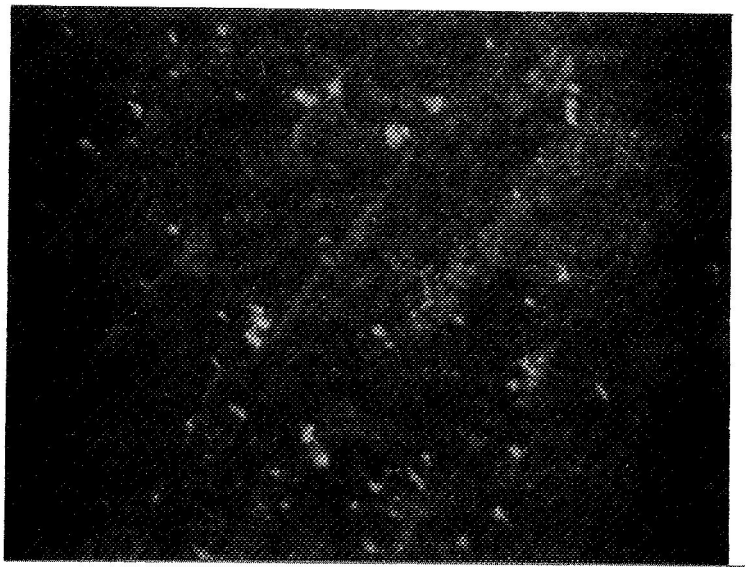

Particle Distribution at 15 mph

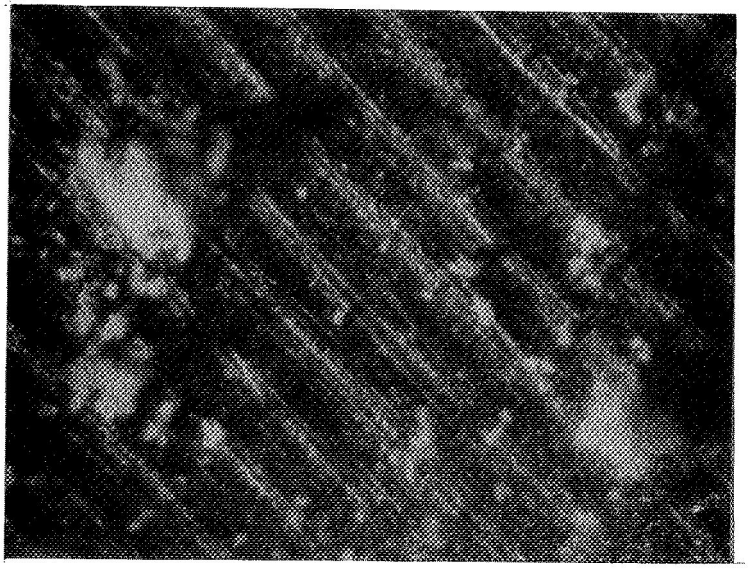

Particle Distribution at 35 mph

Figure P-7

TABLE 4.5

AEROSOL STABILITY WIND TUNNEL

Time (Minutes)	Count*/25 cc Air Sample	
	Not Grounded	Grounded
1	2100	10,000
10	530	500
30	13	40
60	0	4
180	----	8
360	---	0

* Counts before and after reduction of electrostatic charges on chamber walls. Air speed in test area = 15 mph

Although the counts per cc appear small, the total area in the wind tunnel is of the magnitude of 500 liters. Numbers as small as 4 per 25 cc when converted to total organisms within the tunnel become quite large (80,000). These particles driven at 25 mph take approximately 1 second to circumvent the tunnel. Thus the number of organisms challenging a membrane hole becomes quite large in a short period of time.

4.3.4 Microbial Challenge Conditions

4.3.4.1 Quiescent Tests

During some of the test runs, the aerosol was sampled and viable counts were made according to the following procedure, to evaluate the stability of the aerosol.

A sterile 50 ml disposable plastic syringe was attached to a 15 inch sterile French Feeding tube. This in turn was passed through a sterile flexible sampling tube guide which was placed in a rigid sampling tube guide. This was positioned at various depths in the aerosol chamber by inserting it through the rubber stopper at the top of the chamber. A 25 cc air sample was then obtained by withdrawing the syringe plunger to the 25 cc mark. The feeding tube was then removed from the chamber and the tip immersed in sterile deionized water. 25 ml of water was then drawn up into the syringe. The feeding tube was then knotted and the water and air sample mixed by vigorous shaking. Samples were then plated, in appropriate dilutions,mixed with sterile agar tempered to 45°C, and incubated at 37°C for 48 hours and counted. Results from some of these tests are shown in Table 4.6. These tests quantitated the viable counts of the bacterial aerosol still suspended in the chamber at various time intervals during the 72 hour test run.

TABLE 4.6

VIABLE AEROSOL COUNTS IN QUIESCENT CHAMBERS VS SAMPLING POINT

Chamber/Position	Elapsed Time				
	15 minutes	3 hours	5 hours	24 hours	48 hours
Chamber #1					
Top	5700/cc	3900*/cc	2100/cc	165/cc	55/cc
Middle	1800	2100	1800	875	29
Bottom	10700	1700	2600	710	115
Chamber #2					
Top	1700	1500*	1300	120	127
Middle	1500	1330	5100	110	38
Bottom	2300	6200	1600	81	41
Chamber #3					
Top	2200	2200	1600	156	15
Middle	500	2000	1700	16	5
Bottom	4700	2700	7200	71	17

* Estimated

During the early phase of the experimental program one of the viable culture tubes beneath a 190 micron membrane developed a bacterial colony after a period of 18 hours into the test run. This was not consistent with previous results at 0.5 inches water pressure with the 190 micron membrane. It was theorized that such a colony could not have grown from a single particle in such a short time at 23°C, but indeed was present before the final assembly, and overlooked due to its small size.

To test this hypothesis, four sterile culture tubes were exposed to a B. subtilis aerosol for 15 minutes. The tubes were then capped and left at room temperature to determine the time interval required to observe growth. The results are shown in Table 4.7.

TABLE 4.7

INVESTIGATION RESULTS INTO ANOMOLOUS QUIESCENT RUN

Time	Tube I	Tube II	Tube III	Tube IV
16 hours	Neg.	Neg.	Neg.	Neg.
18 hours	Neg.	Neg.	Neg.	Neg.
20 hours	Neg.	Neg.	Neg.	Neg.
22 hours	Neg.	Neg.	Neg.	Neg.
24 hours	Neg.	Neg.	Neg.	Neg.
28 hours	Neg.	Neg.	Neg.	Neg.
40 hours	Pos.	Neg.	Neg.	Neg.
48 hours	Pos.	Pos.	Pos.	Pos.

From these results, it becomes apparent that a minimum incubation time of forty-eight hours is necessary at room temperature to detect visually the growth of B. subtilis under the existing conditions. Hence the observed growth for the 190 micron membrane was due to an unsterile tube and not a penetration.

4.3.4.2 High Velocity Tests

An experiment was carried out to determine the number of organisms that would indeed transgress a 1000 micron membrane hole at zero ΔP in a given period of time at a given velocity.

50 mg. of B. subtilis was aerosolized into the tunnel with the air speed regulated at 15 mph. Tape covered a 1000 micron hole for the usual 5 minutes before being removed. Water replaced the agar in the visible culture tube. After a 5 minute period for the first test, and 30 minutes for the second test, the tubes were removed, and the water assayed for viable counts. Table 4.8 show the results of these two experiments.

TABLE 4.8

CHALLENGE TO 1000 MICRON DIAMETER HOLE*

Time of Exposure	Population Detected
5 minutes	12,000 spores
30 minutes	18,000 spores
* At 15 mph,	

These populations do not represent 12,000 and 18,000 challenges during the period of time exposed but represent the total number of viable bacteria that penetrated the membrane hole.

No direct attempt was made to quantitate the population challenge for the 20 or 200 micron holes. However tests run at zero Δ P during the course of the study did show positive culture tubes - our index of penetration.

5.0 EXPERIMENTS RESULTS AND DISCUSSION

5.1 QUIESCENT PROGRAM

A total of 39 runs at 0.5 inches differential water pressure, and 6 runs at 2.0 inches water pressure have been completed and represent more than 100% of the contractual requirements. Of the 5 runs utilizing membrane holes greater than 1000 microns in diameter, three were run with 1667 micron diameter holes, and two were run using a membrane with a hole diameter of 1887 microns. The 1887 micron hole probably represents the largest size capable of being tested using our present techniques. Hole sizes greater than this caused excessive water evaporation from the culture media, which could lead to erroneous results. (Table 5-1 is a summary of the quiescent test runs.)

The one positive test that appears in Table 5-1 became apparent 18 hours into the test run. This led to the experiment mentioned in Section 4.3.4 whereby 4 tubes were exposed to the aerosol and remained at room temperature for 48 hours. The results of this experiment proved conclusively that the colony was growing on the agar slant prior to its hook-up to the quiescent chamber, but was too small to be observed visually. Two additional tests were run using the same membrane and same holder with no penetration observed on either of them.

TABLE 5-1

QUIESCENT TEST RESULT SUMMARY

Number of Runs	Hole Size	Pressure	Test Results
12	20 Microns	0.5"	No Penetration
11	190 Microns	0.5"	No Penetration
1	190 Microns	0.5"	Penetration*
10	1000 Microns	0.5"	No Penetration
5	1000 Microns	0.5"	No Penetration
6	1000 Microns	2.0"	No Penetration
2	20 Microns	0.0"	Penetration
2	190 Microns	0.0"	Penetration
2	1000 Microns	0.0"	Penetration

* Test positive within 24 hours. Repeated twice with negative results; see Section 4.3.4.

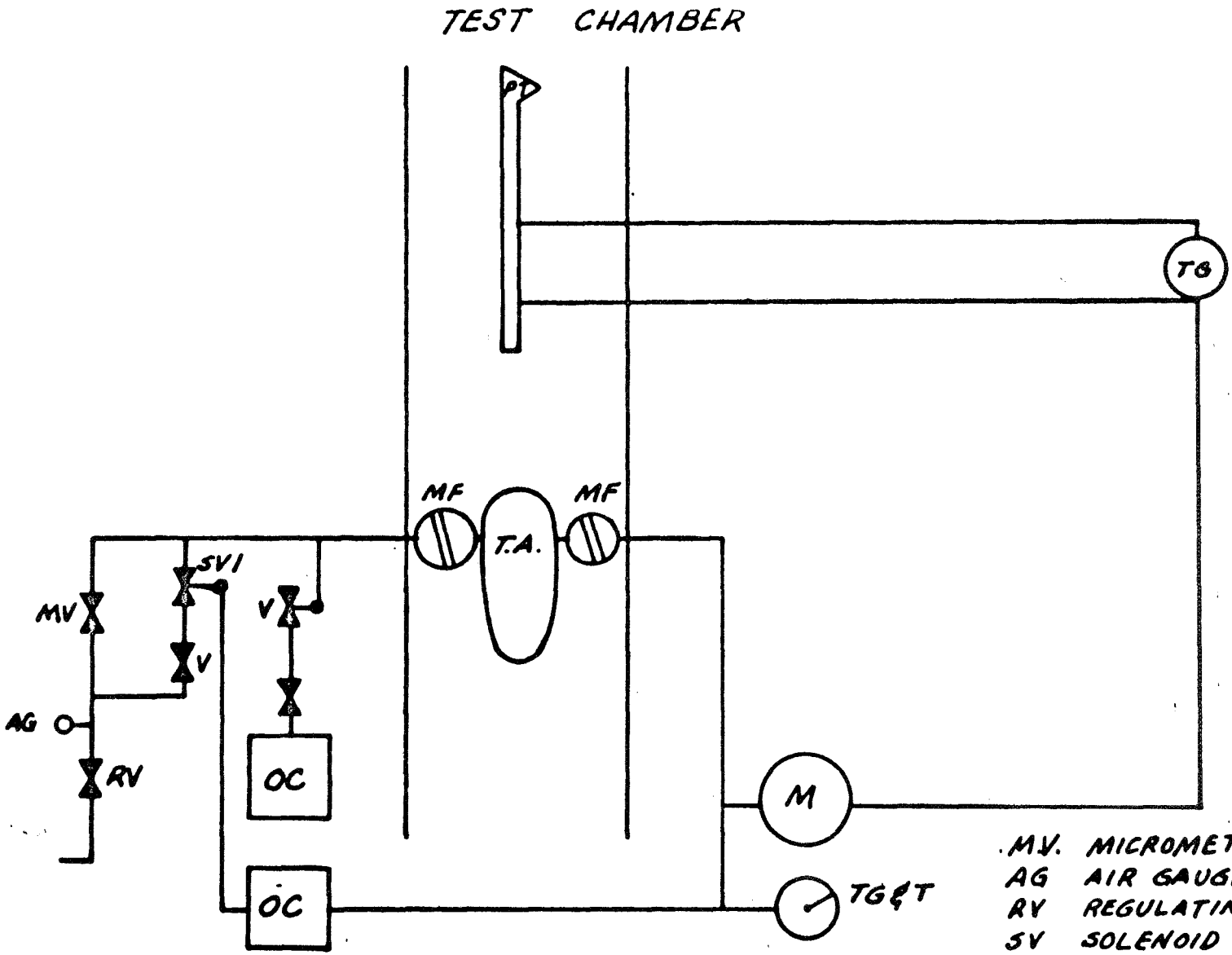

MV. MICROMETER VALVE
AG AIR GAUGE
RV REGULATING VALVE-AIR
SV SOLENOID VALVE
TA TEST ASSEMBLY
MF MILLIPORE AIR FILTER
TG&T MAGNAHELIC GAUGE & TRANSDUCER
M MANOMETER
PT PILOT TUBE
OC ON-OFF RELAY CONTROLLER

FIGURE 5.1

The quiescent test results, as evidenced by the build-up of statistical data, shows results consistent with the theoretical analysis of Section 3.1.2.3 which indicates that a pressure differential only slightly above ambient is all that is necessary to prevent penetration under ambient conditions. The particle approaching the hole at its terminal velocity is stopped by the positive Δ P across the membrane, at some point within the hole, and is swept back out by a pressure differential sufficient to overcome the gravitational settling.

The process of using one-half the prescribed amount of dehydrated culture medium was incorporated into those test assemblies which used the 1000 micron diameter membrane holes. This procedure was necessitated by the severe dehydration of the agar after 72 hours in the test assembly. The air flow across the viable culture tube and up through the membrane hole was sufficient to remove the larger portion of the moisture from the agar. Experimental tests determined that 0.75% to 0.8% agar (1/2 the prescribed amount) showed the least amount of water evaporation, yet was firm enough to maintain its angle of inclination in the viable culture tube.

The testing includes the use of a pressure differential to prevent spore particles with diameters of up to 35 microns and settling due to gravity, from passing through various size microscopic holes. Forty-five

tests on membrane holes ranging from 20 to 1887 microns in membranes 12 mils thick have been conducted. A pressure differential of 0.5 inches of water was found totally adequate in preventing penetration of bacterial particles under quiescent conditions.

Furthermore if one compares the measured flow rates through the various hole sizes (see Section 4.3.1) with the "worst case" settling velocities determined by the analysis in Appendix A, one can observe that penetration by particles of several hundred microns in diameter will be stopped by a Δ P of 0.5" of water.

5.2 HIGH VELOCITY PROGRAM

A total of 83 test runs were made utilizing the 20, 200 and 1000 micron membrane holes at wind velocities ranging from zero mph to 35 mph. Differential pressures from ambient to 3.6 inches water pressure above ambient were employed in an effort to prevent penetration.

The results of these tests are recorded in Figures 5.2, 5.3 and 5.4. The accuracy of the instrumentation controlling the air stream velocity within the wind tunnel (shown in Figure 5.1) is such that the velocity can be controlled to greater than 0.5 mph. Once adjusted to the desired speed, it will maintain that speed for the duration of the 72 hour

test. The only external condition that appears to change the ΔP across the pitot tube used to indicate wind velocity is room temperature. A drastic change in temperature ($10^{o}F$) will alter the fan speed by as much as 0.5 mph. Such a ΔP change is of slow onset, however, and will maintain itself so long as the condition exists. In addition, the flow stability in the test section was shown, by "smoke" tests, to be stable with no visible turbulence and little fluctuation. The combination of stable fan speed and stable flow ensures that the greater majority of particles ($d_s \leq 100$ microns) will challenge the hole with a constant speed. The possibility of a spread in speed values caused by turbulence (see Section 3.2.1) is believed to be eliminated or to be made very small.

From Figures 5.2 and 5.3 it becomes apparent that with the 20 and 200 micron holes, at wind velocities up to 25 miles per hour, a water differential pressure of 0.4 inch above ambient is sufficient to prevent penetration of all the airborne particles that were observed (see Section 4.3.3). As the air velocity increases beyond 25 mph the ΔP required rises sharply to 1.05 inches above ambient at 35 mph. This pressure is well within the 2.0 inch working limits set forth for the MAST program. Data from Figure 5.4, however, shows the effect a 1000 micron hole would have during such a program. Below 25 miles per hour, test data obtained suggests that 1.8 inches water pressure is the maximum amount of pressure required. Above 25 mph the ΔP limits have not been established for particles up to 230 microns in diameter.

20μ HOLES

EFFECT OF IMPINGING AIR STREAM VELOCITY ON MICROBIAL PENETRATION THROUGH MICROSCOPIC HOLES IN MEMBRANES

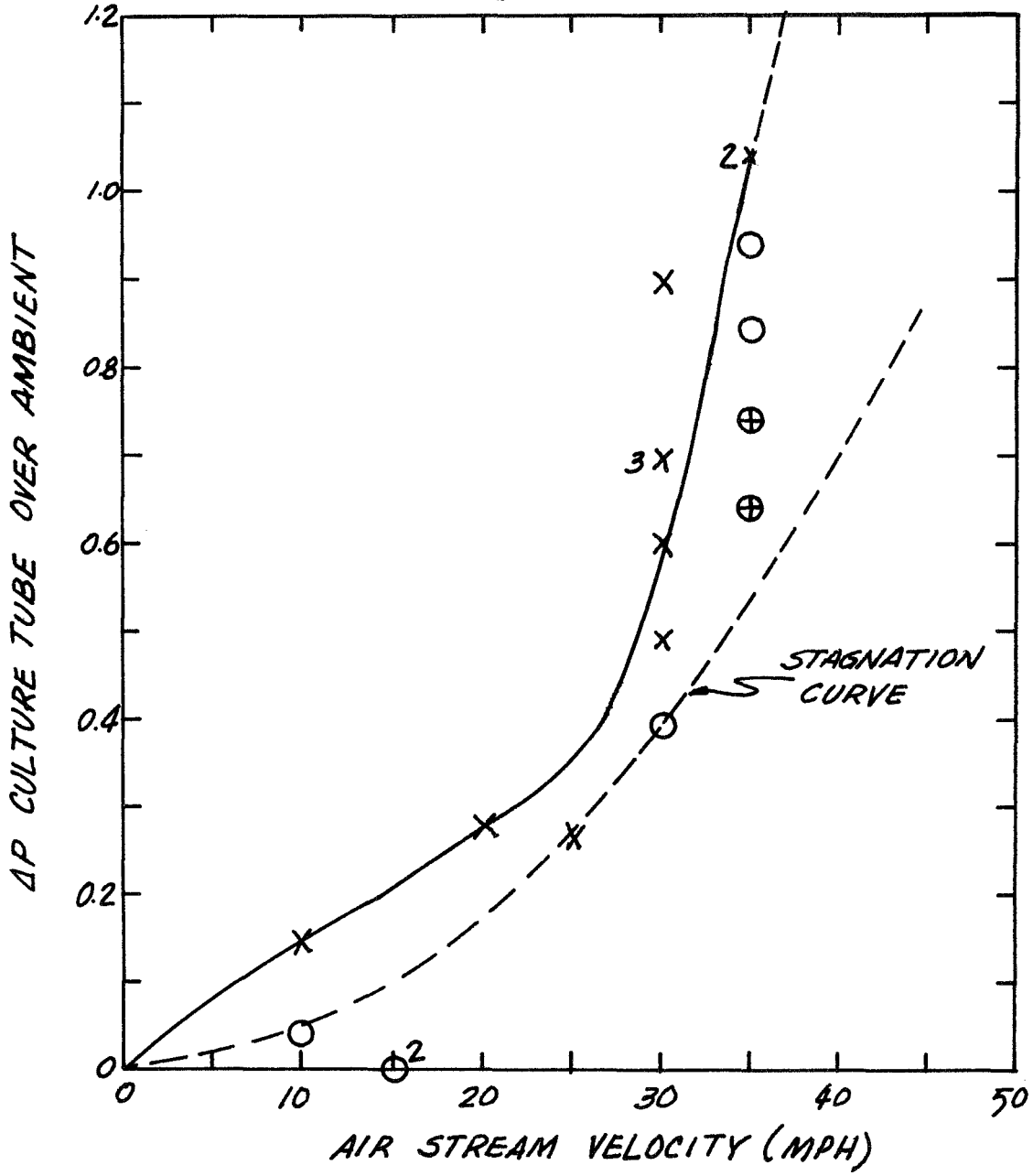

○ = POSITIVE
X = NEGATIVE
⊕ = CLOGGED

FIGURE 5.2

200 μ HOLES

EFFECT OF IMPINGING AIR STREAM VELOCITY ON MICROBIAL PENETRATION THROUGH MICROSCOPIC HOLES IN MEMBRANES

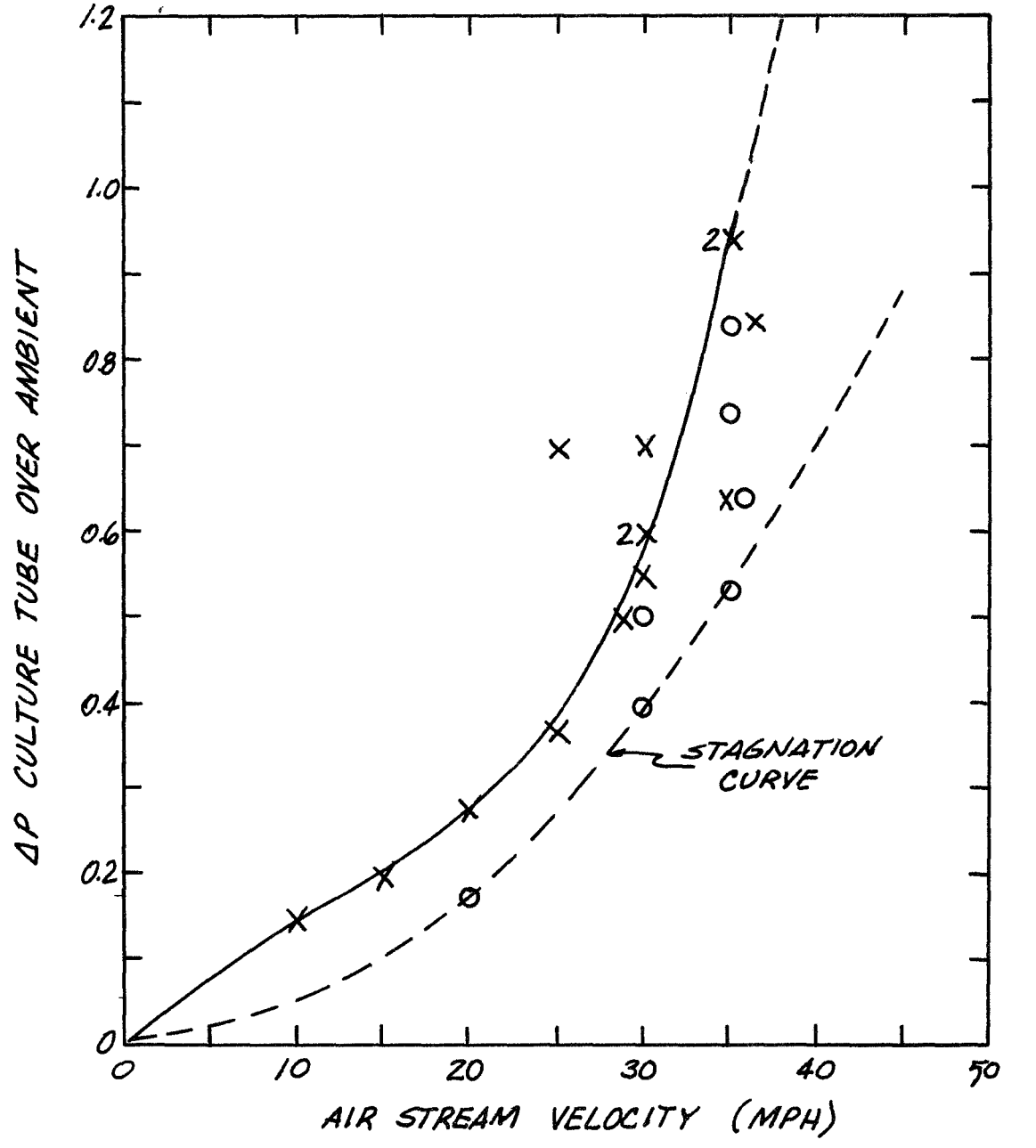

X = NEGATIVE
O = POSITIVE

FIGURE 5.3

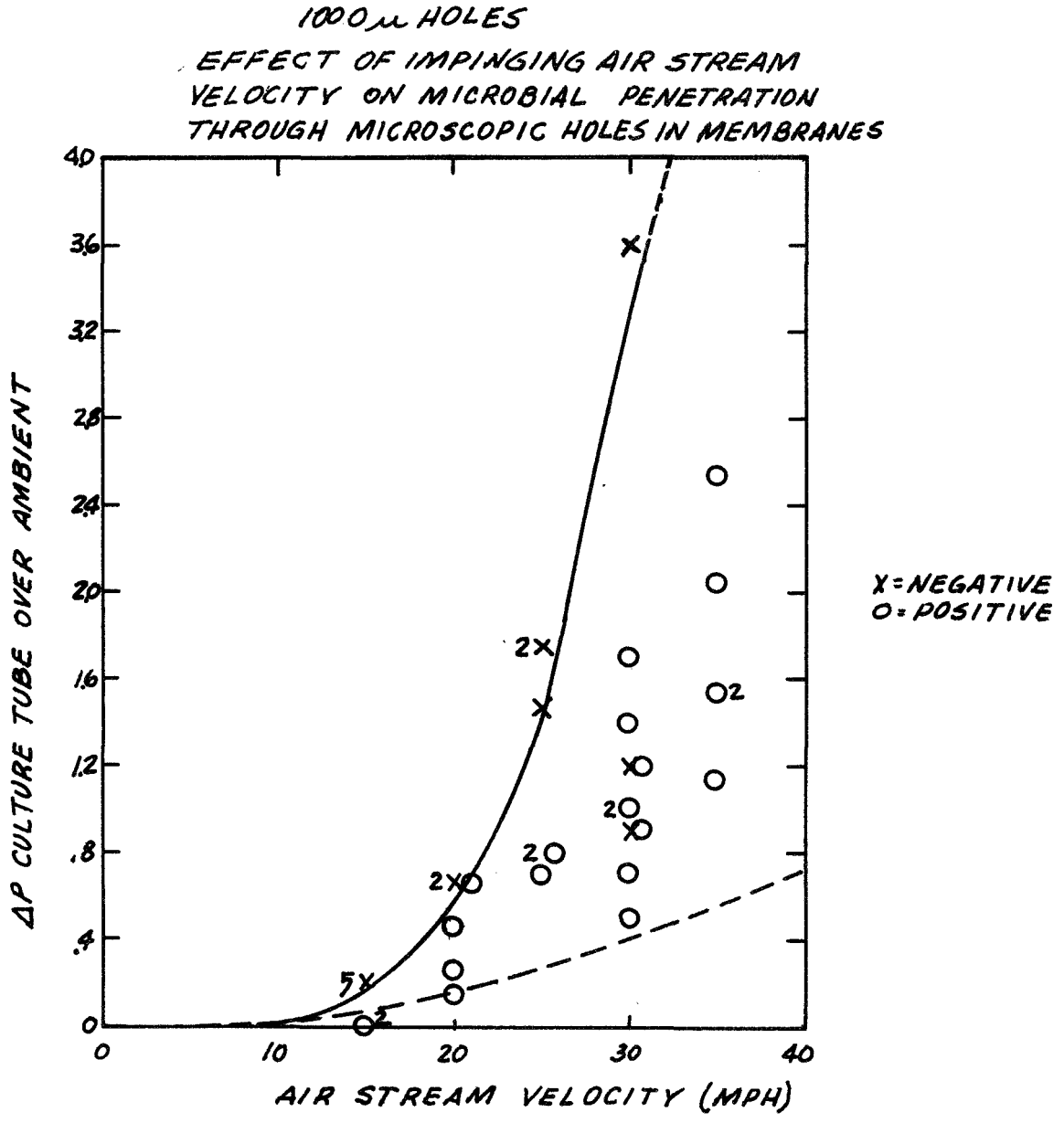
1000μ HOLES
EFFECT OF IMPINGING AIR STREAM
VELOCITY ON MICROBIAL PENETRATION
THROUGH MICROSCOPIC HOLES IN MEMBRANES
ΔP CULTURE TUBE OVER AMBIENT
AIR STREAM VELOCITY (MPH)
X = NEGATIVE
O = POSITIVE
0
.4
.8
1.2
1.6
2.0
2.4
2.8
3.2
3.6
4.0
0
10
20
30
40

FIGURE 5.4

Pressures in excess of 3.5 inches above ambient are required however.

In drawing the slope of the curves for Figures 5.2 and 5.3, a dotted line was included beyond the last data point showing negative results at 35 mph. Insufficient data is available to give a true picture of the slopes of the curves beyond the highest differential pressure points obtained.

The two points on the 20 micron curve designated as "clogged" were included after microscopic examination showed the membrane holes to be blocked. It was impossible to tell, microscopically, whether the hole was blocked by bacterial particulate, or by the formation of aluminum oxide during the sterilization-assembly-incubation procedure. It can be reasonably assumed that the results would indeed have been positive because of the two higher ΔP points showing positive results.

The area in Figure 5.4 which begins slightly above the ΔP reading of 1.8 inches water pressure, at 25 miles per hour, and extends up to 4.0 inches of water is uncertain in regard to the slope of the curve. Only by the accumulation of additional data, can we adequately define the slope in this particular area.

Throughout the experimental program, blank membranes were employed

as diagnostic tools to determine the efficiency of the membrane holders and gas line filters. In all instances, the viable culture tubes were void of microbial growth. It is evident then, that the positive results obtained throughout the experimental program were due to penetration through the membrane hole and not due to extraneous penetration by contaminants.

6.0 CONCLUSIONS

The experience gained with the quiescent and high velocity test equipment has shown that the techniques employed are of the utmost sensitivity. Accumulated test data indicates that the system is potentially sensitive to penetration of one microorganism, which upon transgressing the hole, would be deposited upon the culture media, and, during the 72 hour test run, would grow into a colony large enough to be observed visually.

6.1 QUIESCENT PROGRAM

The testing program has clearly demonstrated that a pressure differential of 0.5 inches of water is adequate to prevent penetration by spore particles with diameters of up to 35 microns. The testing, which covered hole diameters from 20 to 1887 microns, revealed no dependence of penetration on particle size and hole size. The theoretical analysis indicates this is most likely due to the fact that 0.5 inches of water yields efflux gas flow rates (see Figures 4.11 to 4.13) which are at least one hundred times larger than the 0.02 feet per second settling velocity for 15 micron diameter particles. The large relative difference in velocities means that 0.5 inches of water is a conservative pressure level

and any size dependence is being masked. In fact, a reasonable extension of the analysis (Appendix A) indicates 0.5 inch of water should stop the penetration of particles up to 200 microns in diameter under quiescent conditions for hole sizes up to several thousand microns in diameter.

6.2 HIGH VELOCITY PROGRAM

In general, a reasonable correspondence has been observed between the experimental program and simple flow analysis provided the flow velocities are below several hundred microns. The data for the 20 and 200 micron diameter holes in this region are not inconsistent with a v^2-dependence although we have used a straight line of V-dependent fit which is conservative. Moreover the very similar shape of the entire curves for the 20 and 200 micron diameter holes indicates a weak dependence on hole size. The experimental results therefore indicate a relationship of $\Delta P \propto \rho V_\infty^2/g_c$ when $V_\infty \leq$ 25 mph and $D_h \leq$ 200 microns. The difference between the experimental curve and the baseline curve for 1 micron particles is probably due to the discharge coefficient of 0.6 which is associated with sharp-edged orifices.

For larger velocities and hole sizes, both experiment and theory indicate a growing dependent on hole size and particle size. The simple flow analyses conducted in the program however are not sufficient to

describe the increased complexity of the flow conditions in the hole and the particle interactions with these flows. As a result, the experimental data provides the more reliable penetration threshold values. It should be observed that the simple theory shows a $\Delta P = 0.6$ inches of water after correction for discharge coefficient is required for 15 micron diameter particles moving at 30 mph. The experimental data for the 20 and 200 micron diameter holes match the prediction and lend credence to the spore population measurements showing a majority with $d_s \leq 15$ microns.

Prediction of penetration at reduced pressures (increasing altitudes) faces the same complexity of flow phenomena in holes compounded by the flow changing from continuum to free-molecular flow. It appears however that a conservative multiplication factor of 8 to 10 can be applied to the experimental threshold data to establish new curves that are valid for free-space vacuum. This extrapolation, of course, must be verified by an adequate flow analysis and until such an analysis is performed the factor should be used only as an indication of the required ΔP.

In general, the data indicate that practical application of pressurization techniques for maintaining asepsis depends upon control of particle size, particle density, and air velocity in the external environment.

7.0 RECOMMENDATIONS

The conclusions which can be drawn from the present program indicate that the following areas require additional work to fully satisfy the intended use of the AMP program results for the planetary quarantine field.

A. Additional testing should be undertaken under quiescent conditions to increase the confidence limits to acceptable levels.

B. The quiescent testing should concentrate on hole diameters equal to or in excess of 1000 microns since the dependence of penetration on hole size and particle size becomes increasingly significant as the hole size increases.

C. Additional testing should be continued, with the high velocity apparatus, using the larger membrane holes. Emphasis should be placed on the 1000 micron diameter holes at high wind velocities.

D. Experimental and theoretical effort should be expended to improve our understanding of the dependence of penetration on particle size and absolute ambient pressure values.

E. The study should be extended to evaluate the effectiveness of oxyethylene docosanol in preventing dehydration of the nutrient preparation in association with the larger diameter holes.

APPENDIX A

EQUATIONS OF MOTION FOR SPORE PARTICLES

The dimensional analysis study given in Section 3.1.2 is a useful summary of the many variables important to the AMP program. While it is helpful to have such an analysis to guide in organizing a test program, it is difficult to visualize in detail the problem of the drift motion of such small objects unless a quantitative analysis is performed. (Reference A-3)

We take the same dimensions, materials, etc. as in Section 3.1.2. The air is at standard conditions; the excess pressure in the container is of the order of 1 inch of water, which is $\sim$5.2 lbs/ft^2. Compared with the 2116 psf of the standard atmosphere, we neglect this and consider the air incompressible. The mean free path is of the order of 6×10^{-6} cm. The spore size (or aerosol droplet size) is taken to be 1 micron (10^{-4} cm); since the density is roughly the same as water we have its mass equal to $\pi/6 \times 10^{-12}$ grams.

First let us examine some motion histories, assuming that we can set such a small object in motion in still air. We imaging that we can shoot an individual spore at an initial velocity in a horizontal direction, and then see how it decelerates. For this exercise, we neglect the downward drift due to gravity.

If we take the maximum velocity of the test facility as an upper limit to velocity we have the following flow conditions (English units)

$$u = 58.6 \text{ fps (40 mph)}$$
$$\rho = .00238 \text{ slugs/ft}^3$$
$$\mu = 3.72 \times 10^{-7} \text{ slugs/ft sec}$$
$$d = 3.28 \times 10^{-6} \text{ ft}$$

The maximum Reynolds number in the flow is given by

$$R_{e_{max}} = \frac{58.6 \times 0.00238 \times 3.28 \times 10^{-6}}{3.72 \times 10^{-7}}$$

$$= 1.22 \text{ for the flow about the small sphere as it decelerates.}$$

Now, at $R_e = 1.22$ the drag departs only slightly from that given by Stokes' law, see e.g., Reference A-1. For our purposes of visualizing what happens, it is sufficient to assume Stokes' Law applies over the velocity range we are considering. Incidentially, it may be noted that Stokes' law gives C_D values smaller than those measured at $R_e \sim 1$, so that decelerations will not be over-estimated. We have from Stokes' law (again, see Reference A-1, e.g.)

$$\text{Drag} = D = 6\pi\mu r V$$

This is a very simple relation between the force acting on the body and its velocity in the fluid. To use this we make one modification; since the drag is a force directed oppositely to the velocity, we say

$$D = F = -6\pi\mu r V$$

Now if we put F = Ma, we have

$$F = -6\pi\mu r V = Ma = M\frac{dv}{dt}$$

From this we can write

$$\frac{dv}{dt} = \frac{-6\pi\mu r}{M} \cdot v$$

For convenience we set

$$\frac{6\mu\pi r}{M} = \alpha$$

then;

$$\frac{dv}{dt} = -\alpha v$$

$$\frac{dv}{v} = -\alpha dt$$

and $\ln v = \alpha t + C_1$

Now, we may call our particular case an impulsive motion; the velocity of the particle relative to the fluid goes from zero to v_o instantaneously. We set $v = v_o$ at $t = 0$, so that $C_1 = \ln v_o$.

Then $\ln v = \alpha t + \ln v_o$ or $\ln v - \ln v_o = \ln v/v_o = -\alpha t$, or $v = v_o e^{-\alpha t}$. We see that α should have the dimensions $1/t$;

$$\text{Dimensions of } \alpha = [\alpha] = \left[\frac{\mu r}{M}\right] = \frac{gm}{cm \cdot sec} \cdot \frac{cm}{gm} = \frac{1}{sec}.$$

If we put $\tau = 1/\alpha$, we can write this $v = v_o e^{-t/\tau}$. Then in τ seconds $v = v_o e^{-1} = (1/e)\, v_o$; the velocity has dropped to $0.37\, v_o$. In 2τ seconds, the velocity is equal to $(1/e^2)v_o$, or $0.135\, v_o$, etc. Further, at $t = 0$, $dv/dt = -\alpha v_o$, so that

$$\frac{1}{\alpha}\left(\frac{dv}{dt}\right)_{t=0} = \tau\left(\frac{dv}{dt}\right)_{t=0} = -v_o$$

the velocity would drop to zero in τ seconds if it continued to decelerate at its initial rate. We see that τ corresponds to the time constant of an electric current in an inductive circuit. If we consider the fluid in motion with velocity v_o with respect to the particle initially at rest, we can use

this same solution by saying the v, the velocity of the particle with respect to the fluid is equal to v', its velocity with respect to fixed axes, minus the fluid velocity v_o, thus

$$v = v' - v_o$$

As long as v_o is larger than v', the drag is in the direction of v_o, and opposite to v. Further, dv = dv', and when t = 0, $v = -v_o$. Then in our solution we have only to substitute

$$v = v' - v_o = (-v_o)e^{-\alpha t}$$

from which the velocity with respect to fixed axes v' becomes

$$v' = v_o (1 - e^{-\alpha t})$$

while the velocity with respect to the initial station in the fluid is

$$v = -v_o e^{-\alpha t}$$

the negative sign showing that it is a drift velocity opposite in sign to v_o. We can illustrate these results in Figures A1.a. and A1.b. Here the velocity of the particle is shown as a function of time. For convenience, we plot velocities by the ratio v/v_o so that the ordinate runs from zero to unity, while the time is given in units of t/τ. Figure A1.a. shows the particle projected in the fluid with the initial velocity v_o. The

initial rate of deceleration is shown by the straight line from $v/v_o = 1$, $t/\tau = 0$ to $v/v_o = 0$, $t/\tau = 1$. At $t/\tau = 1, 2 \ldots n$, we have $v/v_o = e^{-1}, e^{-2}, e^{-n}$. If we wish to consider a particle initially at rest and being accelerated by the surrounding fluid, we have the diagram of Figure 1A.b.; note that v' is the velocity relative to fixed axes.

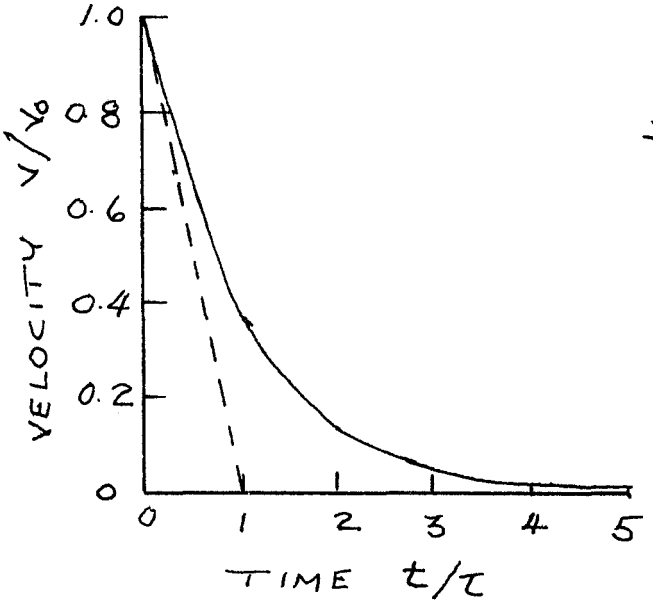

FIGURE A1 a

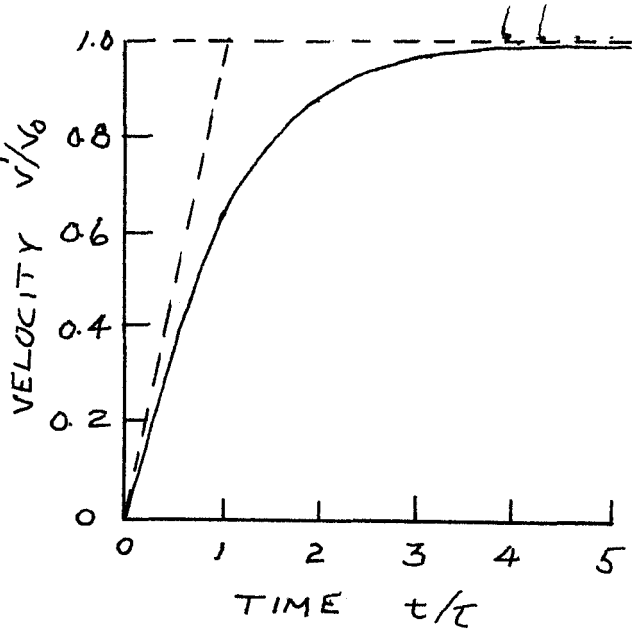

FIGURE A1 b

Let us now go one step further, and find distances associated with this particles impulsive Stokesian motion.

$$v = \frac{ds}{dt} = v_0 e^{-\alpha t}$$

from which

$$ds = v_0 e^{-\alpha t} dt \quad \text{or} \quad s = -\frac{v_0}{\alpha} e^{-\alpha t} + C_2$$

Let us set S = 0 at t = 0; then $C_2 = v_0/\alpha$ and

$$s = \frac{v_0}{\alpha}(1 - e^{-\alpha t}) \quad \text{or} \quad s = v_0 \tau (1 - e^{-t/\tau})$$

This is a very curious result: the particle never moves beyond the distance it would traverse in a time τ if it maintained its initial velocity. Again, let us see if we can represent this result graphically. We plot the ratio $S/v_0\tau$ against t/τ ; Figure A2 shows the results for the particle moving with respect to the fluid. This also shows the displacement of the particle from its original position in the moving fluid, but with the particle initially at rest and the fluid in motion.

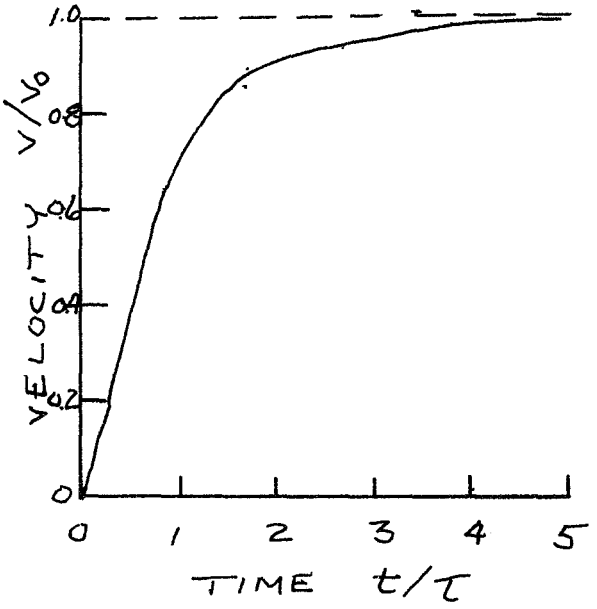

FIGURE A2

In this particular case of impulsive Stokesian motion it is impossible to cause a particle to move in the fluid beyond the distance $v_o \tau$.

Suppose we wish to describe the motion with respect to fixed axes of a particle initially at rest in the fluid moving a velocity v_o. Again we let v' represent the velocity with respect to fixed axes, and say

$$v = v' - v_o$$

from which we get

$$v' = v_0 + v = v_0 (1 - e^{-\alpha t})$$

Now we want

$$s = \int v' dt = \int v_0 (1 - e^{-\alpha t}) dt$$

$$= v_0 t + v_0 \tau e^{-\alpha t} + C$$

$$= v_0 t + v_0 \tau e^{-\alpha t} + C$$

When t = 0 we want S to be zero, so we have

$$C = -v_0 \tau$$

$$s = v_0 t - v_0 \tau (1 - e^{-t/\tau})$$

After a large time interval, the particle falls behind the fluid by the amount $v_o \tau$. Let us now see what magnitudes we have for our particular spore.

At standard atmospheric conditions, $\mu = 1.781 \times 10^{-4}$ gms/cm-sec. For our spore, r = 0.5 microns = 0.5×10^{4} cm = 5×10^{-5} cm.

$$M = \frac{\pi}{6} \times 10^{-12} \text{ gms}$$

Then

$$\alpha = \frac{6\pi\mu r}{M} = \frac{6\pi \times 1.781 \times 10^{-4} \times 5 \times 10^{-5}}{\frac{\pi}{6} \times 10^{-12}}$$

$= 3.207 \times 10^{5}$ sec^{-1}. We will be content to use $\alpha = 3.2 \times 10^{5}$ sec^{-1} and $\tau = 1/\alpha = 3.1 \times 10^{-6}$ sec., 3.1 microseconds.

If we imagine a spore projected at 30 mph (30 mph = 1341 cm/sec) in quiescent air, the velocity will drop to 0.05 x 1341 or about 65 cm/sec in the time 3τ (9.3 microseconds). During this time, the particle traverses a distance

$$S = 3.1 \times 10^{-6} \times 1341 \ (1-0.05)$$

$$S = 3.1 \times 1.34 \times .95 \times 10^{-3} \text{ cm}$$

or about 4×10^{-3} cm, say 40 microns. If we reverse our reference system and consider a particle set free in an air stream at this speed, within the 9 microseconds the particle would be moving at 95% of the stream velocity, and would only be lagging 40 microns behind its original location in the fluid

stream, which has in the meantime move approximately .0125 cm, or 1/8 of a millimeter. These distances are so small and the time so minute that we visualize the particle essentially following the flow as soon as it is introduced into the fluid.

Let us see what effect a sharp turbulent fluctuation in the flow would have on the path of the particle. For simplicity, let us assume: (1) that the droplet is initially moving with the fluid and (2) there is an instantaneous 10% increase in the velocity in its original direction. This corresponds to our impulsive velocity step. We see that the response of the particle is described by $v = (v'(t) - 1.1\ v_o)$, where again v is the velocity relative to the fluid, v' is the particle velocity in space, and $1.10\ v_o$ represents the fluid velocity after the instantaneous turbulent fluctuation. Now the only difference from the previous example is that at $t = 0$, $v' = 1.0 v_o$ so that $v = 0.1\ v_o$ at $t = 0$, and the functional relations become $v = (-0.1\ v_o)e^{-\alpha t}$, from which

$$v' = 1.1 V_o + v = 1.1 V_o - 0.1 V_o e^{-\alpha t}$$

$$= V_o + 0.1 V_o (1 - e^{-\alpha t})$$

Similarly, the lag of the particle behind its original position in the fluid is

$$S = 0.1\ v_o \tau\ (1 - e^{-\alpha t})$$

The relative drift between the particle and the fluid thus cannot exceed $0.1\ v_o \tau$; for our particular spore and for v_o = 1341 cm/sec, this amounts to 4.3 microns. Approximately 95% of this drift has been accomplished in 9 odd microseconds. If we wish to have on the average only 5% of the droplets in the turbulent fluid element left behind (i.e., move out of the fluid element), and if we assume the element is a small spherical volume, it can be shown that the diameter of this element must be approximately 25 times this lag distance, or about 100 microns (0.1mm). Now, it is very difficult to associate a physical length with a turbulent fluid element. Hinze (Reference A-2) gives for subsonic flows of velocity of the order of 100 m/sec, an estimate of the "smallest" eddy size of about 1 mm. We see that we can expect the droplets to follow the turbulent flow fluctuations with considerable exactness.

It is of interest also to consider the spore motion as the ambient pressure is reduced. We recognize that as the density of the gas within the AMP membrane decreases the flow conditions about a tiny sphere may range from continuum flow to what may become free-molecular flow when the ambient pressure is essentially zero and the pressure within the AMP membrane is correspondingly low.

To cover this wide range of flow conditions we make use of three different formulations for the drag on a sphere:

Stokes' Law: $$F = -6\pi\mu r V \tag{1}$$

Millikan's empirical modification of Stokes' law

$$F = -\frac{6\pi\mu r V}{1+\frac{L}{r}\left[A+B\exp\left(-\frac{Cr}{L}\right)\right]} \tag{2}$$

Epstein's relation:

$$F = -k\bar{V}_M \rho r^2 V \tag{3}$$

The nomenclature is given below.

F = force on sphere due to motion through the gas (lbs.)

μ = viscosity of gas (slugs/ft-sec)

V = relative velocity of sphere in gas (ft/sec)

r = radius of sphere (ft.)

L = mean free path of gas moleculars (ft.)

L/r = ratio of mean free path to radius of sphere (dimensionless)

$\bar{V}_M$ = mean molecular speed (ft/sec)

ρ = gas density (slugs/cu.ft.)

k = constant; for specular reflection of molecular impact K = 4 /3

A, B, C } empricial constants. For oil droplets, Millikan found A = 1.23, B = 0.41 and C = 0.88

Table 1 exhibits computations for a range of container pressures. The constant α is a measure of the acceleration of the particle due to its velocity through the gas; thus (Reference 2)

$$\text{acceleration} = \frac{dV}{dt} = \frac{F}{M_s} = \frac{-6\pi\mu r}{M_s} V = -\alpha V$$

for Stokes' law, so that for this flow regime,

$$\alpha = \frac{6\pi\mu r}{M_s}$$

Here M_s is the mass of the spores; the other quantities have been defined. For L/r of the order of unity, we obviously have

$$\alpha = \frac{6\pi\mu r/M_s}{1 + \frac{L}{r}\left[A + B\exp\left(-\frac{Cr}{L}\right)\right]}$$

while for free molecular flow

$$\alpha = \frac{\frac{4}{3}\pi \overline{V_M} \rho r^2}{M_s}$$

The dimensions of α are seconds^{-1}.

It was shown above that the maximum distance that a particle can traverse in a gas under such laws of force is given by

$$S = \tau V_0 \quad \text{where } \tau \text{ is a}$$

characteristic time equal to $1/\alpha$ and v_0 is the initial velocity of the spore in the gas. This parameter S_0 is the "Penetration Distance" given in Table 1.

We see from Table 1 that for a pressure range down to approximately one-thirtieth of an atmosphere the penetration of a one-micron spore into a quiescent gas would not exceed the membrane thickness (300 microns). An efflux velocity just greater than the drift velocity of the particle under gravitational attraction would thus be sufficient to assure aseptic maintenance. The last column in Table 1 gives this drift velocity, calculated either by Stokes' law or by the use of the empirical formulation for the drag force, Equation (2) and assuming constant (sea-level) gravity. Thus

$$F = M_s g = \frac{6\pi\mu r V_s}{1 + \frac{L}{r}\left[A + B\exp\left(-\frac{Cr}{L}\right)\right]}$$

whence

$$V_s = \frac{M_s g}{\left\{\frac{6\pi\mu r}{1 + \frac{L}{r}\left[A + B\exp\left(-\frac{Cr}{L}\right)\right]}\right\}} = \frac{g}{\alpha}$$

where v_s is the settling velocity and α is the constant previously defined.

From Table 1, we see that for a very large range of ambient pressures the general conclusions drawn previously for one micron particles still apply. However, if we go to ambient pressures less than 0.033 atmospheres, we must go beyond our simple "penetration distance" concept. We still wish to use a simple analysis, without solving the problem exactly. We assume for the next step that there is an over-pressure within the barrier. Thus, in Table 2 we tabulate internal pressures from 70.4 psf down to 10.4 psf, and ambient pressures 2" of water (10.4 psf) lower than these.

TABLE 1 PENETRATION DISTANCE FOR ONE MICRON PARTICLES AS A FUNCTION OF PRESSURE LEVEL WITHIN ASEPTIC MAINTENANCE BARRIER

Atm.	Pressure psf	in of H_2O	ρ Slugs/cu.ft.	L feet	L/r	α^{-1} sec	τ Micro-seconds	S_o Microns	V_S ft/sec
1	2116	407	2.38×10^{-3}	2.17×10^{-7}	0.133	3.21×10^{5} 2.86	3.12 3.50	42.0 47.0	1.00×10^{-4} 1.10
0.5	1058	203	1.19	4.36	0.266	2.41	4.15	55.6	1.33
0.2	423	81.2	4.76×10^{-4}	1.09×10^{-6}	0.665	1.70	5.89	79.0	1.89
0.133	282	54.2	3.16	1.64	1.00	1.34	7.50	101	2.40
0.1	211.6	40.7	2.38	2.18	1.33	1.10	9.09	122	2.92
0.0665	140.5	27.0	1.58	3.28	2.00	8.06×10^{4}	12.4	167	3.99
0.0443	93.5	18.0	1.05	4.92	3.00	5.73	17.4	234	5.62
0.04	84.6	16.3	9.52×10^{-5}	5.45	3.32	5.24	18.1	244	6.15
0.0332	70.0	13.5	7.90	6.56	4.00	4.45	22.5	302	7.22

Temperatures within membrane assumed constant at 518.6°R

ρL assumed constant, equal to 5.17×10^{-10} slugs/ft^2

V_o = initial spore velocity = 30 mph = 44 fps = 1342 cm/sec

r = spore radius = 1/2 micron (1.64×10^{-6} ft.)

V_S = settling velocity of spore under standard gravitational force

TABLE 2 APPROXIMATE PENETRATION ANALYSIS AT LOW AMBIENT PRESSURES FOR ONE MICRON PARTICLES

Interior Pressure psf	Ambient Pressure psf	Alt. Corres. to P_∞ kft	Efflux Velocity V_e fps	L feet	L/r	Seconds^{-1} α	Micro-seconds t_1	Microns $v_s t_1$
70.4	60	79.5	526	7.25×10^{-6}	4.4	4.65×10^{4}	1.72	23
50.4	40	88	631	1.08×10^{-5}	6.6	3.07	2.2	30
30.4	20	103	835	2.04	12.4	1.60(Eq.2) 1.12(Eq.3)	3.2 4.6	43 62
20.4	10	119	1020	3.57	21.7	6.23×10^{3}	6.8	91
16.4	6	132	1020	4.43	27	5.04	8.4	113
12.4	2	157	1020	5.86	35.7	3.79	11.1	149
11.4	1	180	1020	6.40	39	3.46	12.2	164
10.9	0.5	198	1020	6.65	40.5	3.34	12.6	169
10.6	0.2	220	1020	6.90	92	3.23	13	175
10.4	0	∞	1020	7.00	42.6	3.17	13.3	179

$\Delta p = p_i - p_\infty = 10.4$ psf $= 2"\ H_2O$

$v = v_o e^{-\alpha t}$;

$v_o = v_e + v_s$, with $v_s = 44$ fps

$v = v_e$ when $t = t_1$, i.e.

$v_e = (v_e + v_s)e^{-\alpha t}$

REFERENCES

A-1 Prandtl - Tietjeus: Applied Hydro and Aeromechanics, McGraw-Hill Book Company, Inc. (1934), (see page 115, Figure 61).

A-2 Hinze: Turbulence, McGraw-Hill Book Company, Inc., (see p. 7).

A-3 Long, M.; "Penetration of Large Contaminants"; GE PIR 9522-103, 11/6/69.

APPENDIX B

WIND TUNNEL FAN - VIBRATION ANALYSIS

B.1 INTRODUCTION

The purpose of this analysis is to determine the cause of the severe vibrations occurring in the wind tunnel fan system. Once this is known corrective recommendations are made to eliminate the vibrations.

The main areas assessed were the shaft alignment in the bearings, the shaft critical frequency, and the support structure resonance. The maximum operating fan speed is 5000 rpm or an equivalent of 83.3 cps. The shaft and support structure resonant frequencies should be far removed from the fan operating speed.

The following analysis assesses the present fan system (Figure 3.1.11) for the above possible causes of vibration (Reference B-1).

II - ANALYSIS

A - ALIGNMENT

The present fan system utilizes 2 sleeve bearings. A small misalignment of the shaft through the bearings would cause a moment at the bearings and during fan operation severe vibrations could occur. A self-aligned bearing would eliminate this problem.

B - SHAFT CRITICAL FREQUENCY

DYNAMIC MODEL FIG-2

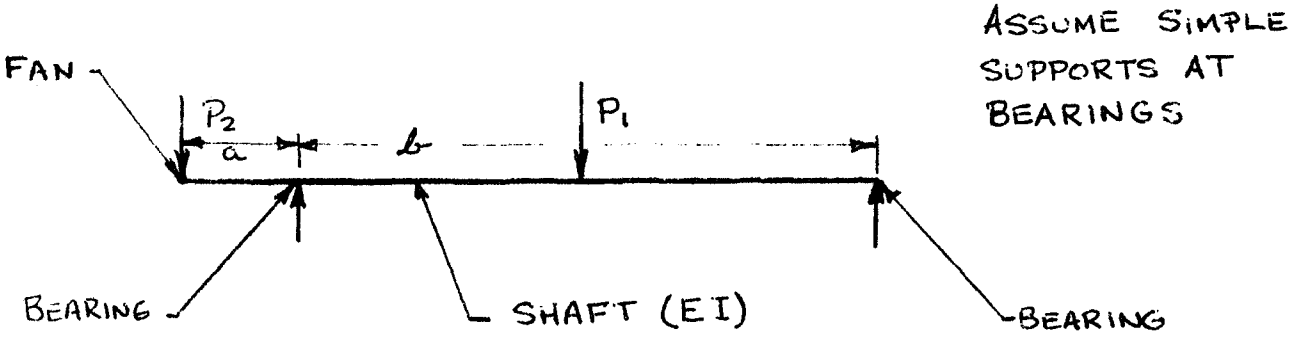

DEFINITIONS:

y_1 = DEFLECTION OF b DUE TO LOAD P_1
y_2 = DEFLECTION OF a DUE TO LOAD P_2
y_{12} = DEFLECTION OF b DUE TO LOAD P_2
y_{21} = DEFLECTION OF a DUE TO LOAD P_1

SOLVING FOR DEFLECTIONS

$$y_1 = \frac{P_1 b^3}{48EI} \qquad a_{11} = \frac{y_1}{P_1} = \frac{b^3}{48EI}$$

$$y_2 = \frac{1}{3}\frac{P_2 a^3}{EI} + (-a)\left[-\frac{1}{3}\left(\frac{P_2 a b}{EI}\right)\right]$$

$$a_{22} = \frac{y_2}{P_2} = \frac{1}{3}\frac{a^3}{EI} + \frac{1}{3}\frac{a^2 b}{EI}$$

$$y_{12} = -a\,\theta_c = -a\,\frac{P_1 b^2}{16EI}$$

$$a_{12} = \frac{y_{12}}{P_1} = \frac{-a b^2}{16EI}$$

AND

$$a_{12} = a_{21}$$

NOW SOLVING THE EQUATION OF MOTION

$$M\ddot{x} + Kx = 0$$

$$\ddot{x} = -\omega^2 x$$

$$-\omega^2 M x + Kx = 0$$

DIVIDE BY ω^2 & MULTIPLY BY $1/K$

$$-K^{-1} M x + \frac{1}{\omega^2} x = 0$$

SOLVING IN MATRIX FORMAT

$$\left\{ \begin{bmatrix} -a_{11} & -a_{12} \\ -a_{21} & -a_{22} \end{bmatrix} \begin{bmatrix} M_1 & 0 \\ 0 & M_2 \end{bmatrix} + \begin{bmatrix} 1/\omega^2 & 0 \\ 0 & 1/\omega^2 \end{bmatrix} \right\} \begin{Bmatrix} x_1 \\ x_2 \end{Bmatrix} = 0$$

LET $1/\omega^2 = \lambda$

$$\begin{bmatrix} -a_{11} M_1 & -a_{12} M_2 \\ -a_{21} M_1 & -a_{22} M_2 \end{bmatrix} + \begin{bmatrix} \lambda & 0 \\ 0 & \lambda \end{bmatrix} = 0$$

$$\begin{vmatrix} -a_{11} M_1 + \lambda & -a_{12} M_2 \\ -a_{21} M_1 & -a_{22} M_2 + \lambda \end{vmatrix} = 0$$

CHANGE SIGNS & SOLVE ABOVE DETERMINANT

$$(a_{11} M_1 - \lambda)(a_{22} M_2 - \lambda) - (a_{12} M_2)(a_{21} M_1) = 0$$

$$a_{11} M_1 a_{22} M_2 - \lambda (a_{11} M_1 + a_{22} M_2) + \lambda^2 - (a_{12} M_2)(a_{21} M_1) = 0$$

REGROUPING

$$\lambda^2 - \lambda (a_{11} M_1 + a_{22} M_2) + M_1 M_2 (a_{11} a_{22} - a_{12} a_{21}) = 0$$

LET :

$$B = a_{11} M_1 + a_{22} M_2 \quad \& \quad C = M_1 M_2 (a_{11} a_{22} - a_{12} a_{21})$$

REDUCES TO :

$$\lambda^2 - B\lambda + C = 0$$

SOLVING FOR λ USING THE QUADRATIC FORMULA

$$\lambda = \frac{B \pm \sqrt{B^2 - 4C}}{2}$$

MUST NOW DETERMINE COEFFICIENT
B & C FROM DATA

DATA - FROM FIGURE -1

a, b, M_1, M_2, & EI

LENGTH

$a = 1.5$ IN. $\quad a^2 = 2.25\ IN^2 \quad a^3 = 3.375\ IN^3$

$b = 22.67$ IN. $\quad b^2 = 518\ IN^2 \quad b^3 = 11{,}750\ IN^3$

MASS

M_1 = MASS OF SHAFT (ASSUME 14" EFFECTIVE)

$$M_1 = \frac{W_T\ (14\ IN)}{g} = \frac{1.74\ lbs}{386\ IN/SEC^2} = 4.5 \times 10^{-3}\ \frac{lbs\text{-}SEC^2}{IN}$$

M_2 = MASS OF SHAFT + FAN $\qquad W_{T\ FAN} = .75$ lbs (MEASURED)

$$M_2 = \frac{W_{T_{FAN}} + W_{T_{SHAFT}}}{g} = \frac{.75\ lbs + .187\ lbs}{386\ IN/SEC^2} = 2.4 \times 10^{-3}\ \frac{lbs\text{-}SEC^2}{IN}$$

EI

$E = 30 \times 10^6\ PSI$ (STEEL SHAFT)

$$I = \frac{\pi d^4}{64} \qquad \text{WHERE: } d = .6875\ IN \ \& \ d^4 = .22\ IN^4$$

$$I = \frac{\pi \times .22}{64} = 1.08 \times 10^{-2}\ IN^4$$

$$EI = 30 \times 10^6\ PSI \times 1.08 \times 10^{-2}\ IN^4 = 3.25 \times 10^5\ lbs\text{-}IN^2$$

THEN: (PAGE 4)

$$a_{11} = \frac{11{,}750}{48 \times 3.25 \times 10^5} = .75 \times 10^{-3}$$

$$a_{22} = \frac{1}{3}\frac{3.375}{3.25 \times 10^5} + \frac{1}{3}\frac{2.25 \times 22.67}{3.25 \times 10^5} = 5.6 \times 10^{-5}$$

$$a_{12} = -\frac{1.5(518)}{16 \times 3.25 \times 10^5} = 15 \times 10^{-5}$$

$$a_{21} = a_{12} = 15 \times 10^{-5}$$

SOLVING FOR COEFFICIENT B & C (PAGE 6)

$$B = a_{11} M_1 + a_{22} M_2$$

$$B = .75 \times 10^{-3} \times 4.5 \times 10^{-3} + 5.6 \times 10^{-5} \times 2.4 \times 10^{-3}$$

$$B = 3.514 \times 10^{-6}$$

$$C = M_1 M_2 (a_{11} a_{22} - a_{12} a_{21})$$

$$C = 4.5 \times 10^{-3} \times 2.4 \times 10^{-3} (.75 \times 10^{-3} \times 5.6 \times 10^{-5} - 15 \times 10^{-5} \times 15 \times 10^{-5})$$

$$C = 2.1 \times 10^{-13}$$

SOLVING FOR λ

$$\lambda = \frac{B \pm \sqrt{B^2 - 4C}}{2}$$

$$\lambda = \frac{3.514 \times 10^{-6} \pm \sqrt{12.4 \times 10^{-12} - 8.4 \times 10^{-12}}}{2}$$

TWO SOLUTIONS

$$\lambda_1 = 1.757 \times 10^{-6} + \tfrac{1}{2}(3.4 \times 10^{-6}) = 3.457 \times 10^{-6}$$

AND

$$\lambda_2 = 1.757 \times 10^{-6} - \tfrac{1}{2}(3.4 \times 10^{-6}) = .057 \times 10^{-6}$$

SOLVING FOR FREQUENCY USING λ_1

$$\lambda_1 = \frac{1}{\omega_1^2}$$

$$\omega_1 = \sqrt{1/\lambda_1} = \sqrt{\frac{1}{3.457 \times 10^{-6}}} = .54 \times 10^3$$

$$f_1 = \frac{\omega_1}{2\pi} = \frac{.54 \times 10^3}{2\pi} = 86 \text{ CPS}$$

SOLVING FOR FREQUENCY USING λ_2

$$\lambda_2 = 1/\omega_2^2$$

$$\omega_2 = \sqrt{1/\lambda_2} = \sqrt{\frac{1}{.057 \times 10^{-6}}} = 4.2 \times 10^3$$

$$f_2 = \frac{\omega_2}{2\pi} = \frac{4.2 \times 10^3}{2\pi} = \underline{670 \text{ CPS}}$$

THEREFORE THE SHAFT CRITICAL FREQUENCY IS 86 CPS

C - INNER BEARING SUPPORT - FREQ. EVALUATION

In the present operating configuration only one lateral threaded bar is connected. The following analysis determines the lateral f_N.

$$f_N = \frac{1}{2\pi}\sqrt{\frac{K g}{W_T}}$$

WHERE:

$g = \underline{386\ IN/SEC^2}$

W_r = Weight of Fan, Bearing, and Portion of Shaft.

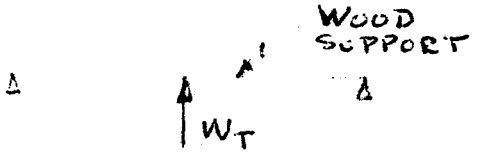

$W_F = .75\#$

$W_{SHAFT} = .125\ \#/IN \times 12\ INCHES = 1.5\#$

$W_{BEARING} = .5\#$

ASSUME SIMPLE SUPPORTS

$W_T = \underline{3.25\ lbs}.$

SOLVING FOR K

$$K = \frac{W_T}{\Delta} = \frac{48EI}{L^3}$$

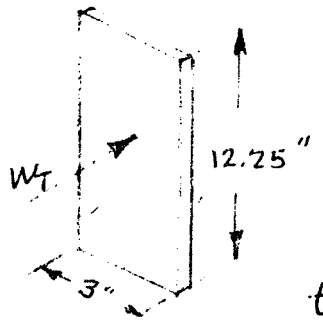

$t = 7/16"$

ASSUMED
PLYWOOD SUPPORT

$E_{WOOD} \approx 2.0 \times 10^6$ PSI

$I = \frac{1}{12} bh^3 = \frac{1}{12} (3.0)(7/16)^3$

$I = .0207$ IN^4

$L = 12.25"$, $L^3 = 1840$ IN^3

$$K = \frac{48\ (2.0 \times 10^6)(.0207)}{1840}$$

$K = 1080$ lbs/IN

SOLVING FOR f_N

$$f_N = \frac{1}{2\pi} \sqrt{\frac{1080 \times 386}{3.25}}$$

$f_N = 57$ CPS

REFERENCES

B-1 Abrams, E. M.; "Wind Tunnel Fan - Vibration Analysis", GE PIR 9333-365; 8/1/69.

APPENDIX C

AIR VELOCITY CALCULATIONS

The air velocity within the wind tunnel was measured by means of a pitot tube located near the beginning of the high velocity leg. This was connected to a pressure transducer gage which read velocity pressure in inches of water. Using this reading and utilizing a standard air density reading of 0.075 lbs/ft^3, the velocity in feet per minute was determined on a Dwyer Air Velocity Calculator slide rule, F. W. Dwyer Manufacturing Company, Michigan City, Indiana. From this reading, the miles per hour were determined.

CONVERSION TABLE PITOT TUBE

ΔP TO MPH

VELOCITY			ΔP Pitot Tube
10 mph	14.7 ft/sec	882 ft/min	0.049"
20 mph	29.3 ft/sec	1760 ft/min	0.19"
25 mph	36.7 ft/sec	2200 ft/min	0.30"
30 mph	44 ft/sec	2640 ft/min	0.43"
35 mph	51 ft/sec	3060 ft/min	0.58"
40 mph	58.7 ft/sec	3520 ft/min	0.78"
45 mph	66 ft/sec	3960 ft/min	0.98"
50 mph	73.3 ft/sec	4400 ft/min	1.24"
60 mph	88 ft/sec	5280 ft/min	1.75"

APPENDIX D

HIGH VELOCITY TEST RESULTS

20 MICRON HOLES

	Experiment #	Wind Velocity mph	Membrane ΔP	Test Results
#1	9	30	0.00	Pos.
#2	11	30	0.30	Neg.
#3	13	30	0.50	Neg.
#4	22	30	0.30	Neg.
#5	23	30	0.30	Neg.
#6	27	25	0.00	Neg.
#7	29	20	0.10	Neg.
#8	33	25	0.10	Neg.
#9	34	10	0.00	Pos.
#10	39	35	0.10	Neg.*
#11	40	35	0.10	Pos.
#12	43	15	0.10	Neg.
#13	48	35	0.20	Neg.*
#14	50	35	0.30	Pos.
#15	69	30	0.20	Neg.
#16	1	15	Ambient	Pos.
#17	5	15	Ambient	Pos.
#18	75	35	0.40	Pos.
#19	77	35	0.50	Neg.
#20	80	35	0.50	Neg.
#21	81	30	0.20	Neg.

* clogged

APPENDIX D

HIGH VELOCITY TEST RESULTS

200 MICRON HOLES

	Experiment #	Wind Velocity mph	Membrane Δ P	Test Results
#1	7	15	0.10	Neg.
#2	15	30	0.30	Neg.
#3	17	30	0.20	Neg.
#4	20	25	0.43	Neg.
#5	21	30	0.00	Pos.
#6	26	25	0.10	Neg.
#7	28	20	0.00	Pos.
#8	32	20	0.10	Neg.
#9	35	35	0.10	Neg.
#10	37	35	0.00	Pos.
#11	41	30	0.10	Neg.
#12	44	10	0.10	Neg.
#13	46	30	0.10	Pos.
#14	47	35	0.10	Pos.
#15	52	35	0.30	Pos.
#16	53	35	0.40	Neg.
#17	57	35	0.20	Pos.
#18	59	35	0.30	Neg.
#19	65	35	0.40	Neg.
#20	71	30	0.15	Neg.
#21	74	30	0.20	Neg.

APPENDIX D

HIGH VELOCITY TEST RESULTS

1000 MICRON HOLES

	Experiment #	Wind Velocity mph	Membrane ΔP	Test Results
#1	2	15	0.1	Neg.
#2	3	15	0.1	Neg.
#3	4	15	0.1	Neg.
#4	5	15	0.1	Neg.
#5	8	30	0.1	Pos.
#6	10	30	0.3	Pos.
#7	12	30	0.5	Neg.
#8	14	30	0.3	Pos.
#9	16	25	0.4	Pos.
#10	18	25	0.53	Neg.
#11	19	25	0.43	Pos.
#12	24	20	0.00	Pos.
#13	25	20	0.10	Pos.
#14	30	30	0.50	Pos.
#15	31	20	0.30	Pos.
#16	36	30	0.60	Pos.
#17	38	35	0.60	Pos.
#18	42	35	1.00	Pos.
#19	45	35	1.00	Pos.
#20	49	20	0.50	Pos.

APPENDIX D

HIGH VELOCITY TEST RESULTS

1000 MICRON HOLES

	Experiment #	Wind Velocity mph	Membrane ΔP	Test Results
#21	51	15	0.10	Neg.
#22	54	20	0.50	Neg.
#23	55	25	0.50	Neg.
#24	56	30	0.60	Pos.
#25	58	30	0.80	Neg.
#26	61	35	1.50	Pos.
#27	62	20	0.50	Neg.
#28	63	30	0.80	Pos.
#29	64	35	2.00	Pos.
#30	66	25	0.55	Pos.
#31	67	30	1.00	Pos.
#32	70	30	1.30	Pos.
#33	72	25	1.50	Neg.
#34	72	25	1.50	Neg.
#35	76	35	3.00	Pos.
#36	78	25	1.20	Neg.
#37	79	30	3.20	Neg.
#38	81	20	0.75	Neg.
#39	1a	15	Ambient	Pos.
#40	1b	15	Ambient	Pos.